INFORMATION TO USERS

This manuscript has been reproduced from the microfilm master. UMI films the text directly from the original or copy submitted. Thus, some thesis and dissertation copies are in typewriter face, while others may be from any type of computer printer.

The quality of this reproduction is dependent upon the quality of the copy submitted. Broken or indistinct print, colored or poor quality illustrations and photographs, print bleedthrough, substandard margins, and improper alignment can adversely affect reproduction.

In the unlikely event that the author did not send UMI a complete manuscript and there are missing pages, these will be noted. Also, if unauthorized copyright material had to be removed, a note will indicate the deletion.

Oversize materials (e.g., maps, drawings, charts) are reproduced by sectioning the original, beginning at the upper left-hand corner and continuing from left to right in equal sections with small overlaps. Each original is also photographed in one exposure and is included in reduced form at the back of the book.

Photographs included in the original manuscript have been reproduced xerographically in this copy. Higher quality 6" x 9" black and white photographic prints are available for any photographs or illustrations appearing in this copy for an additional charge. Contact UMI directly to order.

UMI

A Bell & Howell Information Company
300 North Zeeb Road, Ann Arbor MI 48106-1346 USA
313/761-4700 800/521-0600

CHARACTERIZATION OF EXCITED STATE REACTIONS IN TRIS(8-HYDROXYQUINOLINE) ALUMINUM (ALQ3)

by

RICHARD S. PRIESTLEY

A dissertation submitted to the Graduate Faculty in Engineering in partial fulfillment of the requirements for the degree of Doctor of Philosophy, The City University of New York.

1998

This manuscript has been read and accepted for the Graduate Faculty in Engineering in satisfaction of the dissertation requirement for the degree of Doctor of Philosophy.

12/16/97
Date:

Prof. Ardie D. Walser (Thesis Advisor)
Associate Professor
Dept. of Electrical Engineering
Chairman of the Examining Committee

12/16/97
Date:

Prof. Gerard D. Lowen
Executive Officer

Dr. Roger Dorsinville — Professor, Dept. of Electrical Engineering The City College of the City University of New York

Dr. Ping Pei Ho — Professor, Dept. of Electrical Engineering The City College of the City University of New York

Dr. Kai Shum — Associate Professor, Dept. of Electrical Engineering, The City College of the City University of New York

Dr. Nan-Lou Yang — Professor, Dept. of Chemistry College of Staten Island; The City University of New York

Supervisory Committee

THE CITY UNIVERSITY OF NEW YORK

ABSTRACT

CHARACTERIZATION OF EXCITED STATE REACTIONS IN TRIS(8-HYDROXYQUINOLINE) ALUMINUM (ALQ_3)

by

RICHARD S. PRIESTLEY

Thesis Advisor: Professor Ardie D. Walser

Recently organic materials have sparked a great deal of interest for their potential use in electroluminescent (EL) displays and thin film light emitting diodes (LED's). Light emitted from these organic materials is produced by the radiative decay of singlet excitons formed by way of charge carrier injection or photoexcitation. Any reactions which cause these excitons to decay nonradiatively will reduce the luminescence quantum efficiency of the material and hence, the optimum performance of electroluminescent devices. Therefore, an understanding of exciton interactions directly associated with luminescence quenching is vital before we can effectively exploit these devices for technological applications.

In this thesis we have examined the underlying mechanisms of various reactions which can produce a low luminescence quantum efficiency in tris(8-hydroxyquinoline) aluminum (Alq_3), a prominent material currently being used as the emitting layer of organic LED's.

Our experimental results are summarized as follows:

i) We have examined exciton-exciton interactions due to the formation of a high concentration of singlet excitons. Measurements show that such reactions reduce the photoluminescence (PL), radiative excited state lifetime and PL quantum efficiency in Alq_3. Calculations were obtained for the bimolecular recombination rate constant, singlet exciton diffusion coefficient and exciton diffusion length.

ii) We investigated the photooxidation reaction of singlet excitons with UV light and oxygen/water. Our measurements indicate that Alq_3 light emission degrades as a result of exposure to UV light and water, or UV light and oxygen molecules. Products of photooxidation act as quenching centers for singlet excitons thereby decreasing the peak photoluminescence, radiative excited state lifetime and PL quantum efficiency in Alq_3.

iii) We studied the temperature dependence of the dynamics of singlet excited states in Alq_3. Our results revealed an increase in the peak PL, radiative excited state lifetime and PL quantum efficiency with decreasing temperature from 300K to 77K. At low temperature we observed a decrease in the bimolecular recombination rate, singlet exciton diffusion coefficient and diffusion length. These results are explained in terms of a singlet exciton trapping model.

This thesis is dedicated to my parents Allan & Marva Priestley.

"Success is to be measured not so much
by the position that one has achieved
in life as by the obstacles which he
has overcome while trying to succeed."

- Booker T. Washington

ACKNOWLEDGMENTS

First and foremost I would like to thank God for blessing me with the knowledge, skills, ability and understanding for accomplishing my goals. I would like to thank my parents, Allan & Marva Priestley and my fiancee, Donzaleigh Maitland for the years of understanding and support they gave me during the challenging times in obtaining my Doctoral Degree. To them I am most thankful.

I wish to thank my thesis advisor Prof. Ardie D. Walser for giving me the opportunity to accomplish my goal of achieving the highest attainable degree within my field of engineering. His guidance, training and support is well appreciated. I also would like to thank Prof. Roger Dorsinville for the supervision he has provided over these past years. I am grateful to Dr. Igor Sokolik, whom I have worked closely with, for his contributions and our many fruitful discussions.

Many thanks to present and past staff members of the Center for Analysis of Structures and Interfaces (CASI) for their continuous guidance, administrative assistance and financial support during my years of study. I would like to thank the Program for the Retention of Engineering Students (PRES) for their support during my undergraduate and graduate years at

CCNY. I am appreciative to Prof. Ping Pei Ho, Prof. Kai Shum and Prof. Nan-Lou Yang for serving on my thesis supervisory committee. Finally, I would like to thank all my friends for their support and inspiration.

CHARACTERIZATION OF EXCITED STATE REACTIONS IN TRIS(8-HYDROXYQUINOLINE) ALUMINUM (ALQ_3)

by

RICHARD S. PRIESTLEY

TABLE OF CONTENTS

List of Figures

List of Tables

CHAPTER ONE

1. INTRODUCTION

The development of organic materials for use in thin film light emitting diodes (LED's) and electroluminescent (EL) devices has become one of the most intensively studied research topics over the last decade. The range of applications for such devices stems from simple backlights for portable battery-operated equipment, through alphanumeric displays, to complex multi-color video screens for computers and televisions.[1] Other potential applications such as light modulators,[2] optical amplifiers,[3] photodetectors,[4] organic thin film transistors[5], and laser gain mediums[6] have also stimulated interest in organic materials and the optical technology field.

To date, conventional EL devices are fabricated with inorganic direct-bandgap semiconductors such as gallium arsenide (GaAs) and indium gallium arsenide (InGaAs).[7] ZnS:Cu dispersed in a polymer matrix is the most efficient inorganic powder system which emits in the visible spectra and has an external quantum efficiency (photons emitted per input electrons) of 3%.[8] However it requires high drive voltage, has poor

stability and little color tunability. Conversely, devices fabricated from thin films of organic materials will have many advantages over such competing technologies. They have high quantum efficiency, low operating voltage, and emission in many colors from deep blue to infrared.[9,10,11,12] In addition, high resolution and emission from a flexible substrate have been demonstrated.[13] Another unique property of many organic molecules which is not found in inorganic semiconductors is that the luminescence band is red-shifted from the absorption band[14] by as much as 0.5eV. This shift results in an organic LED that is highly transparent over its own emission spectrum, and indeed throughout most of the visible region of the spectrum. Hence, any reabsorption of the emitted light is very minimal.

The pioneering work in electroluminescence from an organic material was first demonstrated in the 1960's by Pope et al. in anthracene crystals.[15] Thereafter other groups also observed this phenomenon in organic crystals and thin films[16] but high operating voltages and low quantum efficiencies made these organic EL devices unattractive and consequently they did not draw much attention. Then in 1987, Tang and Van Slyke successfully demonstrated efficient EL from multilayers of sublimated organic compounds.[17] Their device was based on the fluorescent metal chelate, tris(8-hydroxyquinoline) aluminum (Alq_3). By fabricating the device in a multilayer configuration, they observed a

dramatic reduction in the operating voltage of the LED along with an enhancement in the quantum efficiency. Moreover, by doping this material with fluorescent dyes such as coumarin 6 or quinacridone, they noticed an increase in the quantum efficiency or a shift in the spectral emission.[18,19] Similar improvements were found in other hosts.[20]

In later years Burroughes et al.[21] constructed the first organic polymer based EL device utilizing poly(p-phenylene vinylene) (PPV) as the emitting layer. This and other polymer-based devices took advantage of the low manufacturing cost and the ability to alter the emitting bandgap energy by varying the effective conjugation length of the polymer. Figure 1.1 shows the chemical structure of Alq_3 and PPV, two of the most prominent organic luminescent materials.

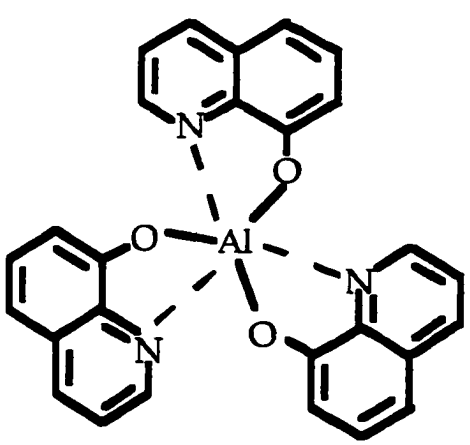

Alq3

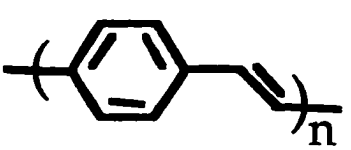

PPV

Figure 1.1 Chemical structure of Alq_3 and PPV

Since the first demonstrations of electroluminescence (EL), the field has advanced rapidly towards the development of organic compounds for light emitting diodes. Multilayered cell structures currently show luminance of over 100,000 cd/m^2,[22] about twelve times brighter than a common fluorescent lamp (8,000 cd/m^2). Other recent discoveries in organic light emitting diodes (OLED's) includes white light emission[23] and color-tuning through microcavity based designs.[24] With these progressions one can justify an increased interest towards commercialization of this technology, but many factors still exist which prevents the advancement of OLED's for commercial use.

A schematic of a typical single layer organic LED is shown in Figure 1.2. An Indium-Tin-Oxide(ITO) semi-transparent electrode and an Aluminum(Al)/Calcium(Ca) electrode serves as the hole-injecting and electron-injecting layers, respectively. The light emitting material, which is about 100nm thick, is sandwiched between these two layers. In most devices electron and hole transport layers are used to increase the injection efficiency of charge carriers into the emitting layer since these materials do not possess good bipolar transport properties.[25]

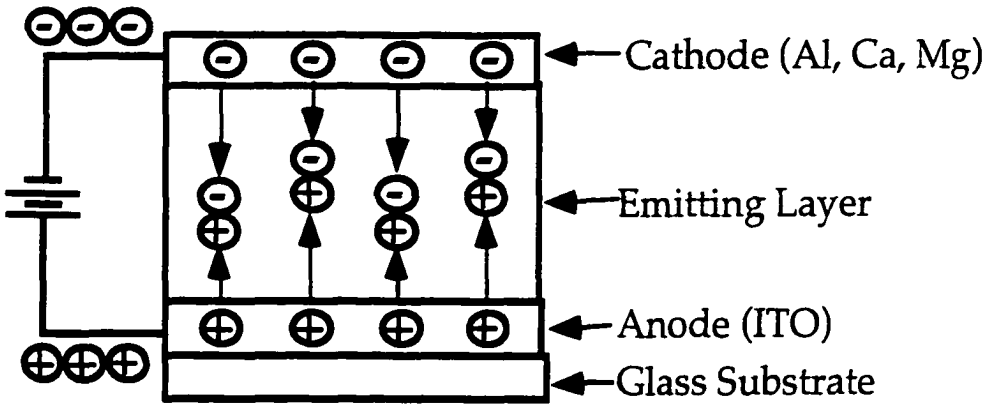

Figure 1.2 Schematic of a typical organic LED

When a forward biased voltage is applied across the electrodes, the electric field created pulls low-energy electrons from the organic material near the positively charged electrode, or anode, leaving behind electron vacancies, or holes. On the other hand, the negative electrode, or cathode, injects high-energy electrons into the adjacent material. With the aid of the electric field, the electrons and holes migrate towards each other in the emitting layer where they form both singlet and triplet excitons. These excitons can both decay radiatively or nonradiatively though it is the radiative decay of the singlet excitons that is primarily responsible for light emitted from the device. Almost all the OLED's reported so far exhibit EL originating from the radiative decay of singlet excitons in the emitting material and only a preliminary study has been undertaken on the EL originating from triplet excitons.[26,27,28]

In OLED's, the formation of excitons involves charge carrier injection, transport, and carrier combination. These are all of primary importance to efficient device operation. Another important process is the decay or recombination of singlet excitons. This involves a competition between the radiative and nonradiative decay channels. While a portion of the singlet excitons will recombine radiatively emitting light, some may give up their energy as phonons. In addition to these nonradiative processes, impurities or irregularities in the emitting layer may exist and create defects or low-energy trapping sites which are nonradiative decay channels for the excitons.

The EL efficiency may also be reduced by the formation of excitons close to the contacts where a large number of defect sites may be located.[29,30] Other nonradiative decay mechanisms such as intersystem crossing from singlet to triplet states, exciton-exciton annihilation at high excitation densities, charge carrier generation due to exciton dissociation, and exciton migration to quenching sites have all been demonstrated to occur in organic materials.[31,32,33] Such nonradiative decay channels produces a decline in brightness and a reduction in the light emitting efficiency. Moreover, the device properties of OLED's degrade as a result of exposure to UV light, water and oxygen molecules.[34,35] This degradation is related to the corrosion of contacts, the presence and migration of impurities, and to the chemical decomposition of the emissive material.

Singlet excitons formed within the emitting layer are primarily responsible for light emission and any interactions causing nonradiative recombination of these excitons will affect the quantum efficiency and optimum performance of EL devices. Before we can effectively exploit these devices for technological applications, we must first have a better understanding of various singlet exciton quenching mechanisms. Therefore, the overall focus of this study will be to examine the underlying reactions of singlet excited states which attribute to a reduction in PL and EL quantum efficiency.

To perform these studies we will simultaneously observe the transient photoluminescence (PL) and photoconductivity (PC) response of thin-film layers of Alq_3. Through PL measurements we can observe the reactions and relaxation dynamics of singlet excitons in organic light emitting materials. Also, there are fewer variables to control in studying the photoluminescence than the electroluminescence. On the other hand, PC measurements will help us in understanding one of the nonradiative channels for singlet exciton energy dissipation. We believe the PC response is a byproduct of singlet-singlet exciton interactions with the generation of charge carriers (electrons and holes) through exciton dissociation. Combined together, simultaneous PL and PC measurements will provide two channels from which we can observe the reactions of photoexcited singlet excitons.

1.1 Thesis Statement

This thesis is focused on understanding the reactions of singlet excitons in organic EL materials while studying various factors which affects the dynamics of these states and consequently the overall performance of OLED's. The following objectives have been investigated:

1. Determine the optical properties of Alq_3. These optical properties includes absorption spectra, photoluminescence (PL) spectra, PL excitation spectra, fluorescence lifetime and relative PL quantum efficiency.
2. Study the bimolecular reactions of singlet excitons. We will determine how the concentration of singlet excitons affects both the peak PL and fluorescence lifetime. We will investigate how bimolecular interactions contribute to the generation of charge carriers and the PC response. Theoretical calculations of the bimolecular rate coefficient, diffusion coefficient, and diffusion length of singlet excitons will be performed.
3. Investigate the photochemical reactions of UV light and oxygen/water on EL materials. We will show that such reactions act as quenchers for singlet excited states and are responsible for quenching the PL and fluorescence lifetime, which in turn leads to a degradation in the device performance.

4. Determine the temperature dependence of the transient PL. We will observe how this affects the quantum efficiency of the PL. Temperature dependent calculations of the bimolecular rate coefficient, diffusion coefficient, and diffusion length of singlet excitons will be provided along with an explanation in terms of a singlet exciton trapping model.

The information gathered from this thesis is significant in the advancement of organic thin film light emitting devices. The cause of light emission quenching needs to be clearly understood before problem solving approaches can be made. Once this is resolved the potential of higher efficiencies and longer device lifetimes can be attained.

1.2 Thesis Outline

Chapter 2 of this thesis will provide a review on the background of our material of interest, tris(8-hydroxyquinoline) aluminum (Alq_3). We will discuss the physical structure of Alq_3 along with its optical properties and the primary photoexcitations of this material.

Chapter 3 involves a discussion of the experimental techniques and apparatus used to investigate the various reactions of singlet excitons. A description of the laser system used in this study and the procedures for fabricating the samples will be presented.

In chapter 4, we report on the investigation of bimolecular reactions of singlet excitons in Alq_3. We have studied the singlet excited state dynamics and results show that bimolecular recombination dominates the singlet exciton decay in pristine films at high intensities.

In chapter 5, we report the investigation of photooxidation reactions of singlet excitons in Alq_3. This experiment demonstrates for the first time the process of photooxidation by UV light and oxygen/water in Alq_3.

In chapter 6, we report the investigation of the temperature dependence on the behavior of singlet excitons in Alq_3.

Chapter 7 summarizes the major results and conclusions drawn from this thesis and discusses the future research experiments to be performed.

1 R.W. Gymer, *Endeavour*, **20**, p. 115 (1996)

2 M. Hiramoto, K. Yoshimura, and M. Yokoyama, *Appl. Phys. Lett.* **60**, p.324, (1992)

3 T. Katsume, M. Hiramoto, and M. Yokoyama, *Appl. Phys. Lett.* **66**, p.2992, (1995)

4 G. Yu, K. Pakbax, and A.J. Heeger, *J. Electron. Mater.*, **23**, p. 925, (1994)

5 G. Robinson, *Electronic Engineering Times*, p. 35, (1997)

6 M.A. Diaz-Garcia, F. Hide, B.J. Schwartz, M.D. McGehee, M.R. Andersson and A.J. Heeger, *Appl. Phys. Lett.*, **70**, p. 3191 (1997)

7 Y. Yang, *MRS Bulletin.* **22**, p. 31 (1997)

8 D.D.C. Bradley, *Adv. Mater.*, **4**, p. 756, (1992)

9 D. Braun and A.J. Heeger, *Appl. Phys. Lett.* **58**, p. 1982, (1991)

10 Y. Ohmori, M. Uchida, K. Muro and K. Yoshino, *Solid State Comm.* **80**, p. 605, (1991); Y. Ohmori, M. Uchida, K. Muro and K. Yoshino, *Jpn. J. Appl. Phys.*, **30**, p. L 1938, (1991)

11 G. Grem, G. Leditzky, B. Ullrich and G. Leising, *Adv. Mater.*, **4**, p. 36, (1992)

12 P.L. Burn, A.B. Holmes, A. Kraft, D.D.C. Bradley, A.R.Brown, R.H. Friend and R.W. Gymer, *Nature*, **356**, p. 47, (1992)

13 G. Gustafsson, Y. Cao, G.M. Treacy, F. Klavetter, N. Colaneri, and A.J. Heeger, *Nature*, **357**, p. 477-479, (1992)

14 P.E. Burrows, Z. Shen, V. Bulovic, D.M. McCarty, S.R. Forrest, J.A. Cronin and M.E. Thompson, *J. Appl. Phys.* **79**, 1991 (1996)

15 M. Pope, H.P. Kallmann, and P. Magnante, *J. Chem. Phys.* **38**, p. 2042, (1963)

16 W. Helfrich and W.G. Schneider, *Phys. Rev. Lett.* **14**, p. 229, (1965)

17 C.W. Tang and S.A. Van Slyke, *Appl. Phys. Lett.* **51**, p. 913-15, (1987)

18 C.W. Tang, S.A. VanSlyke and C.H. Chem, *J. Appl. Phys.* **65**, p. 3610, (1989)

19 R. Murayama, T. Wakioto, H. Nakada, M. Nomura and G. Sato. U.S. Patent 5,227,252.

20 T. Sano, M. Fujita, T. Fujii, Y. Nishio, Y. Hamada and K. Shibata, "Extended Abstracts." The 41st Spring Meeting, 1994 of the Japan Society of Applied Physics and Related Societies, 25 p-N-2.

21 J.H. Burroughes, D.D.C. Bradley and A.R. Brown, *Nature* **347**, p. 539-541, (1990)

22 R. Murayama, "Extended Abstracts." The 54th Autumn Meeting of the Japan Society of Applied Physics, p. 1127, (1993)

23 J. Kido, M. Kimura, and K. Nagai, *Science,* **267**, p. 1332, (1995)

24 A. Dodabalapur, L. Rothberg, and T.M. Miller, *Appl. Phys. Lett.*, **64**, p. 2308, (1994)

25 J. Kido, *TRIP*, Vol. 2, No.10, p. 350 (1994)

26 T. Tsutsui, C. Adachi, and S.Saito, in *Photochemical Processes in Organized Molecular Systems*, edited by K. Honda (Elsevier, North Holland, Amsterdam. p. 445, (1991)

27 M. Moridawa, C. Adachi, T. Tsutsui, and S. Saito, "Extended Abstracts." The 51th Autumn Meeting of The Japan Society of Applied Physics, p. 1041, (1990)

28 S. Hoshino and H. Suzuki, *Appl. Phys. Lett.*, **69**, p. 224 (1996)

29 D.D.C. Bradley and R.H. Friend, *J. Phys. Cond. Matt.*, **1**, p. 3671 (1989)

30 K.E. Ziemelis, A.T. Hussain, D.D.C. Bradle, A.R. Brown, R.H. Friend, and R.W. Gymer, *Nature*, **356**, p. 47 (1992)

31 N.F. Colaneri, D.D.C. Bradley, R.H. Friend, P.L. Burn, A.B. Holmes, and C.W. Spangler, *Phys. Rev. B.*, **42**, p. 11670, (1990)

32 H.S. Woo, S.C. Graham, D.A. Halliday, D.D.C.Bradley, R.H. Friend, P.L. Burn and A.B. Holmes, *Phys. Rev, B.*,

33 R. Kersting, U. Lemmer, M. Deussen, H.J. Bakker, R.F. Mahrt, H. Kurz, V.I. Arkhipov, H. bassler, and E.O. Gobel, *Phys. Rev. Lett.*, **73**, p. 1440 (1994)

34 F. Papadimitrakopoulos, K. Konstadinidis, T.M. Miller, R. Opila, E.A. Chandross, and M.E. Galvin, *Chem. Mater.*, **6**, p.1563 (1994)

35 J.C. Scott, J.H. Kaufman, P.J. Brock, R. Dipietro, J. Salem, and J.A. Goitia, *J. Appl. Phys.*, **79**, p. 2745 (1996)

CHAPTER TWO

2. TRIS (8-HYDROXYQUINOLINE) ALUMINUM, (ALQ_3)

2.1 Introduction

Our interest in tris(8-hydroxyquinoline) aluminum stems from its application as the first material used in organic low molecular weight light-emitting diodes. In fact, it has become the prototypical material among numerous organic electroluminescence (EL) systems. In this chapter we begin with a summary on the structure of Alq_3 along with a discussion on the primary photoexcited species in this material. A brief overview of the photoluminescence (PL) and EL processes in Alq_3 will then be given followed by a discussion on the optical properties in Alq_3 and mechanisms behind charge transport.

2.2 Alq_3 Structure and Theory

A large portion of fluorescent organic-metallic compounds are found among metal chelates.[1] Typically, these compounds consist of a single metal ion joined to one or more molecules of an organic compound. This bonding results in a rigid molecule containing several fused ring systems in

which the metal atom is incorporated. Alq_3 is one type of metal-chelate composed of an aluminum ion surrounded by three 8-hydroxyquinoline (8-HQ) ligands. In a thin film Alq_3 is one of the most fluorescent materials in this class of metal-chelates.

Figure 2.1 shows the chemical structures of the Alq_3 complex and the ligand. The 8-HQ ligand is a fluorescent chelating agent composed of two fused benzene rings with two functional groups, the nitrogen atom and the hydroxy (OH) group. These functional groups combine with the metal ion to form the chelate compound. Three ionized 8-HQ ligands bonds with the aluminum ion via the oxygen and nitrogen atoms and forms the neutral trivalent aluminum oxinate (Alq_3). The functional groups on the ligand are bonded to the aluminum ion with regular covalent bonds and coordinate covalent bonds, shown by the straight lines and broken lines, respectively. In the covalent bonds a pair of electrons are shared by two adjoining atoms. The coordinate covalent bonds represents a bond in which the nitrogen atoms donates a pair of unshared electrons to the aluminum ion.

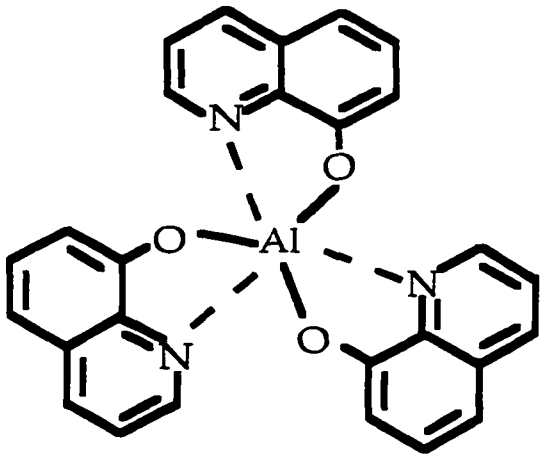

Alq3

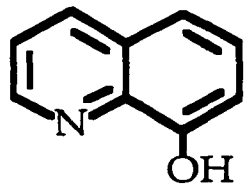

8-hydroxyquinoline

Figure 2.1 Chemical structure of Alq_3 and 8-hydroxyquinoline

The carbon atoms within the fused benzene rings contains three trigonal sp^2 hybrid orbitals on the same molecular plane which form a σ-bond formation. A lone $2p_z$ orbital remains with its axis perpendicular to the molecular plane and the overlapping of two $2p_z$ orbitals forms a π-bond. Therefore, the carbon-carbon double bonds are composed of one σ-bond and one π-bond and the alternating single and double bonds results in a π-conjugated network. Since the π-bond is weaker it is more reactive and easier to break. This allows the delocalization of π-electrons along the conjugated carbon atoms, permitting them to move freely within the molecule.

The energy level diagram for Alq_3 and the aluminum ion is shown in Figure 2.2.

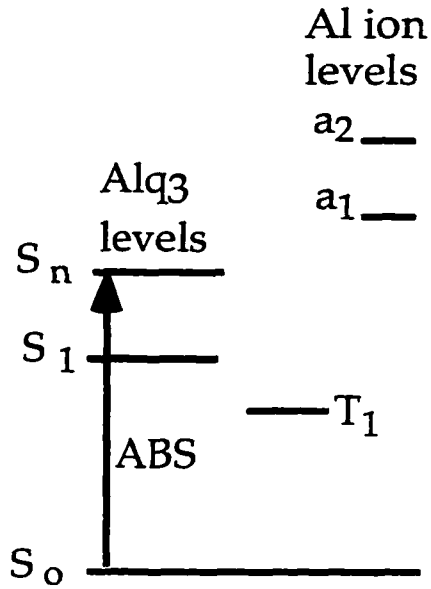

Figure 2.2 Energy levels of metal chelate Alq_3

Since the aluminum ion forming part of the chelate does not contain partly unfilled inner shells of electrons, the excited state energy levels of the metallic ion is much larger than the singlet and triplet excited state energy levels in the organic part of the molecule. This prohibits any type of energy transfer from the ligands to the aluminum ion. Therefore, the ligands are primarily responsible for both photon absorption and emission and the metal ion merely serves as the link holding the various parts of the Alq_3 molecule together.[2] The similarity observed in the PL and EL spectra of other metal chelate materials such as Gaq_3 and Inq_3 to the spectra of Alq_3[3] also indicates that the metal ion does not play a major role in the

emission spectra. From this it is presumed that the quinolate ligand, rather than the central metal ion, is the site of the excited state. However, some metal chelates do produce emission spectra originating from the metal ions such as lanthanide-organic complexes.[4,5]

2.3 Photoexcitations and Luminescence in Alq_3

The origin of photoluminescence and electroluminescence in Alq_3 stems from the radiative decay of singlet excited states. In this section a discussion on the primary excitations leading to these excited states will be presented along with their recombination process.

2.3.1 Electronic Excitation in Alq_3

In organic materials the absorption of energy from an incident photon excites an electron from the highest occupied molecular orbital (HOMO) to the lowest unoccupied molecular orbital (LUMO). The electron spin can be oriented in the same or opposite direction to that of the electron remaining in the original orbital and this produces one of two possible excited electronic states. In one state, the electron spins are paired (antiparallel) resulting in a spin quantum number of '0'. In the presence of a magnetic field this state remains a single state, referred to as a singlet state, with a magnetic quantum number of '0' and a state multiplicity equal

to '1'. In the other state the spins are unpaired (parallel) with a resultant spin quantum number of '1'. This unpaired state will interact with a magnetic field and splits into three quantized states with a corresponding magnetic quantum number of '+1, 0, or -1'. These three values coincides with three different energy levels and the molecule is said to be in a triplet state, with a multiplicity equal to '3'. Figure 2.3 shows a pictorial description of this absorption process with the arrows intersected by the levels representing electrons and the direction of the arrow representing the orientation of the electron spin.

In Alq_3, photoexcitation mainly creates singlet excited states because population of the triplet level by direct absorption of light is a difficult process. This is due to both the weak singlet-triplet absorption band and the required spin inversion.[6] Analogous to photoexcitation by the absorption of a photon, the basis of electroluminescence involves the injection of charge carriers (electrons and holes) into Alq_3 and subsequently, the formation of singlet and triplet excited states. Both states are formed due to the random spin of the injected carriers. However, there is a 75% probability of forming triplet excited states and a 25% probability of forming singlet excited states. This originates from the four possible spin orientations that the injected carriers can form, with three of the four orientations contributing to the triplet state along with the single orientation which forms the singlet state.

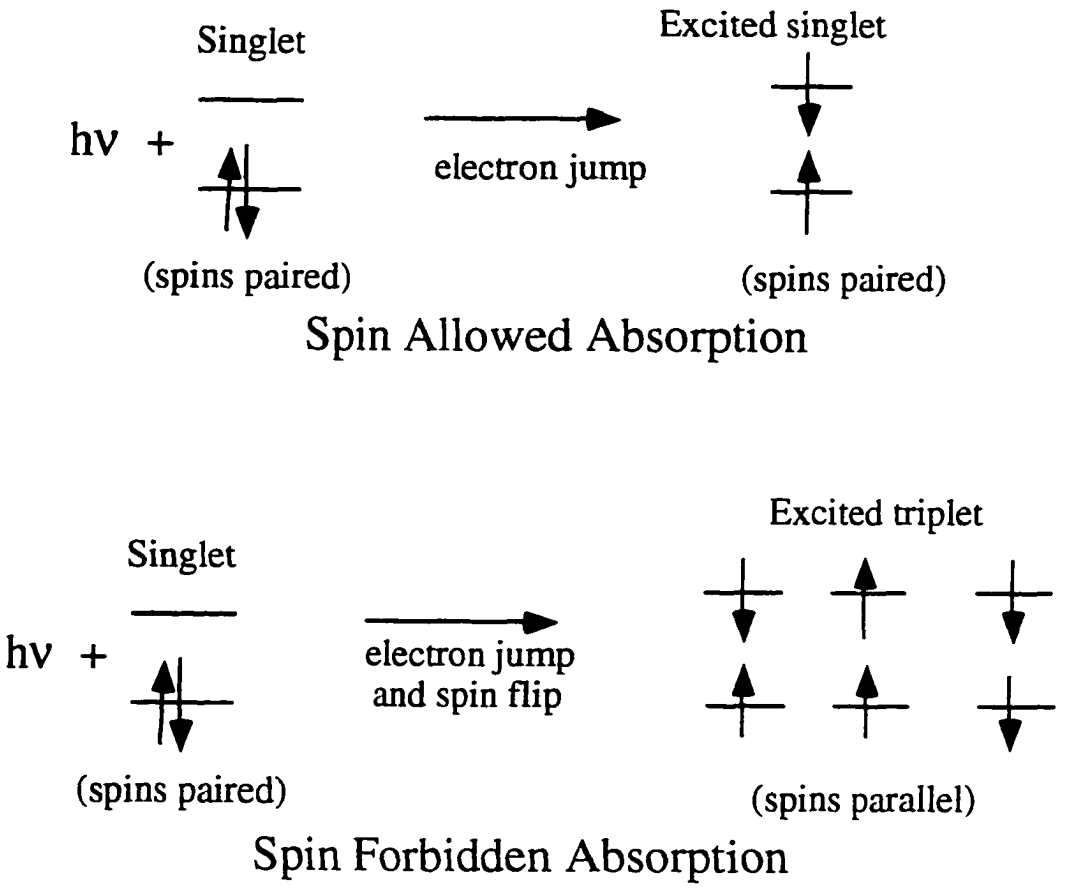

Figure 2.3 Orbital energy level description of absorption process for singlet and triplet exciton generation

2.3.2 Exciton Formation in Alq_3

In Alq_3, a π-electron photoexcited into the LUMO level is electrostatically bound with the remaining hole in the HOMO level. This electron-hole pair is bound by their coulombic attraction and forms an exciton.[7] Depending on the binding energy of the electron-hole pair, these excitons can be classified into two groups: Frenkel excitons or Wannier excitons. In Frenkel excitons the electron in the excited state occupies an empty molecular orbital of higher energy and the excitation is confined within or near the molecule. This confinement produces weak intermolecular coupling between the excited molecule and its neighbors. For Wannier excitons the coulombic interaction between the electron and hole is lower than in Frenkel excitons since there is no confinement of the electron to a single molecule. This allows the excited electron to undergo strong interaction with other molecules which can result in the dissociation of the electron-hole pair.

The exciton binding energy is dependent on the strength of coupling between electron-electron interactions and the electron-lattice coupling.[8] This topic has recently been at the center of debate in organic luminescent materials, mainly organic polymers.[9] Depending on the strength of coupling, optical transitions in organic materials can be described in terms of an exciton model or a semiconductor band model. For example, weak

coupling and interaction between an electron and neighboring molecular sites favors the generation of strongly correlated electron-hole pairs upon photoexcitation. This strong association results in a large binding energy on the order of 1eV[10] and suggests that the exciton model should be applied to the system. In the case of organic polymers this leads to the formation of intrachain excitons.[11,12] On the other hand, strong electron coupling between adjacent molecular sites results in the formation of uncorrelated electron-hole pairs. In this case Pakbaz et al.[13] suggested that the Coulombic binding energy of the exciton is negligible and on the order of a few meV, so the primary photoexcitations in organic polymers are free carriers that later self-localize to form polaron-excitons. For such negligible binding energies a semiconductor band model can be applied. Such low binding energies of excitons are found in semiconductor materials such as silicon and germanium, which has a 14.7 meV and 4.15 meV binding energy, respectively.[14]

The binding energy of Alq_3 is about 3.1 eV,[15] suggesting that the intermolecular coupling is weak and allowing the exciton picture to be more valid. Thus, Frenkel excitons are formed since the molecular excitation is confined within the vicinity of one molecule.[16]

2.3.3 Photoluminescence in Alq_3

Photoluminescence in Alq_3 mainly occurs with exciton transitions from the lowest vibrational level of the S_1 state to the vibrational levels of the ground state, S_0. This is regardless of what level the molecule is originally excited to. Higher excited singlet excitons may exist but they would rapidly decay nonradiatively to the lowest singlet exciton state by the liberation of heat or phonons. Equations 2.1 & 2.2 describe the absorption and PL process for Alq_3 and a general pictorial description is shown in Figure 2.4, where S_n^* denotes a highly excited singlet state.

The absorption of sufficient energy in Alq_3 excites an electron across the π-π^* gap which is approximately 2.85eV[17] and results in the formation of singlet excitons. However, only a portion of the absorbed energy is emitted upon radiative decay of these excitons. This is due to Stokes Law where part of the absorbed energy is lost via internal conversion and transferred to the lattice as phonons. Therefore, the wavelength of the emitted photon is red-shifted from the wavelength corresponding to the optical bandgap.

$$S_o + h\nu\ (355nm) \longrightarrow S_1 \qquad \text{Equation 2.1}$$

$$S_1 \longrightarrow S_o + h\nu\ (500nm) \qquad \text{Equation 2.2}$$

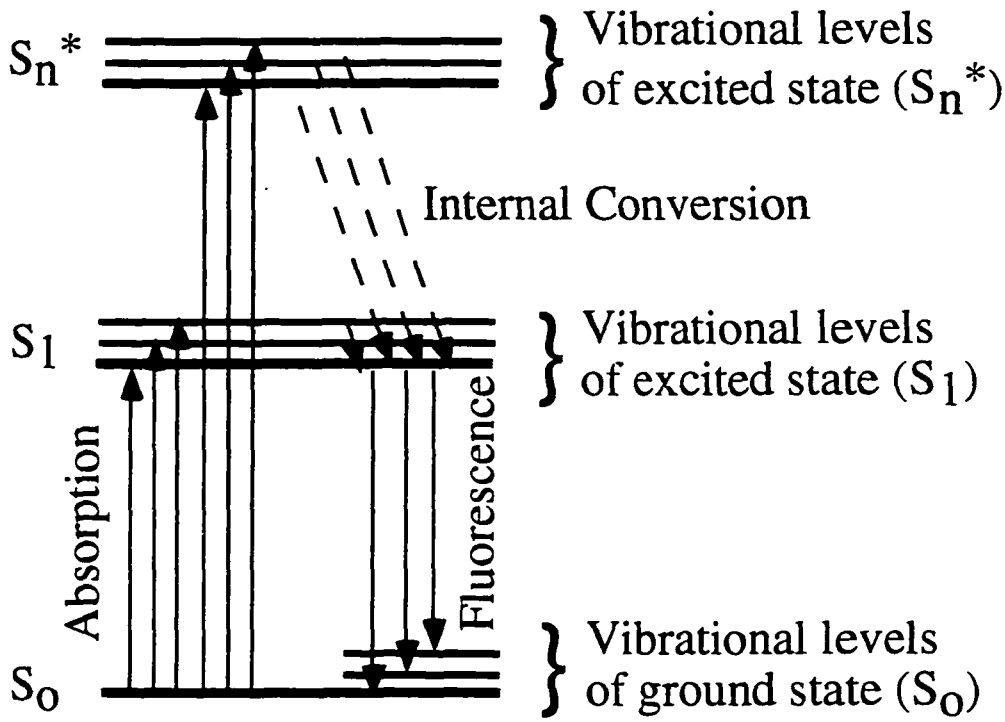

Figure 2.4 Energy level transitions for absorption and fluorescence

2.3.4 Electroluminescence in Alq_3

In electroluminescence, mobile electrons and holes are injected into the emitting layer where they recombine with oppositely charged carriers and form singlet and triplet excitons. The EL in Alq_3 originates from the decay of the singlet excitons, similar to the PL process described in equation 2.2. The difference between the two phenomena is in the formation of the singlet excitons, as shown in Figure 2.5.

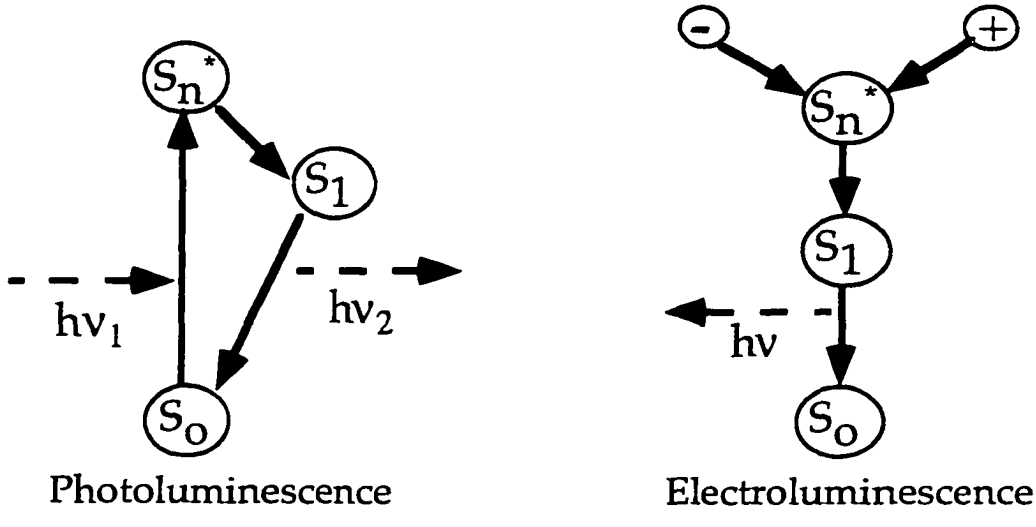

Figure 2.5 Singlet exciton formation in PL and EL processes

The great similarity between the electroluminescence and photoluminescence spectra of Alq_3, shown in Figure 2.6, suggests that charge injection produces the same excited state as photoexcitation and the light emitting mechanism is identical in both cases.[1,13] This implies that an

increase in the photoluminescence yield of Alq_3 will result in improvements in the electroluminescence efficiency, assuming that carrier injection, transport, and recombination are not the limiting factors.

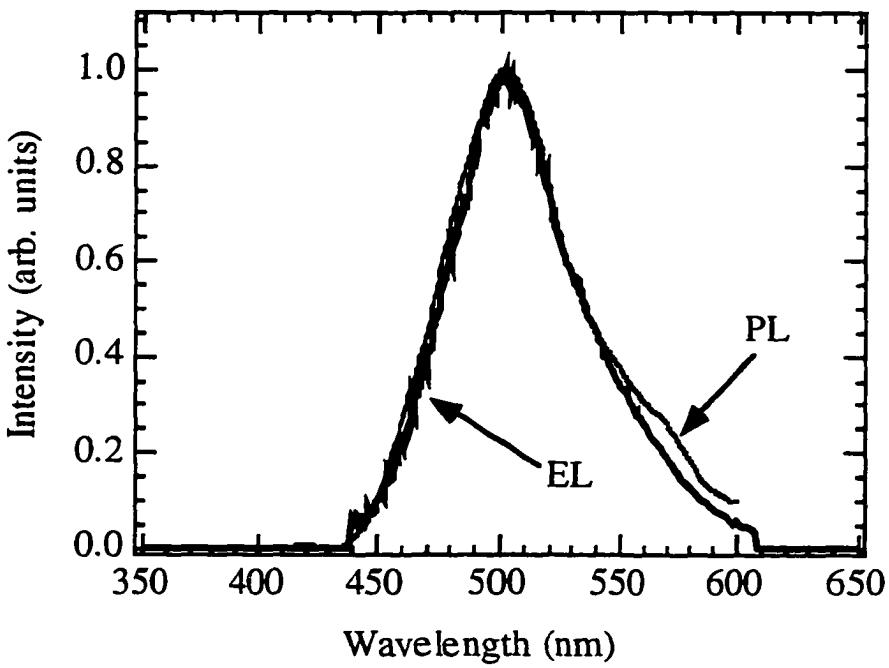

Figure 2.6 PL of Alq_3 thin film and EL of Alq_3 device

The triplet excitons formed in EL could possibly contribute to the luminescence via phosphorescence emission or triplet-triplet fusion. However, in most organic luminescent materials deactivation from triplet excited states results in a non-radiative decay.[18] On the other hand, the triplet-triplet fusion process described by equation 2.3 could contribute to the EL in OLED's:

$$T_1 + T_1 \longrightarrow S_0 + S^*_n \qquad \text{Equation 2.3}$$

where T_1 is an excited triplet state. The vibronically excited singlet exciton S^*_n can subsequently relax to the lowest excited singlet exciton state, S_1, and decay radiatively, similarly to a singlet exciton produced directly by charge carrier injection.

The fluorescence emitted in this process would be delayed from the emission of singlet exciton formed directly by charge injection. This is due to the time required for the triplet excitons to annihilate, form the vibronically excited singlet exciton and then deactivate to the first excited state. However, in EL devices operating under a constant DC bias, this emission would be difficult to detect since emission is constantly being produced.

2.4 Optical Properties of Alq_3

In this section is a discussion on some of the optical properties of the emitting material Alq_3. Such information is crucial for the in-depth understanding of the operation of OLED's. For example, one important criteria for emitting layers is that they possess a high photoluminescence quantum efficiency. This is defined as the percentage of photons emitted per photons absorbed. Ideally one would desire an emitting material with a 100% PL quantum efficiency and, when used in an OLED configuration, a 25% EL quantum efficiency. However, this would be difficult to achieve because of competition between the radiative and nonradiative decay channels.

Alq_3 is a relatively good luminofore with an internal PL quantum efficiency of 8% in the solid state according to C.W. Tang.[19] This value however, has been referenced from unpublished experimental data. According to recent work in Alq_3 by D.Z. Garbuzov et al.[20] the PL quantum efficiency of the prominent luminescence band centered at 530nm was found to be 32%. Their results were obtained by immersing a thin film of Alq_3 into an index-matching fluid and measuring the emitted radiation using UV-enhanced photodiodes. In this technique the influence of waveguiding effects within the sample and losses due to the substrate are

all reduced. Normally these effects can distort the results of PL quantum efficiency measurements taken using an integrating sphere.

Shown in figure 2.7 is the absorption (ABS), photoluminescence excitation (PLE) and photoluminescence (PL) spectra of Alq_3 in solid state. These measurements were taken on Alq_3 films approximately 1-2μm thick. From the PL spectra of Alq_3 we observed a peak fluorescence emission at 500nm when photoexcited at 355nm. This demonstrates the potential use of Alq_3 as a green emitter in EL devices.

Both the ABS and PLE spectra extended from about 450nm into the UV region. The (PLE) spectra of Alq_3 measures the fluorescence intensity with respect to the excitation wavelength and it defines the incident photoexcitation wavelength which produces the strongest fluorescence. The PLE spectra in figure 2.7 was taken for a fluorescence emission at 500nm. The maximum emission occurred at an excitation wavelength of 394nm. From the absorption spectra, and using Beer-Lambert's Law, we calculated the absorption coefficient of Alq_3 thin film to be 4.14×10^4 cm^{-1} at an excitation wavelength of 355nm. This indicates that excitation will occur in the bulk of the Alq_3 thin films used in our measurements.

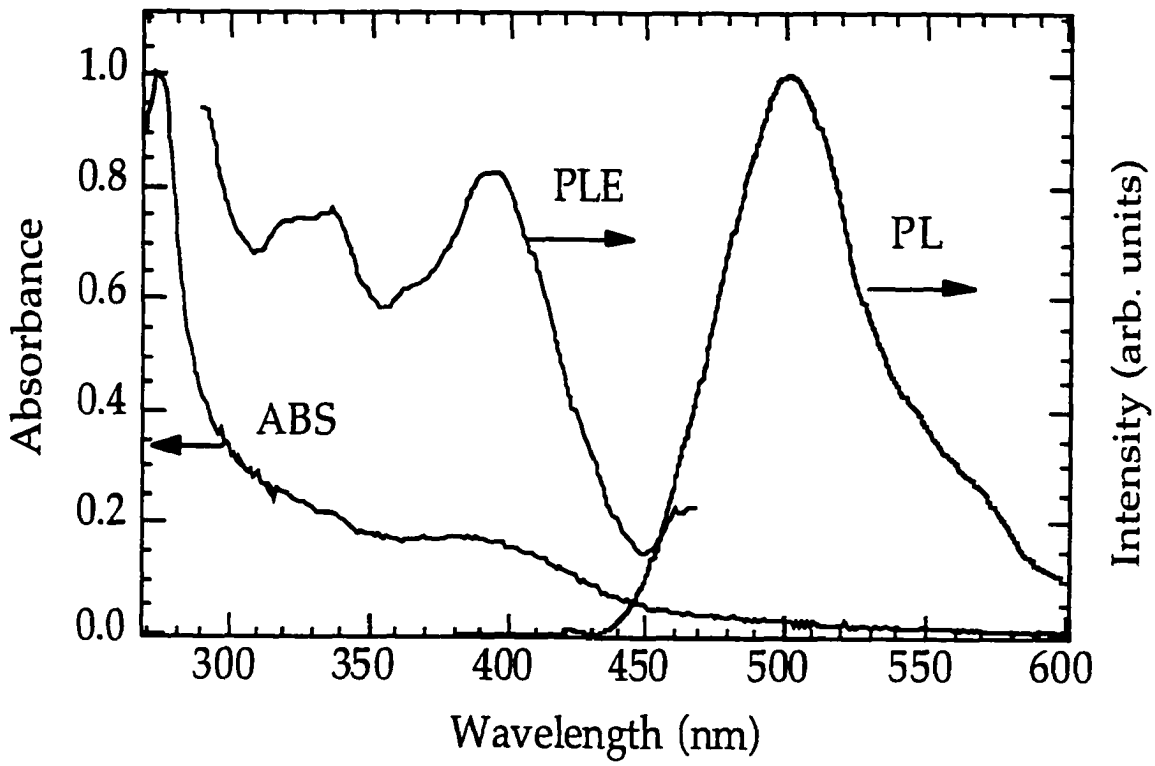

Figure 2.7 ABS, PLE, & PL spectra of Alq_3 thin film

The singlet excited states responsible for light emission in Alq_3 can be characterized by their molecular fluorescence lifetime, which is defined as the reciprocal of the sum of all decay rates from that state. In terms of the parameters shown in Figure 2.8, the fluorescence lifetime, τ, is defined as:

$$\tau = (k_r + k_{nr} + k_{is})^{-1}, \qquad \text{Equation 2.4}$$

where k_r is the radiative transition decay rate, k_{nr} is the nonradiative transition decay rates such as heat or phonon generation, and k_{is} is the rate for intersystem crossing from singlet to triplet states. Here we have neglected any nonradiative decay due to intermolecular interactions, trapping or free-carrier interactions although these processes can occur in organic molecular crystals.[21,22,23,24,25] In upcoming chapters we will demonstrate how some of these additional processes can affect the excited state lifetime.

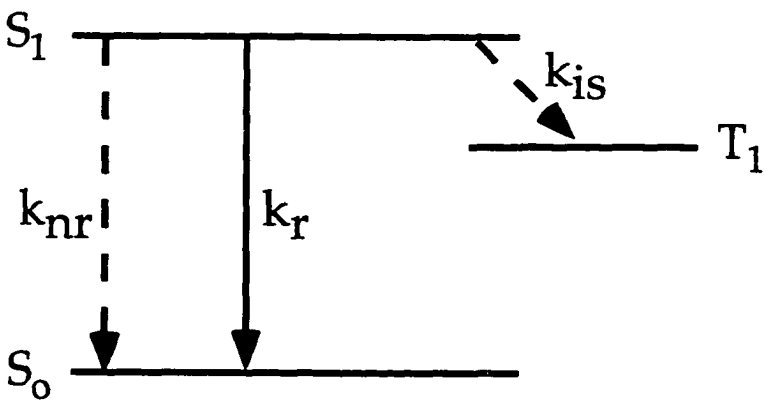

Figure 2.8 Decay rate constants from first excited state, S_1

For Alq_3, the fluorescence lifetime has been measured for both thin films and toluene solutions.[13] This was done at low intensity excitations where bimolecular interactions are minimal. The singlet state population decays exponentially with a decay time, τ_s of 14-16 nsec. In pristine Alq_3 samples we have observed single exponential PL decays with a lifetime of 15-16 nsec (Figure 2.9), consistent with other reported values. In OLED's operating under pulsed DC bias, the fluorescence lifetime places a limit on the fastest possible response of the device. To date EL response times have been measured to be on the order of 10^{-6}-10^{-7} sec[13,26] with the slower response due to the time required for carriers to travel into the emititng layer and form excitons.

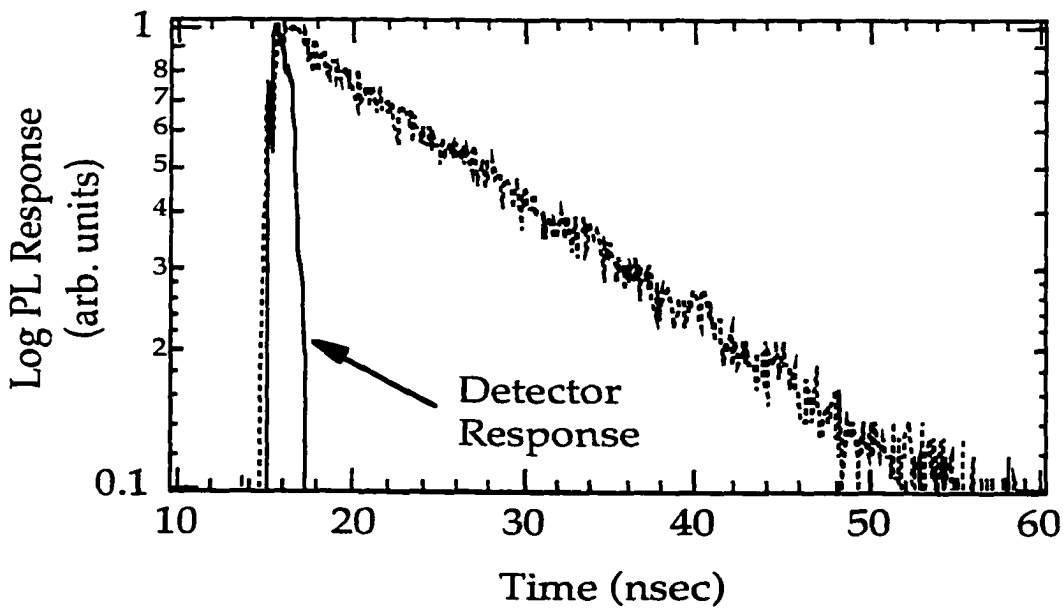

Figure 2.9 PL decay of Alq_3 thin film.

The chelate compound Alq_3 is composed of an aluminum ion surrounded by three ligands. The aluminum ion can be replaced by other group III metal ions such as indium, gallium, or scandium, however different absorption and emission spectra will be observed.[27] Table 2.1 illustrates the luminescent properties of other metal quinolate complexes.[24]

		Alq_3	Gaq_3	Inq_3	Scq_3
Solution	Peak λ	520	542	541	530
	$\eta_{PL\text{-}Solution}$	1.00	0.23	0.32	0.52
Thin film	Peak λ	520	541	540	542
	$\eta_{PL\text{-}Film}$	1.00	0.23	0.25	0.093
Atomic Weight		26.98	69.72	114.8	44.95

Table 2.1 Photoluminescence properties of several Mq_3 complexes

From the above table, Alq_3 is shown to have the highest PL efficiency among all other metal-chelate compounds. This is attributed to the fact that the aluminum ion has a lower atomic weight compared to the other metal atoms. The substitution of heavy atoms increases the rate of intersystem crossing from S_1 to T_1. Normally triplet-singlet transitions are spin-forbidden. However, the magnitude of the spin-orbit coupling between the wavefunctions of the singlet and triplet states increases with the atomic number[28] and this results in a decrease in the fluorescence efficiency for heavier molecules.

2.5 Charge Transport Properties in Alq_3

The charge transport properties in Alq_3 are important since this material serves as an electron-transport layer in addition to the emitting layer. This emitting layer does not possess good bipolar charge transport properties. Therefore, in LED's the electron-hole recombination and exciton formation will occur closer to the interface of the emitting layer and hole transport layer.

Different models have been used to explain charge transport in solids. For example, the conduction mechanism in most inorganic semiconductors has been explained using the band model[29] while charge transport and conduction in organic semiconductors have been explained using a hopping or tunneling model.[30] These models will be discussed briefly in the following sections.

2.5.1 Charge Transport via Band Model

The band model assumes that the free carrier mobility is large and the π-electrons are highly delocalized and moves as a plane wave throughout the lattice. Delocalized charge carriers are considered to have a mobility greater than 1 cm^2/Volt-sec. If the electron motion fast such that the lattice vibration is considered stationary, the electron can be thought of as a wave traveling over several lattice sites before being scattered by the

lattice. However, in a real crystal there are always lattice vibrations or phonons that scatter the electron and reduce the carrier mobility. These strong electron-phonon interactions which occurs in organic compounds is not taken into consideration with the band model.

Measurements of the electron mobility in Alq_3 thin films were reported by Hosokawa et al.[31] in which he attributed the electron mobility to the time delay between the application of a step function voltage pulse and the appearance of electroluminescence from a device. He evaluated the mobility to be $(5\pm2)x10^{-5}$ cm^2/Volt-sec, independent of the applied electric field.

More recently, Kepler et al.[32] determined the mobility of electrons and holes in vapor deposited films of Alq_3 using time-of-flight measurements. This involves generating carriers near one electrode with a short pulse of light while observing the current displaced in the external circuit by the motion of the carriers through the sample.[33] From these measurements, the electron and hole mobility were evaluated to be $1.4x10^{-6}$ and $2x10^{-3}$ cm^2/Volt-sec, respectively.

In the case of organic semiconductors such as Alq_3, which possess very small carrier mobilities, the band model would not be applicable in explaining the charge transport phenomena.

2.5.2 Charge Transport via Hopping

Most undoped organic semiconductors are characterized by an extremely low density of thermally generated free charge carriers and a correspondingly low carrier mobility.[34] In such low-mobility solids, hopping conduction may be expected, characterized by incoherent jumps of carriers between isolated molecular sites. [35]

In Alq_3 Burrows et al. proposed that charge transport and conduction occurs via the hopping model, with carriers hopping between LUMO states of adjacent molecules.[36] In this model a carrier can move from one molecule to another by jumping over the potential barrier separating the two states. The exciton is localized on a molecular state $^1M^*$ and exciton migration occurs as a random walk process in which the excitation energy hops between neighboring molecules.

2.5.3 Charge Transport via Tunneling

The tunneling model assumes that an electron in a π-molecular orbital on one molecule can tunnel through a potential barrier to a non-occupied state of a neighboring molecule when initially excited to a higher energy level, such as a singlet state. This occurs with energy conserved in the tunneling process. The electron in the excited state may tunnel to its neighboring molecules or return to the ground state. However, in general, the probability for molecules returning to the ground state is much larger.

1 D.C. Freeman and C.E. White, *J. Am. Chem. Soc.*, **78**, p. 2678 (1956)

2 C.A. Parker, Photoluminescence of solutions,, p. 474 (1968)

3 P.E. Burrows, L.S. Sapochak, D.M. McCarty, S.R. Forrest, and M.E. Thompson., *Appl. Phys. Lett.*, **64**, p. 20, (1994)

4 A. Heller and E. Wasserman, *J. Chem. Phys.*, **42**, p. 949 (1964)

5 H. Samelson, A. Lempicki and C. Brecher, *J. Chem. Phys.*, **40**, p. 2553 (1964)

6 M. Pope and C.E. Swenberg, *Electronic Processes in Organic Crystals,* (Oxford University Press) p. 64 (1982)

7 C. Kittel, *Introduction to Solid State Physics*, 6 ed. (Wiley) p. 296 (1986)

8 C.H. Lee, G.Yu, and A.J. Heeger, *Phys. Rev. B-Cond. Matt.* **47**, p. 15543 (1993)

9 J.L. Bredas, J. Cornil, and A.J. Heeger, *Adv. Mater.*, **8**, No. 5, p. 447 (1996)

10 J.W. Blatchford, S.W. Jessen, L.B. Lin, J.J. Lih, T.L. Gustafson, A.J. Epstein and T.M Swager, *Phys. Rev. Lett.*, **9**, p. 1513 (1996)

11 U. Rauscher, L. Schutz, A. Greiner and H. Bassler, *J. Phys.: Cond. Matt.*, **1**, p. 9751 (1989)

12 R.N. Marks, J.J.M. Halls, D.D.C. Bradley, R.H. Friend and A.B. Holmes, *J. Phys.: Cond. Matt.*, **6**, p. 1379 (1994)

13 K. Pakbaz, Synth. Met., 64, p. 295 (1994)

14 C. Kittel, *Introduction to Solid State Physics*, (John Wiley & Sons, New York), p. 298 (1986)

15 P.E. Burrows and S.R. Forrest, *Appl. Phys. Lett.*, **64**, p. 2285 (1994)

16 Z. Shen, P.E. Burrows, V. Bulovic, D.M. McCarty, M.E. Thompson, and S.R. Forrest, *Jpn. J. Appl. Phys.*, **35**, Part 2, No. 3B, p. L401 (1996)

17 P.E. Burrows and S.R. Forrest, *Appl. Phys. Lett.*, **64**, p. 2285 (1994)

18 T. Tsutsui, *MRS Bulletin*, Vol. 22, p. 40 (1997)

19 C.W. Tang, S.A. VanSlyke and C.H. Chen, *J. Appl. Phys.*, **65**, p. 3610 (1989)

20 D.Z. Garbuzov, V. Bulovic, S.R. Forrest, *Chem. Phys. Lett.*, **249**, p. 433 (1996)

21 I. Sokolik, R. Priestley, A.D. Walser, and R. Dorsinville, *Appl. Phys. Lett.*, **69** p. 4168 (1996)

22 W. Helfrich and F.R. Lipsett, *J. Chem. Phys.*, **43**, p. 4368 (1965)

23 S.A. Rice and J. Jortner, *Physics and Chemistry of Organic Solid State*, Vol. 3, p. 199 (1967)

24 H.C. Wolf and K.W. Benz, *Pure Appl. Chem.*, **27**, p. 439 (1971)

25 N.I. Wakayama, N. Wakayama, and D.F. Williams, *Mol. Cryst. Liq. Cryst.* **26**, p. 275 (1974)

26 C. Hosokawa, H. Tokailin, H. Higashi, and T. Kusumoto, *Appl. Phys. Lett.*, **60**, p. 1220 (1992)

27 P.E. Burrows, L.S. Sapochak, D.M. McCarty, S.R. Forrest and M.E. Thompson, *Appl. Phys. Lett.*, **64**, p. 2718 (1994)

28 M. Pope and C.E. Swenberg, *Electronic Processes in Organic Crystal*, (Oxford University Press, New York, 1982), p. 26

29 R.F. Pierret, *Semiconductor Fundamentals*, Vol. 1 (Addison-Wesley, Massachusetts), p. 23.

30 H. Bassler, G.Schonherr, M.Abkowitz and D.M. Pai, *Phys. Rev. B.*, **24**, p. 3105 (1982)

31 C. Hosokawa, H. Tokailin, H. Higashi and T. Kusumoto, *Appl. Phys. Lett.*, **60**, p. 1220 (1992)

32 R.G. Kepler, P.M. Beeson, S.J. Jacobs, R.A. Anderson, M.B. Sinclair, V.S. Valencia and P.A. Cahill, *Appl. Phys. Lett.*, **66**, p. 3618 (1995)

33 R.G. Kepler, *Phys. Rev.*, **119**, p. 503 (1960)

34 L.B. Schein and D.W. Brown, *Mol. Cryst. Liq. Cryst.*, **87**, p. 1 (1982)

35 T. Holstein, *Ann. Phys.*, **8**, p. 343 (1959)

36 P.E. Burrows, Z.Shen, V. Bulovic, D.M. McCarty, S.R. Forrest, J.A. Cronin and M.E. Thompson, *J.Appl. Phys.*, **79**, p. 7991 (1996)

CHAPTER THREE

3. EXPERIMENTAL TECHNIQUES AND APPARATUS

3.1 Introduction

In this section is a discussion on the main equipment employed in the experiments conducted for this thesis. A description of the laser system, experimental setup, and other equipment used in characterizing Alq_3 will be given. In addition, procedures for the fabrication of Alq_3 thin films will be discussed.

3.2 Laser System

The laser source used in the experiments was a Continuum PY61C-20 actively/passively mode-locked Nd:YAG laser. As shown in Figure 3.1, this laser consists of three main sections: the oscillator which includes components #1-11, the amplifier (#15), and the harmonic generators (#16). In addition to these optical components are the electronic functions necessary for normal laser operation. The oscillator head (#9) consists of a single laser rod (Nd^{3+} doped YAG) which is excited by a Xenon arc flashlamp. When a pump intensity greater than the laser threshold is

reached, decay from the fluorescent level of the laser rod produces spontaneous and stimulated radiation, with the latter producing the laser output beam. By utilizing an Nd:YAG rod as the lasing medium, radiation is emitted at 1.064μm.

The radiation inside the laser cavity consists of a large number of discrete spectral lines spaced by the axial mode interval c/2L, where L is the cavity length. Each mode oscillates independently of the others with randomly distributed phases and the interference of these modes leads to random fluctuations in the light intensity. If the oscillating modes are forced to maintain a fixed phase relationship to each other this will result in a well-defined single pulse circulating within the laser cavity and the laser now becomes mode-locked. Components 1, 3, and 4 of Figure 3.1 all participate in mode-locking the laser.

The oscillator cavity employs both active and passive mode-locking techniques. Combined together, this method of mode-locking produces smooth Gaussian pulses with very little modulation and ultrashort output pulses with temporal duration in the picosecond regime. For perfect mode-locking a single TEM_{00} mode must oscillate within the cavity and this is accomplished by placing a pinhole aperture (#2) about 1mm in diameter within the laser cavity.

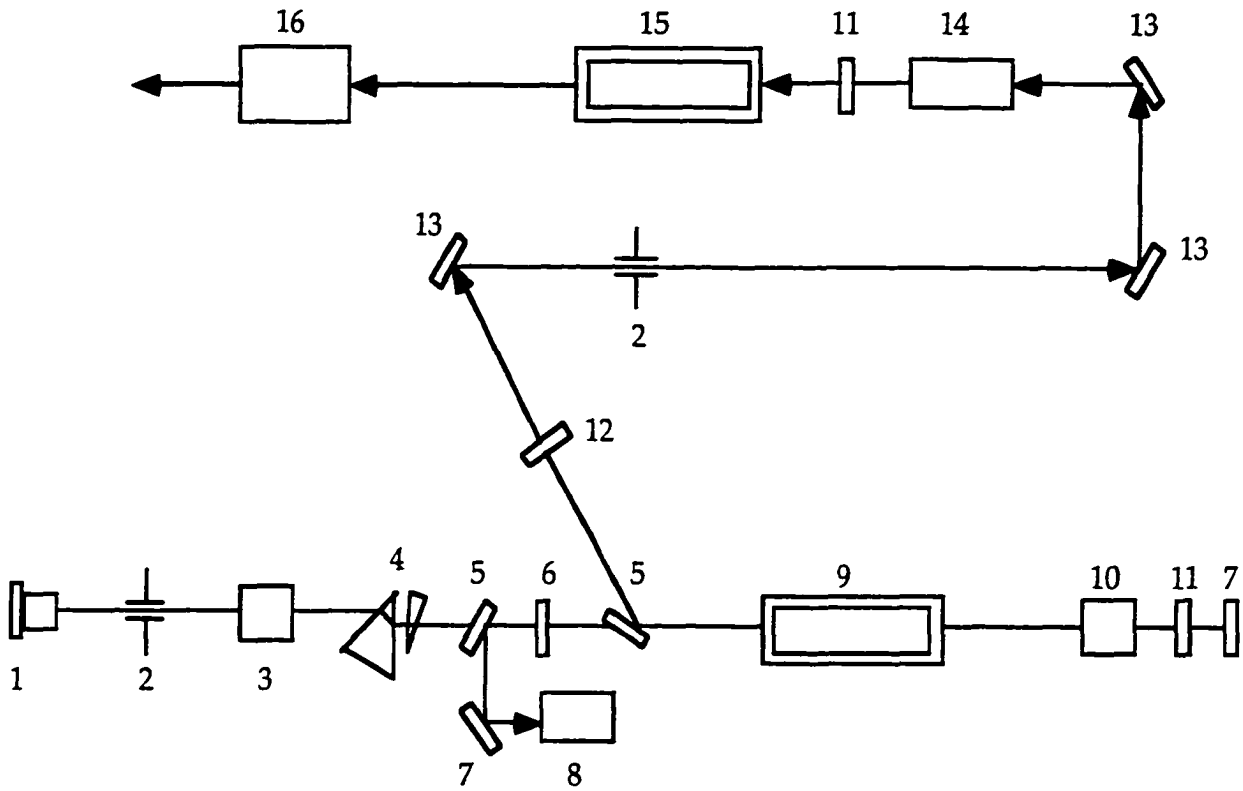

LEGEND

1. Dye Cell w/Mirror
2. Pinhole Aperture
3. Acousto-Optic Modulator
4. Delay Adjustment Prisms
5. Polarizer
6. Half-wave Plate
7. Mirror
8. Photodiode for Cavity Dumper
9. Single Rod/Flashlamp Laser Oscillator
10. Pockels Cell Cavity Dumper
11. Apodizer
12. Lens
13. 45 Degree Turning Mirror
14. Telescope
15. Single Rod/Dual Flashlamp Amplifier
16. Harmonic Generating Crystals

Figure 3.1 Continuum Nd:YAG laser system

Active mode-locking is achieved by inserting into the resonator an acoustooptic (AO) modulator (#3). The AO modulator is electrically modulated at a drive rate equal to the frequency separation of the axial modes, c/2L. This results in the creation of sidebands on each oscillating axial mode with frequencies corresponding to that of adjacent axial modes. Similarly, this occurs to the other axial modes and continues until all axial modes falling under the laser linewidth are coupled together with a well-defined amplitude and phase. Since the AO mode-locker requires an accurate match of the drive rf frequency with the frequency spacing of the cavity modes, synchronization is achieved by adjusting the cavity length with the cavity delay prisms (#4).

In conjunction with coupling of the axial modes, the AO modulator repeatedly reshapes the laser field distribution on each consecutive round trip within the cavity. This is accomplished by providing losses to the light incident on the modulator at a certain time during the modulation cycle. All light will suffer losses except the light that passes through the modulator when the modulator loss is zero. The end result is a buildup of light in narrow pulses at the position of the modulation cycle where losses are minimum.

In this laser system, the action of the active mode-locker is supported by a passive dye mode-locker. Passive mode-locking is achieved by using a dye cell (#1) containing a nonlinear saturable absorber dye, Eastman

Kodak A9740. The dye has an absorption line at the laser wavelength, a linewidth equal to or greater than the laser line width, and a recovery time of about 8psec. The recovery time is important since it restricts the pulse duration. The combination of the dye cell in direct contact with a cavity mirror helps to achieve the most reliable mode-locking operation and obtain the shortest pulses. Furthermore, this configuration helps reduce the number of reflective surfaces in the laser cavity and minimize the possibility of secondary reflections.

In passive mode-locking the laser radiation travels through the saturable absorber and encounters the nonlinear absorption properties of the dye. The dye absorption characteristics are such that for low intensity radiation, the absorption is constant. However, as the intensity increases and exceeds a certain value, the absorption decreases. Therefore, the most intense fluctuations bleach the dye and grow quickly in intensity while the smaller fluctuations are absorbed. Over time, this technique results in a smoothening of the laser amplitude fluctuations. Moreover, consecutive passages of the high-intensity radiation pulse through the oscillator results in a pulse train at the laser output with a Gaussian beam profile and very little modulation.

In addition to the mode-locking techniques used, this oscillator utilizes cavity dumping as an efficient technique for increasing the single pulse energy by selecting a pulse from the laser pulse train. Cavity

dumping is achieved via an electro-optic Pockels cell (#10) which is driven by a Marx board and triggered by a photodiode (#8). The photodiode senses the intensity buildup inside the cavity and applies a voltage pulse across the Pockels cell when a predetermined intensity level is reached. The electro-optic effect of the Pockels cell rotates one of the initially p-polarized pulses within the pulse train to an s-polarized pulse. The s-polarized pulse is then ejected from the oscillator via a polarizer (#5). This pulse is directed into a single rod/dual flashlamp head amplifier (#15) where the pulse energy is amplified to 75mJ. Lastly, the laser pulse, with a duration of 25psec, is sent into the harmonic generating crystals (#16) where wavelength conversion takes place.

3.3 Experimental Setup

The main experimental setup used for the experiments in this thesis is shown schematically in Figure 3.2.

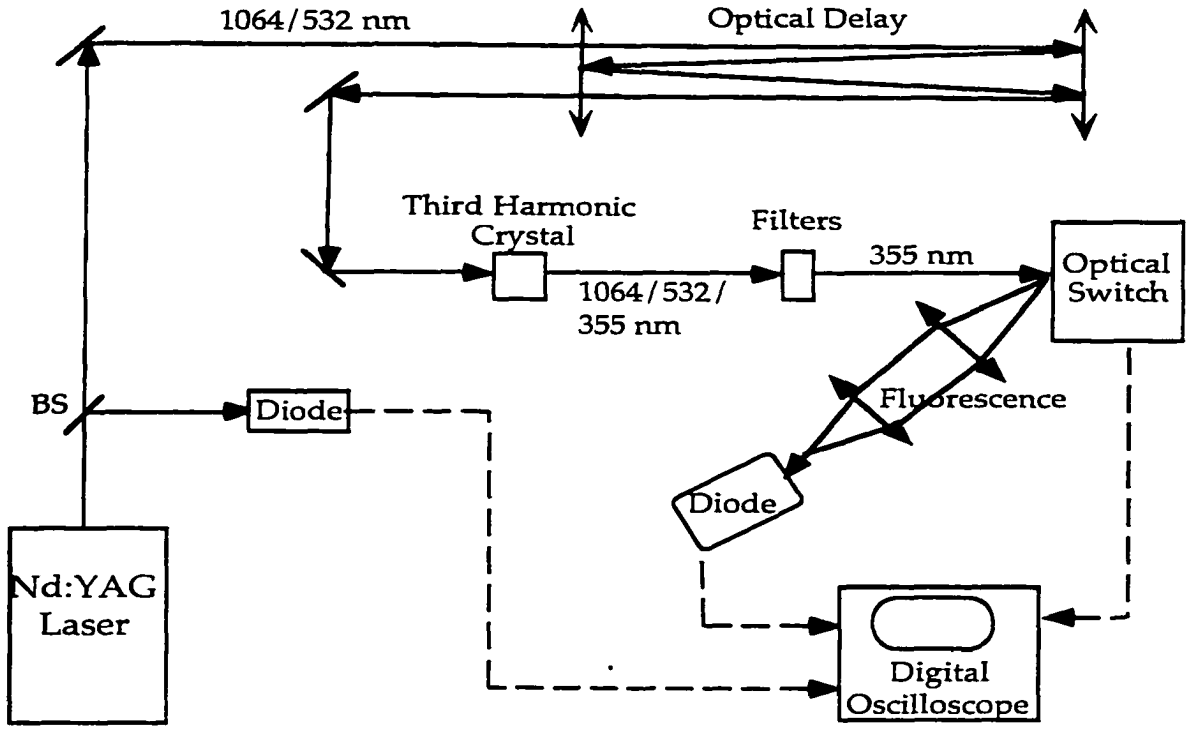

Figure 3.2 Schematic of experimental set-up

As previously discussed, a Continuum Model PY61-C active-passive mode-locked Nd:YAG oscillator is used to provide 1064 nm pulses at 20Hz with a pulse duration of 25 psec. About 35 mJ at 532 nm is generated after passing the amplified pulse through a type II second harmonic generating Potassium Dideuterium Phosphate (KD*P) crystal. The combined laser output of 1064 nm and 532 nm then passes through a beam

splitter (BS) where the reflected portion of the laser energy is directed onto a photodiode (PD) that externally triggers the signal processing unit. The transmitted portion of the beam is sent into an optical delay line where it is delayed with respect to the triggering optical pulse by making several round trips through a white-cell. This delay is necessary to compensate for the trigger lag time inherent in electronic devices such as the signal processing unit. The transmitted beam then passes through another type II KD*P crystal for third harmonic generation and produces the desirable wavelength for photoexcitation of our samples: 355 nm pulses with an average energy of 15 mJ. Narrow-band filters are used to block both the 1064 and 532 nm light and the 355 nm pulses are focused onto an optical switch.

A schematic of the optical switch, known as an Auston switch,[1] is shown in Figure 3.3. Using an Auston switch as the substrate for our luminescent samples allows us to simultaneously observe the photoluminescence and photoconductivity response of the material. The switch is made from a copper base block with a copper cladding dielectric substrate epoxied to the base. As shown by the top view in Fig. 3.3, the switch is fabricated in a planar configuration in which two copper microstrip transmission lines are etched out of the substrate using copper etchant. A gap of dimension 'L' is formed between the two microstrip

lines and serves as the active region of the switch upon which the sample is deposited.

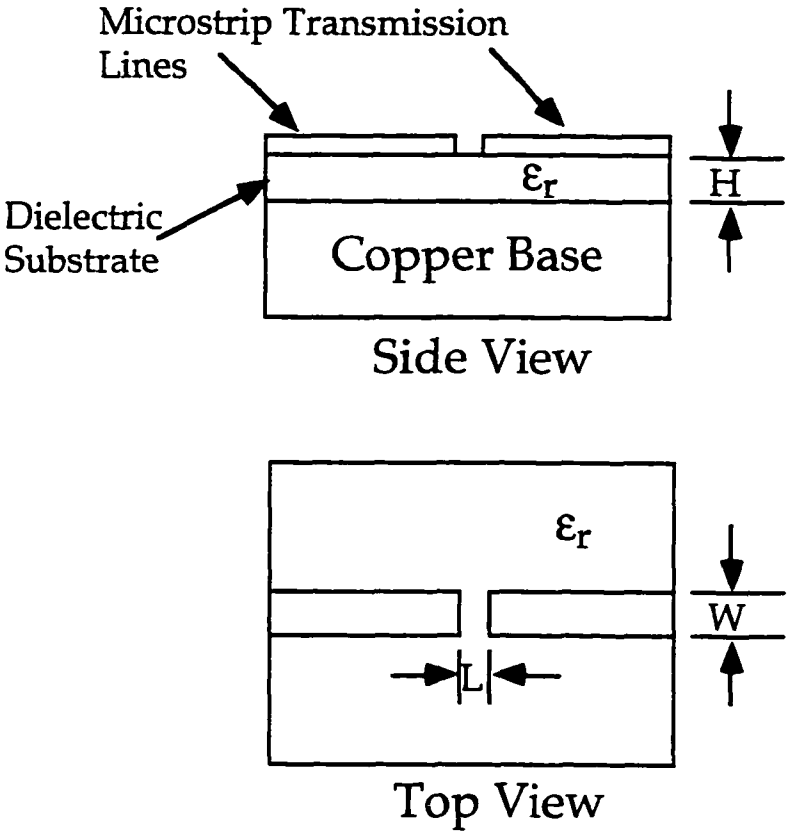

Figure 3.3 Schematic of Auston switch in planar configuration

The transmission line dimensions are made such that the characteristic impedance of the line, Z_0, is 50Ω. This corresponds to the impedance of the plug-in units on our oscilloscope. The relative dielectric constant of the substrate, ε_r, the thickness of the substrate, H, and the width

of the copper microstrip lines, W, are the parameters which determine the microstip line impedance.[2,3,4,5] The W:H ratio is given by the following:

For A>1.52

$$\frac{W}{H}=\frac{8*\exp(A)}{\exp(2A)-2},$$

and for A < 1.52

$$\frac{W}{H}=\frac{2}{\pi}\left\{B-1-\ln(2B-1)+\frac{\varepsilon_r-1}{\varepsilon_r+1}\left(\ln(B-1)+0.39-\frac{0.61}{\varepsilon_r}\right)\right\}$$

where

$$A=\frac{Z_o}{60}\left(\frac{\varepsilon_r+1}{2}\right)^{1/2}+\frac{\varepsilon_r-1}{\varepsilon_r+1}\left(0.23+\frac{0.11}{\varepsilon_r}\right)$$

and

$$B=\frac{60\pi^2}{Z_0\sqrt{\varepsilon_r}}.$$

The dielectric substrate used in our Auston switch had a relative dielectric constant of 2.55 and a thickness, H, of 30 mils. Using the above equations we obtained a transmission line width of W= 2.26mm for a characteristic impedance of 50Ω.

Electrical contact to the switch is made by using Omni-Spectra OSM coaxial-to-microstrip connects. These stripline launchers are placed on both sides of the Auston switch. For photoconductivity measurements, one side is biased with a 250 Volt power supply and the other side is the output PC response. The output signal is first sent into a ComLinear 20db amplifier and then directly into a dual channel Tektronix CSA-803 digital sampling oscilloscope using SMA wide-bandwidth cables.

In reference to figure 3.2, the sample fluorescence is collected by using two 15 cm focal length lens and then focusing the fluorescence onto a silicon PIN photodiode. The photodiode has a time resolution of approximately 500psec. The output from the photodiode is also sent into the digital sampling oscilloscope where both the PC & PL responses are averaged, plot, and stored. Individual scans can then be transferred from the sampling scope to the computer through a custom modified LabView[6] instrument driver.

For spectral measurements, the photoluminescence and PL excitation spectra was collected using a Perkin-Elmer LS-50B spectrofluorometer. Absorption spectra was measured on a Perkin-Elmer Lambda 9 UV-Vis spectrophotometer. In conducting temperature measurements the optical switch was placed inside a Janis Research VPF-100 liquid nitrogen Dewar. This provided adjustable temperatures ranging from 300K to 77K. To

measure the optical pulse energies, we used a LaserProbe RM-3700 Universal Radiometer.

3.4 Sample Fabrication

The Alq_3 material used for the experiments was synthesized at the Eastman Kodak Co. and purified by the train sublimation technique. A thin film was deposited onto the 0.5 mm active region of the Auston switch by thermal evaporation techniques. Figure 3.4 shows a schematic of the thermal evaporation process used for deposition.

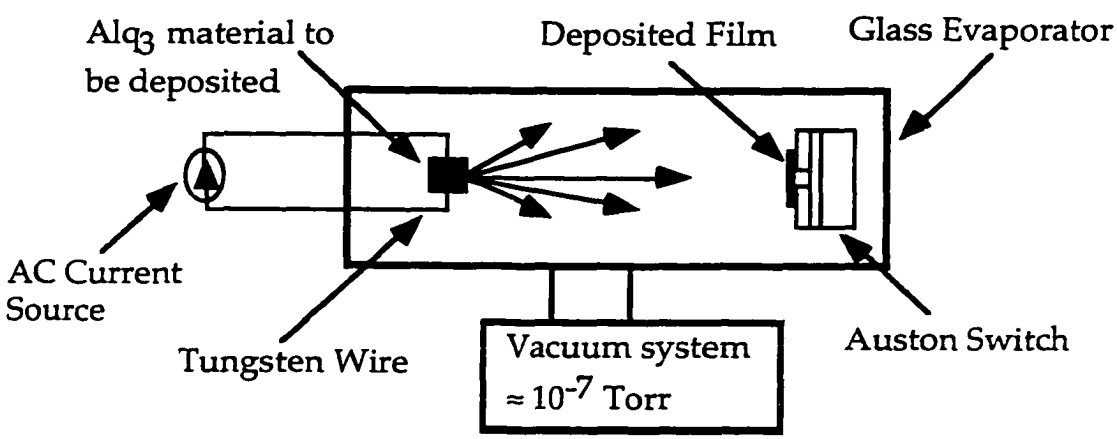

Figure 3.4 Alq_3 film deposition by thermal evaporation

First the Auston switch is mounted into a custom-made glass evaporator which is assembled under a nitrogen atmosphere inside a glove box. Alq_3 in powder form is placed in a quartz crucible at the other end of

the evaporator and the unit is then transported to the vacuum system where thermal evaporation takes place.

The vacuum system consists of a mechanical roughing pump, a diffusion pump, valves, vacuum gauges, and other instrumentation. In the operation of the vacuum system, first the roughing valve is opened and this allows the mechanical pump to lower the evaporator pressure to an vacuum level of approximately 10^{-2} - 10^{-3} Torr. Once this level is reached, the roughing valve is closed and the foreline and diffusion pump valves are opened. The roughing pump maintains a vacuum on the output of the diffusion pump. A liquid nitrogen cold trap is used with the diffusion pump to achieve an ultimate pressure in the vacuum chamber of 10^{-7} Torr. Both ion and thermocouple gauges are used to monitor the pressure at various points in the vacuum system. Other valves are used as vents to return the vacuum system to atmospheric pressure once evaporation is completed.

Evaporation of Alq_3 is accomplished by gradually increasing the temperature of the tungsten wire wrapped around the quartz crucible. This in turn heats the Alq_3 to the point of vaporization. The temperature of the wire is regulated with a high AC current source and we typically use a AC current of 9 amps. This corresponds to an evaporation rate of 3-5 Å/sec when performed in a vacuum of about $3x10^{-7}$ Torr. The result is an evenly

deposited film of Alq_3 about 2-3 μm thick, as measured using a Tencor Instruments Alpha Step 1000 stylus profilometer.

After deposition, the sample remains under a high vacuum and is transported in the sealed evaporator back to the glove box. Here it is stored under nitrogen or argon gas until the experiment. When conducting experiments, the optical switch is transferred to the sample site under nitrogen atmosphere. Such precautions are taken as to prevent any oxidation of the sample. Measurements are then conducted under an inert gas.

1 D.H. Auston, *IEEE J. Quant. Elec.*, **3**, p. 636 (1983)

2 H.A. Wheller, *IEEE Trans. Microwave Theory Tech.*, **13**, p. 172 (1965)

3 H.A. Wheller, *IEEE Trans. Microwave Theory Tech.*, **25**, p. 631 (1977)

4 E.O. Hammerstad, *Proc. European Microwave Conf.*, p. 268 (1975)

5 S. Etemad, A. Pron, A.J. Heeger,, A.G. MacDiarmid, E.J. Mele, and M.J. Rice, *Phys. Rev. B.*, **23**, p. 5137 (1981)

6 LabView is a registered trademark of the National Instruments Corporation.

CHAPTER FOUR

4. BIMOLECULAR REACTIONS OF SINGLET EXCITONS IN TRIS(8-HYDROXYQUINOLINE) ALUMINUM (ALQ_3)

4.1 Introduction

Alq_3 serves as the emitting layer for organic light emitting diodes with light emission originating from the radiative decay of singlet excitons. Prior to their decay, diffusion allows the excitons to interact with impurities and defects in the emitting material or in other adjoining layers. If the first excited singlet state of the impurity or defect lie below that of the exciton, exciton quenching can occurdue to energy transfer. In this same manner, mobile Alq_3 excitons can interact with other excitons via diffusion resulting in exciton-exciton annihilation, non-radiative decay, and a reduction in the PL efficiency or EL quantum yield.

In this chapter we address the issue of exciton-exciton interactions. We investigate how the concentration of singlet excitons affects both the peak PL, fluorescence lifetime, and PL quantum yield. From these observations we speculate on what impact this reaction will have on Alq_3 based OLED's and other potential EL devices such as organic lasaers.

The investigation of exciton interactions in organic solids is an issue that has been widely studied in the past.[1,2,3] Previous work has demonstrated that exciton interactions can affect both the emissive and absorptive spectral properties of organic crystals.[4] In tetracene crystals observations were made showing the effects of exciton interactions on the fluorescence quantum yields and radiative lifetimes.[5,6] The low absolute quantum efficiency observed in crystalline tetracene resulted from singlet exciton fission, where the singlet exciton decayed into two triplet excitons. By analyzing the time dependence of the tetracene fluorescence with respect to excitation intensity, they observed a delayed fluorescence at high excitation intensities. This was attributed to triplet exciton annihilation with the triplet excitons being formed by the random recombination of charge carriers produced by singlet exciton annihilation and autoionization. These results demonstrated the affects of bimolecular exciton annihilation on the fluorescence decay.

In anthracene crystals, work by Braun[7] demonstrated that under high intensity conditions, exciton-exciton interactions dominates the singlet exciton concentration, $[S_1]$. In this case $[S_1]$ no longer increases linearly with the input optical flux, but increases proportionally to the square root. This decrease in singlet exciton concentration is revealed in the reduced fluorescence quantum efficiency observed at high excitation levels. In

these organic crystals it is observed that exciton-exciton interaction and annihilation becomes a dominating nonradiative decay channel.

With bimolecular interactions proven to influence the efficiency of other fluorescent materials such as anthracene and tetracene, it is possible for this to occur in Alq_3 due to the similarity in chemical structures as shown in Figure 4.1. Therefore, we have chosen to closely examine the affects of exciton-exciton interactions on the behavior of singlet excited states in Alq_3 and its effect on electroluminescent devices.

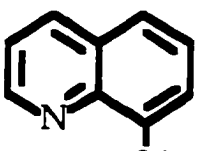

8-hydroxyquinoline

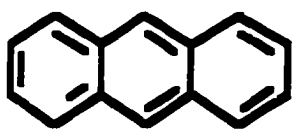

Anthracene

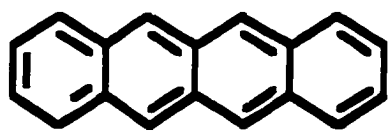

Tetracene

Figure 4.1 Chemical Structure of 8-hydroxyquinoline, anthracene, and tetracene.

In the experiments conducted we have shown that at high singlet exciton concentrations, the mutual annihilation of these excitons becomes a dominating non-radiative decay channel which leads to a significant decrease in the peak photoluminescence. We have also demonstrated that for high excitation intensities, bimolecular decay via exciton-exciton annihilation dominates the temporal response of singlet excited states. This

results in a decrease in the singlet excited state lifetime and a reduction in the luminescence quantum efficiency. We have calculated the bimolecular recombination rate constant due to these interactions. From this value we are able to determine the diffusion constant and diffusion length for singlet excitons since these parameters are crucial in the design of electroluminescent devices.

Furthermore, we have observed how the mutual annihilation of singlet excitons leads to the generation of the photoconductivity (PC) response of Alq_3. We attribute the PC to the dissociation of vibronically excited singlet excitons via bimolecular interactions and the subsequent creation of charge carriers. As discussed in chapter 2, Alq_3 has a large exciton binding energy (3.1eV) as compared with inorganic semiconductor materials (4-15meV). Therefore, the quantum yield for the generation of charge carriers in Alq_3, which is in the range of 10^{-7}-10^{-3}, would be lower than that of inorganic semiconductor materials.[8] Such low quantum yield values indicates that charge carrier generation originates from excitons via some secondary process, such as exciton dissociation.

Northrop and Simpson[9] proposed that exciton-exciton interactions can result in the production of free charge carriers through internal ionization. Evidence of this and other mechanisms for charge carrier generation were observed via photoconductivity measurements. Investigations demonstrated that the slope of the peak photocurrent versus

intensity depends on the various methods of charge carrier generation.[10,11] For example, in organic systems where charge carriers are generated through exciton-exciton interactions or exciton-surface interactions[12,13] the slope can vary between 0.5 and 3.0 depending on the excitation intensity and wavelength used.[14,15,16] In the case of direct carrier band to band generation as in many semiconductors, the slope is generally 1.0.[17]

In our experiments we have simultaneously measured the transient PL response in Alq_3 while observing the PC response. The simultaneous observation of these channels will assist us in determining the dynamics of singlet excitons which participate in the PL and those which results in the photogeneration of charge carriers. By using PC as an observation channel for the non-radiative decay of singlet excited states we have shown that at high excitation intensities, exciton-exciton annihilation is the mechanism responsible for the production of charge carriers.

4.2 Experimental

The experimental setup used to perform measurements presented in this section was discussed in Chapter 3. An abridged diagram of the experimental setup is shown in Figure 4.2.

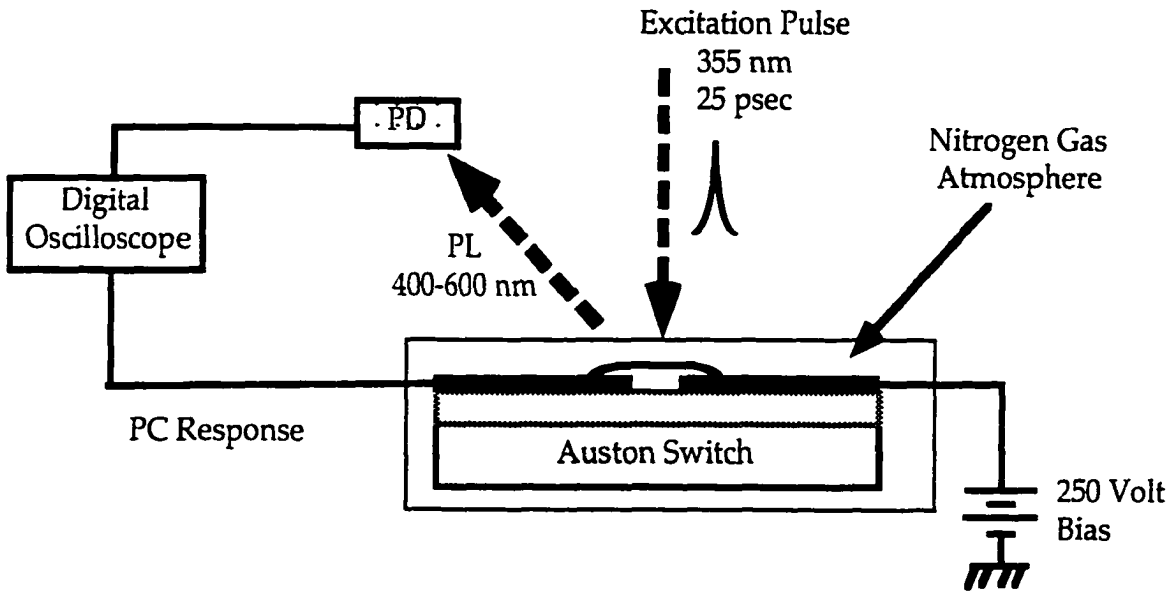

Figure 4.2 Diagram of set-up used to measure the transient PL & PC response in Alq_3 thin films.

We conducted both transient photoluminescence and photoconductivity measurements on pristine thin films (1-2μm) of Alq_3. All measurements were performed at room temperature while the sample cell was purged with nitrogen gas to prevent the occurrence of photooxidation. The excitation intensities for our measurements ranged between $3x10^{13}$ - $6x10^{15}$ photons/cm^2 per pulse. These fluence levels were

sufficient for observing exciton-exciton annihilation without causing any damage to the sample.

4.3 Results and Discussion

The results presented in this section are broken up into different sub-sections. First we discuss our experimental results of the exciton-exciton interactions and its affect on the peak PL and the PL excited state lifetime in Alq_3. Next, we use two different methods to determine the bimolecular recombination rate constant, γ_{ss}. The first method involves modeling the kinetic equation describing the concentration of singlet excitons with our experimental data. From this model we can extract γ_{ss}. The second method involves modeling an expression for the PL quantum efficiency as a function of excitation intensity with PL efficiency calculations made from our experimental data. Using this additional method we again extract γ_{ss} as confirmation of the value obtained previously. From the value obtained for the bimolecular recombination rate constant we determine singlet exciton diffusion parameters such as the diffusion coefficient and the diffusion length, and discuss their significance to OLED's. Finally we discuss the byproduct observed in Alq_3 due to these exciton-exciton interactions, mainly the photoconductive response.

4.3.1 Exciton-Exciton Interactions

Exciton-exciton annihilation occurs when a high concentration of singlet excitons are generated in close proximity of each other. Such a large density can be created by photoexcitation at high intensities. In this process, two singlet excitons approach each other and their interaction causes one exciton to return to the ground state while the other is raised to a higher excited state. The additional energy needed to excite the exciton to a higher state is gained from the annihilated exciton. Equation 4.1 summarizes this reaction as:

$$S_1 + S_1 \longrightarrow S_n^* + S_0 \qquad \text{Equation 4.1}$$

where S_1 represents an exciton in the first excited state and S_n^* is the vibronically excited singlet state ($n \geq 1$). From S_n^* the molecule can deactivate internally to S_1 and decay back to the ground state with the emission of light, as shown in equation 4.2 or ionization of the vibronically excited state can occur producing charged carriers, equation 4.3. These transition processes will be discussed in more detail in upcoming sub-sections.

$$S_n^* \longrightarrow S_1 \longrightarrow S_0 + h\nu, \qquad \text{Equation 4.2}$$

$$S_n^* \longrightarrow e + h, \qquad \text{Equation 4.3}$$

4.3.2 Exciton-Exciton Interactions on Photoluminescence in Alq_3

To understand the affects of exciton-exciton interactions in Alq_3 we have examined the fluence dependence on the peak PL and the PL decay dynamics. Observation of a peak PL transition from a linear dependence on intensity ($I^{1.0}$) to a square-root dependence ($I^{0.5}$) is typical of a bimolecular process. The PL transition can be explained by using the following kinetic equation describing the concentration of singlet molecular excitons $[S_1]$:[18,19]

$$d[S_1]/dt = \alpha I(t) - k[S_1] - f\gamma_{ss}[S_1]^2 \qquad \text{Equation 4.4}$$

where α is the absorption coefficient for Alq_3 thin film, I is the excitation intensity, k is the sum of the radiative and nonradiative transition rates for monomolecular decay of singlet excitons, γ_{ss} is the rate constant for bimolecular recombination, and f is a parameter that takes into account losses due to autoionization and direct nonradiative relaxation to the ground state (S_0) from states above the singlet exciton state.[20,21]

For low excitation intensities the unimolecular decay term, $k[S_1]$, of equation 4.4 becomes dominant and causes the singlet exciton concentration and photoluminescence to have a linear dependence on the excitation intensity.

$$PL \sim [S_1] \sim I^{1.0} \qquad \text{Equation 4.5}$$

On the other hand, high excitation intensities causes the bimolecular singlet exciton-exciton annihilation term, $f\gamma_{ss}[S_1]^2$, to dominate and equation 4.4 predicts a square root intensity dependence of the singlet exciton concentration and photoluminescence.

$$PL \sim [S_1] \sim I^{0.5} \qquad \text{Equation 4.6}$$

Using this model, we measured the PL from Alq_3 thin films as a function of excitation intensity. Our results illustrated in Figure 4.3 demonstrate the occurrence of a PL transition from a linear dependence to a square root dependence on excitation intensity. The onset of this transition occurs at an excitation intensity of $3x10^{14}$ photons/cm^2. Therefore, we presume that for excitation intensities less than $3x10^{14}$ photons/cm^2, bimolecular processes in Alq_3 thin film can be neglected. With the absorption coefficient of Alq_3 = $4.14x10^4$ cm^{-1},[22] this transition threshold corresponds to a singlet exciton concentration of $1.2x10^{19}$ cm^{-3} where we have assumed that each absorbed photon creates a singlet exciton.

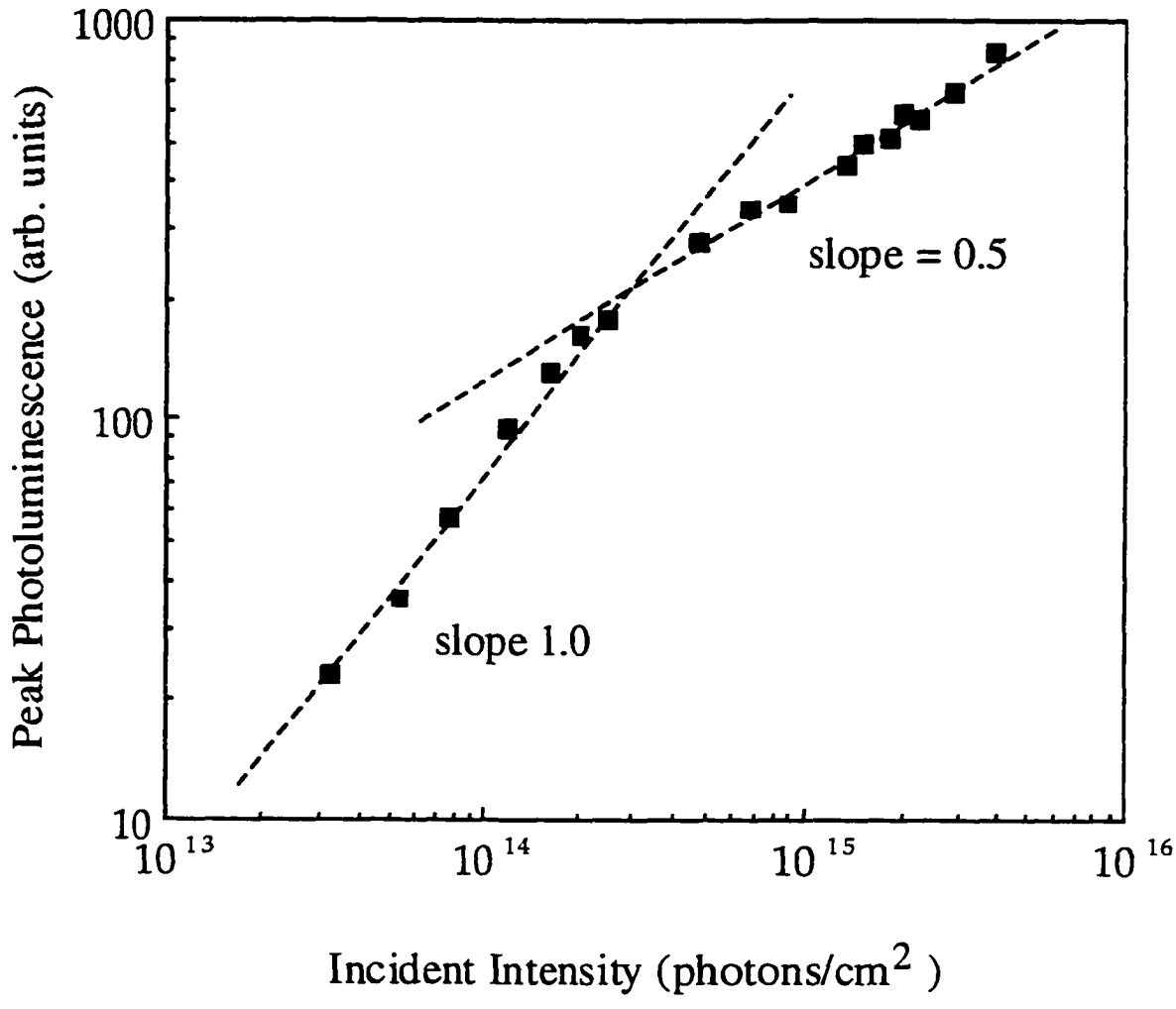

Figure 4.3 Incident intensity dependence of the peak PL in Alq_3 thin film.

Figure 4.4 shows the fluorescence decay on Alq_3 pristine thin films measured at low ($4x10^{13}$ photons/cm^2) and high ($2x10^{15}$ photons/cm^2) excitation intensity, upper and lower curves respectively. For low excitation the PL decays exponentially with a lifetime of 12-16 nsec, consistent with reported values.[23] A similar single exponential decay was observed for the PL of a diluted solution of Alq_3 in methanol and chloroform. When the excitation intensity is increased, the thin film PL decay became nonexponential. In photoluminescence measurements a non-exponential PL decay is another key signature of bimolecular singlet exciton annihilation.[20]

Previously in equation 2.3, we defined the "true" singlet excited state lifetime (equation 4.7).

$$\tau = (k_r + k_{nr} + k_{is})^{-1} \qquad \text{Equation 4.7}$$

It is considered "true" since it only involves the decay of an excited state in a single molecule and free carrier, trapping or bimolecular interactions are all neglected. However, if bimolecular interactions occur then an additional channel for the excited state decay evolves. This is the case under high excitation where the relationship between the observed fluorescence response and the rate parameters is now given as:

$$\tau = (k_r + k_{nr} + k_{is} + \gamma_{ss}[S_1])^{-1} \qquad \text{Equation 4.8}$$

where k_r, k_{nr}, and k_{is} have been previously defined and the additional term $\gamma_{ss}[S_1]$ is due to the bimolecular interaction. The excited state lifetime will shorten because of the added decay term.

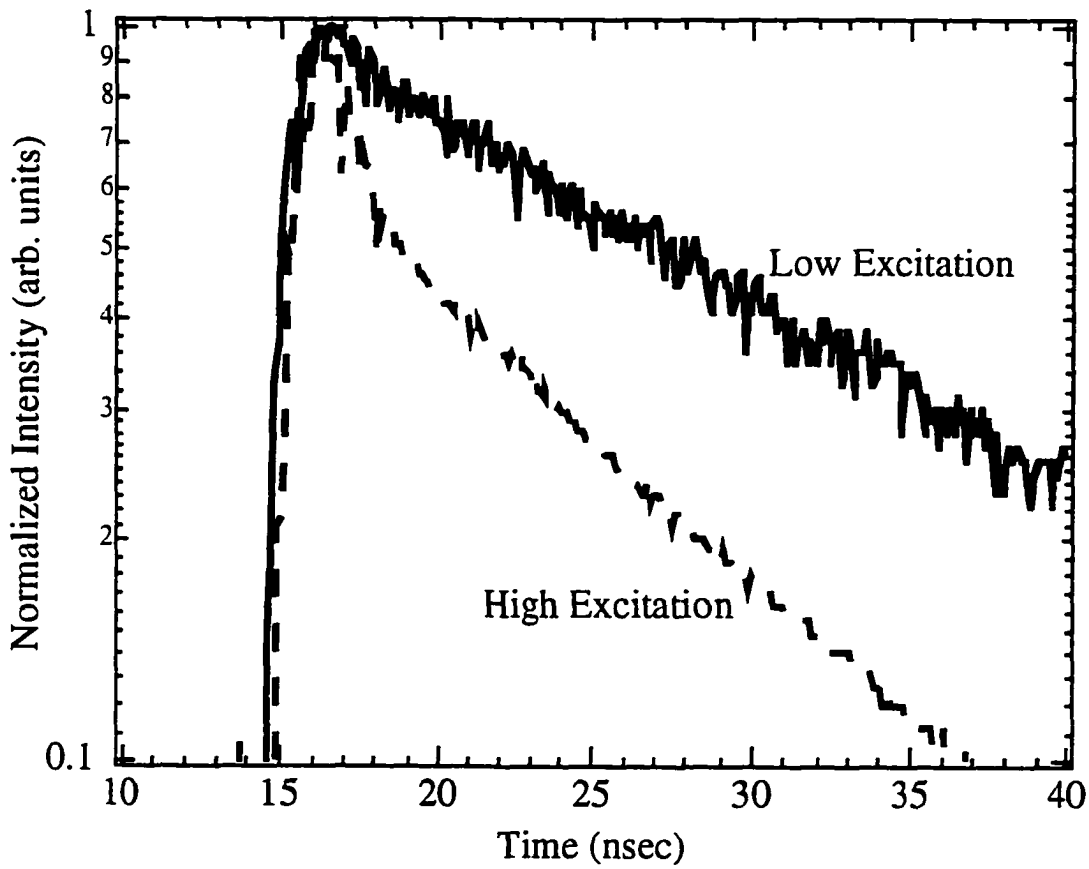

Figure 4.4 Fluorescence decay of Alq_3 thin films.
Broken and solid lines denote high & low intensity,respectively.

4.3.3 Calculations of Bimolecular Recombination Rate Constant

We have used two different methods for determining the bimolecular recombination rate constant in Alq_3. In the first method we have modeled the singlet exciton rate equation 4.4 with our experimental PL decay curve for high excitation. An example of such a fit is presented in figure 4.5 (solid lines). From this fit we extracted a value for $\gamma_{ss} = (2\pm1)x10^{-11}$ cm^3 sec^{-1}. Modeling the rate equation with our experimental PL decay curve for low excitation resulted in $\gamma_{ss} = 0$ cm^3 sec^{-1}. This validated our assumption that bimolecular recombination can be neglected at low excitation.

The second method used to confirm the value of γ_{ss} involved calculating the PL quantum yield, ϕ_{PL}, over a range of excitation intensities. For the monomolecular decay of singlet excitons, the PL quantum yield is defined as the ratio between the radiative transition rate constant, k_r, and the sum of all transition rate constants (ie: $k_r+k_{nr}+k_{is}$):

$$\phi_{PL} = k_r/(k_r + k_{nr} + k_{is}) \qquad \text{Equation 4.9}$$

However, at high excitation intensities where exciton-exciton interactions occur, the bimolecular decay term of equation 4.4, $f\gamma_{ss}[S_1]$ becomes another decay channel for singlet excitons. The PL quantum yield is now defined as:

$$\phi_{PL} = k_r/(k_r + k_{nr} + k_{is} + \gamma_{ss}[S_1]) \qquad \text{Equation 4.10.}$$

where the additional bimolecular decay term results in a decrease in ϕ_{PL}.

We have shown that as the excitation intensity is increased and exciton-exciton interactions begins to occur, a reduction in the fluorescence quantum yield will be observed. We calculated the PL quantum yield at various excitation intensities and using equation 4.11 which describes the PL quantum efficiency as a function of excitation intensity, $\phi(I)$, [24] we determined the bimolecular recombination rate constant, γ_{ss}.

$$\phi(I) = \frac{2k\phi_o}{\Gamma I} \int_0^{\frac{\Gamma I}{2k}} \frac{\ln(1+z)}{z} dz \qquad \text{Equation 4.11}$$

where ϕ_0 is the PL quantum efficiency at low intensities (8%), k is the sum of the radiative and nonradiative rate constants, $\Gamma=\alpha\gamma_{ss}$,, I is the incident intensity (photons/cm^2) and z is the variable of integration.

Figure 4.6 shows the theoretical fit of equation 4.11 to our experimental data where the relative quantum efficiency is defined as $\phi(I)/\phi_0$. From this fit we obtained a value of γ_{ss} = (5.0±0.5)x10^{-11} cm^3 sec^{-1}. Based on the two methods just demonstrated, we have found the value of the bimolecular recombination rate constant in Alq_3 to be between 1.0x10^{-11} and 5.5x10^{-11} cm^3 sec^{-1}.

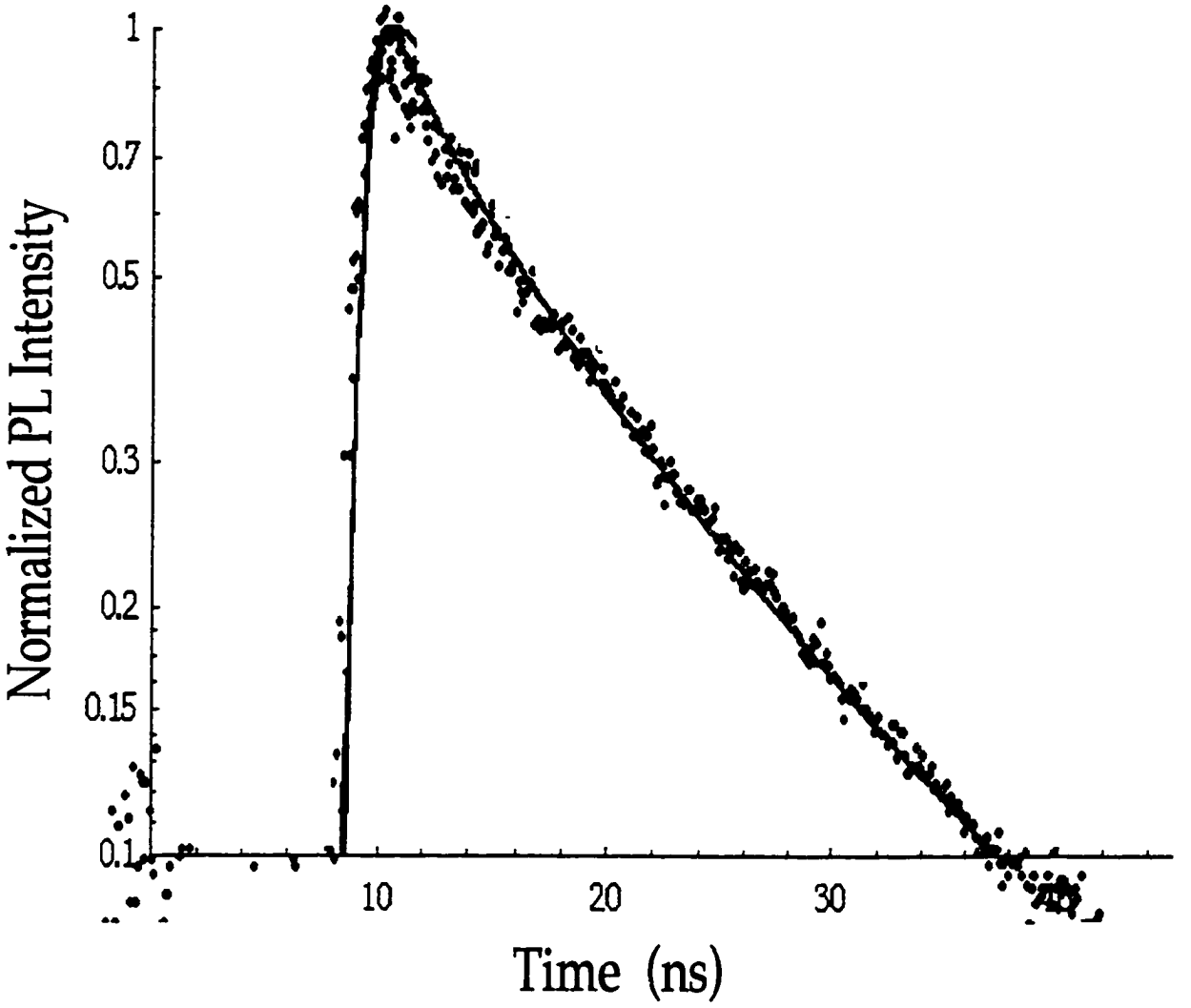

Figure 4.5 Theoretical fit of Alq_3 thin film decay.

PL decay curves of Alq_3 thin film measured for high excitation intensities ($9x10^{14}$ photons/cm^2). Solid lines through the experimental points were theoretically calculated.

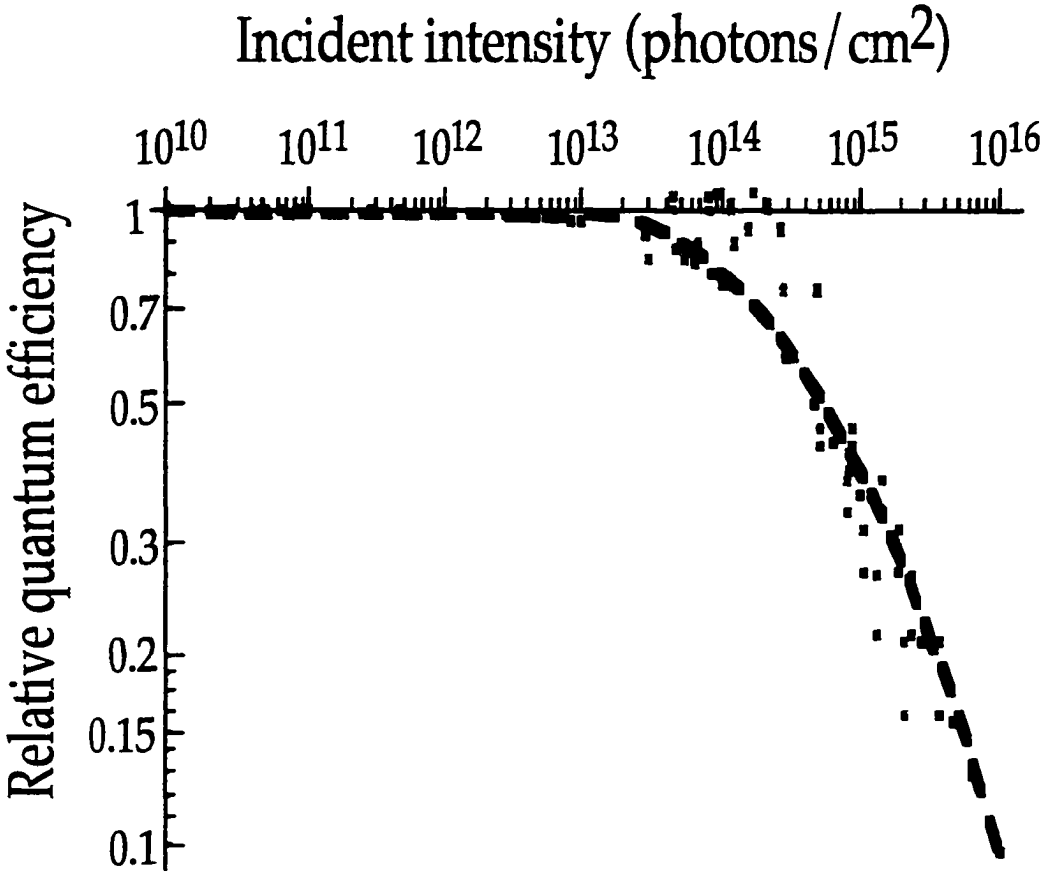

Figure 4.6 Dependence of relative fluorescence quantum efficiency on excitation intensity.

Dots represent experimental points. Broken line represents the calculated fit to equation 4.10 using $\gamma_{-} = 5x10^{-11}$ cm^3 sec^{-1}.

4.3.4 Singlet Exciton Diffusion Coefficient and Diffusion Length

In OLED's understanding the exciton diffusion parameters are important for efficient device operation since they govern the EL emission zone. These parameters are the exciton diffusion coefficient and the exciton diffusion length. After the singlet excitons are formed within the emitting layer they may diffuse towards the emitter/electrode or emitter/transport layer interface where traps are abundant. Impurity sites within the emitting layer can also act as trapping sites for these excitons. This may lead to exciton quenching and a reduction in the EL quantum efficiency.

Using the values calculated for the bimolecular recombination rate constant, one can estimate the value of the diffusion coefficient of singlet excitons, D_s, from the equation: [25]

$$\gamma_{ss} = 8\pi D_s R + 8\pi R^2 (D_s k)^{1/2} \qquad \text{Equation 4.12}$$

where k is the sum of radiative and nonradiative decay rate constants and R is the spherical reaction radius which defines the distance between the two excitons at which interactions can occur. Typically, energy transfer in exciton-exciton interactions results from electron interactions which takes place over distances $\approx$ 6-15Å.[26] Therefore, taking R = 10Å, we obtained values for D_s within the range $(1.2 \pm 0.8)\times10^{-5}$ cm^2 sec^{-1}. This estimate is

about one order of magnitude smaller than the value obtained by Tang et al for Alq_3.

Tang et al.[27] were able to evaluate the singlet exciton diffusion coefficient and diffusion length by placing a doped EL sensing layer at different locations within the Alq_3 emitting layer and measuring the overall EL emission spectra of the LED. For different locations of the sensing layer within the Alq_3 emitting layer, they made simulations of the EL spectra. Comparing the simulations with the actual EL spectra resulted in a diffusion length of 200Å from which they calculated the exciton diffusion coefficient, D_s, to be 7.6×10^{-4} cm^2 sec^{-1}.

The difference between singlet exciton diffusion coefficient values can be attributed to the fact that the latter value for D_s was estimated from EL measurements where the singlet lifetime, τ_s, can be affected by different factors such as high electric fields, quenching by charge carriers, and electrodes. This could significantly differ from τ_s in thicker films and solutions. Therefore the D_s value estimated from EL measurements may tend to be less accurate than the value calculated from PL measurements. In addition, since Alq_3 films have a microcrystalline structure,[2] it is natural to expect the diffusion coefficient in these films to be smaller than in single molecular crystals where D_s lies in the range of 10^{-4}-10^{-2} cm^2 sec^{-1}.[28]

Knowing the singlet exciton diffusion coefficient allowed us to then calculate the singlet exciton diffusion length, L. This is a measure of the

average distance an exciton moves from its initial point during its lifetime. The diffusion length is related to the diffusion coefficient through the exciton lifetime, τ. This relationship depends on whether the diffusion is restricted to one, two, or three dimensions. For exciton motion characterized by an isotropic diffusion coefficient, the general relationship is:

$$L \approx (Z\tau D_s)^{1/2}, \qquad \text{Equation 4.13}$$

where Z is equal to 2, 4, or 6 for a one, two, or three-dimensional diffusion, respectively.[29] Assuming that the exciton diffusion is three-dimensional in isotropic Alq_3 films, we obtained a diffusion length of 98±40Å.

4.3.5 By-Product of Exciton-Exciton Interactions

As previously mentioned, the interaction of two excitons leads to a higher vibronic excited state, S_n^*, and from this state ionization can occur as shown in Equation 4.14:

$$S_n^* \rightarrow e^- + h^+ \qquad \text{Equation 4.14}$$

Therefore, the photogeneration of charge carriers and the observed PC response is a byproduct of exciton-exciton interactions. The PC is proportional to the square of the singlet exciton concentration:

$$PC \sim [S_1]^2 \qquad \text{Equation 4.15}$$

We have previously shown in equation 4.6 that at high excitation intensities the singlet exciton concentration has a square root intensity dependence, $[S_1] \sim I^{0.5}$. This leads to a linear relationship between the peak PC and the incident optical flux,

$$PC \sim I^{1.0} \qquad \text{Equation 4.16}$$

As illustrated in Fig. 4.7 we observe a linear intensity dependence of the measured PC with input intensity.

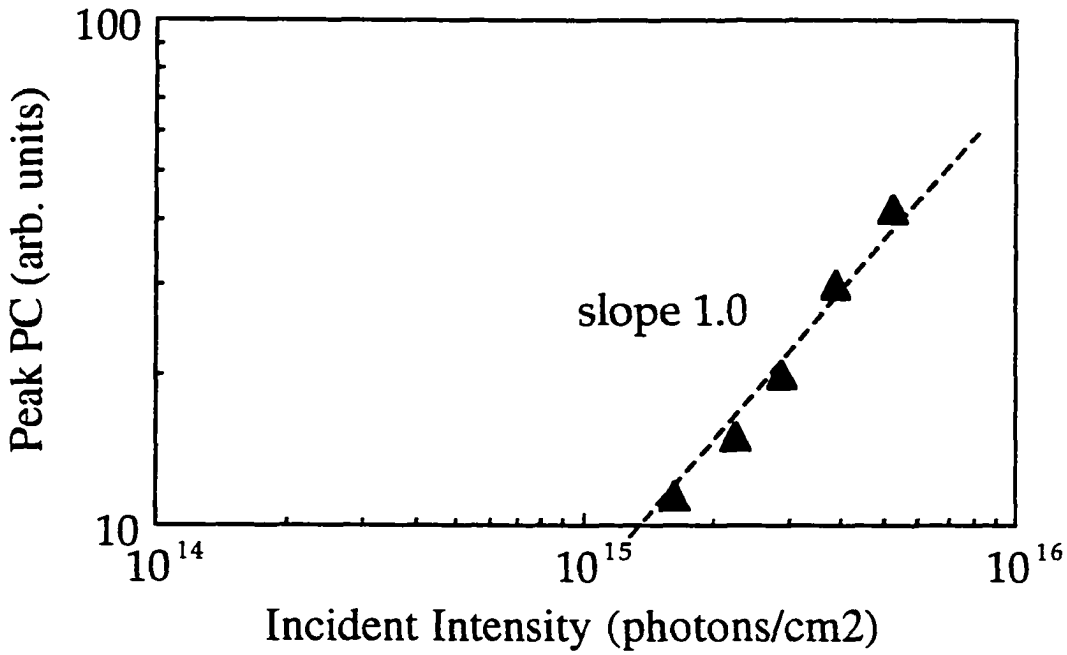

Figure 4.7 Peak PC vs. incident intensity in Alq_3 thin films

We were unable to observe the production of photoexcited charge carriers at low excitation intensities. In this regime the PC was dominated by noise and could not be measured accurately with our setup due to its low sensitivity. However, our model indicates that the PC is a byproduct of exciton-exciton interactions and is proportional to the square of the singlet exciton density, PC ~ $[S_1]^2$. Therefore, at low excitation intensities where $[S_1] \sim I^{1.0}$, we would expect the PC to have a quadratic dependence on the intensity, PC ~ I^2.

By calculating a theoretical curve using equation 4.4, we demonstrated in Figure 4.8 that the photoconductivity is proportional to the square of the molecular exciton concentration at low fluence. This curve also confirms the linear slope of the photocurrent vs. incident fluence for the intensity range used in the measurements.

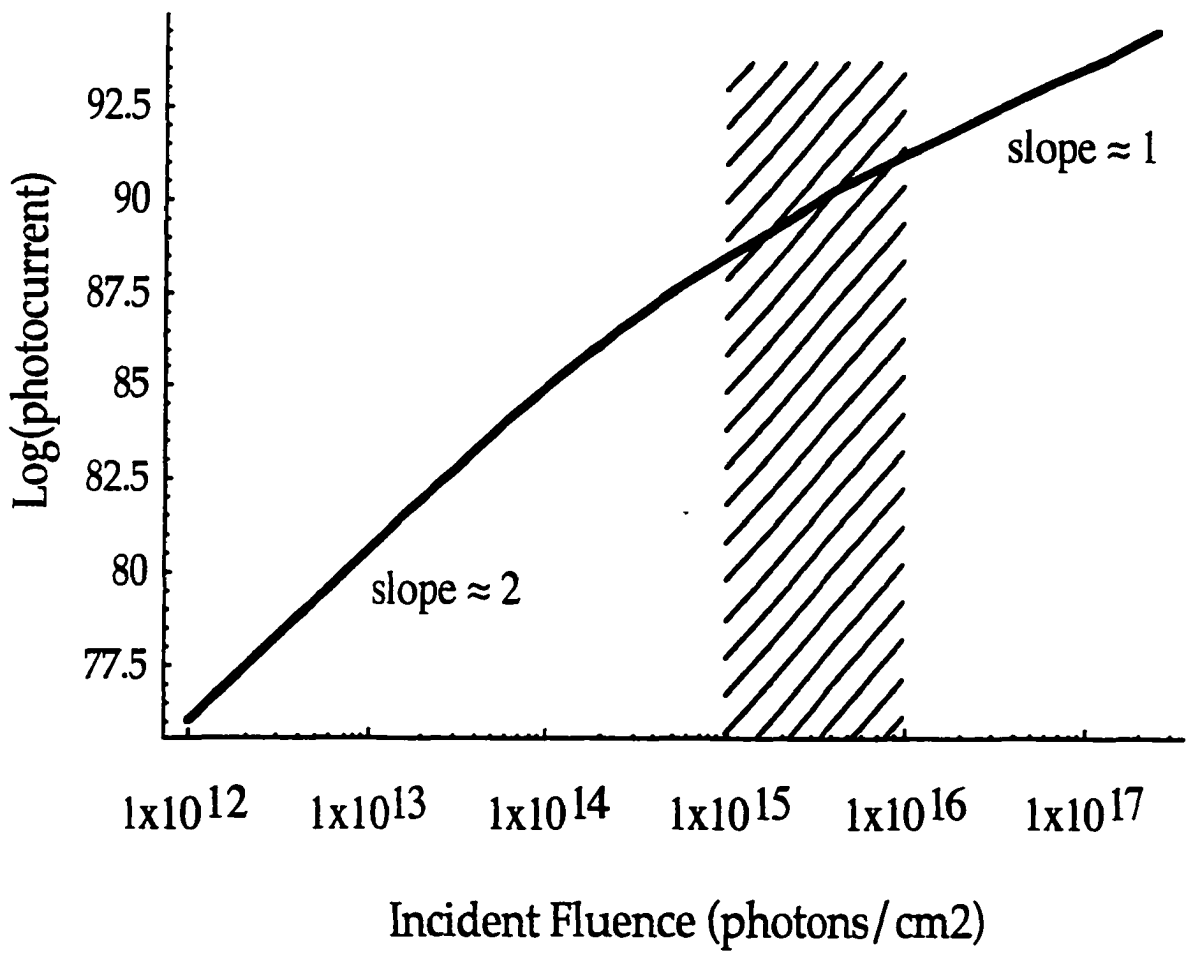

Figure 4.8 Theoretical plot of peak PC vs. fluence in Alq_3 Calculation made using Equation 4.4.

4.4 Conclusion

In conclusion, we have demonstrated that the process of bimolecular recombination of singlet excitons in Alq_3 films affects the kinetics of the PL decay and decreases the quantum efficiency at high exciton concentrations. However, for practical purposes, it is important to estimate whether such concentrations are achieved under normal LED operation.

For a typical OLED utilizing ITO as the anode, TPD as the hole transport layer, Alq_3 as the emitting/electron transport layer, and Mg:Ag as the cathode, an operating voltage of less than 10 Volts is required to achieve a brightness of 1000cd/m^2. This is 10 times the average brightness of a computer display. With an overall device thickness of 10μm the electric field across the device is $1x10^6$ V/cm, corresponding to an electron drift mobility in Alq_3 of $5x10^{-5}$ cm^2/V sec.[30] If we place a maximum limit of 1A/cm^2 on the injection current density, which is required for dot-matrix display applications, then the charge carrier concentration can be obtained from equation 4.17.[31]

$$J_{drift} = q\mu_n nE, \qquad \text{Equation 4.17}$$

where J_{drift} is the injected drift current density, q is the electron charge, μ_n is the electron mobility in Alq_3, n is the charge carrier concentration and E

is the electric field. Using equation 4.16 we obtain a charge carrier density $n \approx 1.25 \times 10^{17}$ cm^{-3} and if we assume that 25% of these carriers form singlet excitons, then the singlet exciton concentration, $[S_1]$, equals $n/4 \approx 3.1 \times 10^{16}$ cm^{-3}. From our PL measurements we estimated that exciton-exciton interactions begins at a singlet exciton concentration of 1.2×10^{19} cm^{-3}. The exciton concentration in OELD's is three orders of magnitude smaller than the concentration needed to observe exciton-exciton interactions. Therefore, it appears unlikely that this phenomenon would affect the performance and efficiency of OLED's.

On the other hand, exciton-exciton interactions can occur in other organic emitting devices such as the proposed electrically pumped solid state polymer diode laser[32] where the organic emitting layer serves as the active gain medium and a higher injection current density is required. For example, spectral narrowing (SN) and stimulated emission (SE) are both a manifestation of laser action and have been observed in thin films of several PPV derivatives such as DOO-PPV[33] and BuEH-PPV[34]. In the case of DOO-PPV films photoexcited at 532nm and emitting at 627nm, considerable SN occurred at $100 \mu J/cm^2$. This corresponds to a photon density of 2.7×10^{14} photons/cm^2. With an absorption coefficient of 5×10^4 cm^{-1},[35] the absorbed photon concentration is 1.35×10^{19} photons/cm^3. This value corresponds to the singlet exciton concentration if we again assume each absorbed photon creates a singlet exciton. This exciton concentration

is the same order of magnitude at which we observed exciton-exciton interactions in Alq_3. Moreover, significant SN can be observed at even higher excitation intensities where bimolecular interactions are more probable. Therefore, singlet exciton-exciton interactions would need to be addressed in fluorescent materials used for this type of application.

1 P. Avakian, *Pure Appl Chem.*, **32**, p. 1 (1974)

2 P. Avakian and R.E. Merrifield, *Mol. Cryst.*, **5**, p. 37 (1968)

3 C.E. Swenberg and N.E. Geacintov, *Organic Molecular Photophysics*, Vol. 1, ed. J.B. Birks, Chapter 10, (1973)

4 A.S. Davydov, *Theory of Molecular Excitons*, McGraw-Hill, New York (1962)

5 N.E. Geacintov, M. Pope and F. Vogel, *Phys. Rev. Lett.*, **22**, p. 593 (1969)

6 F. Heisel, J.A. Miehe, B. Sipp and M. Schott, *Chem. Phys. Lett.*, **3**, p. 534 (1976)

7 C.L. Braun, *Phys. Rev. Lett.* **21**, 215 (1968)

8 K.C. Kao and W. Hwang, *Electrical Transport in Solids*, (Pergamon Press, Vol. 14), p. 386 (1981)

9 D.C. Northrop and O. Simpson, *Proc. Roy. Soc.* **A244**, p. 377 (1958)

10 T Mori, K. Miyachi and T. Mizutani, *J. Phys. D.*, **28**, p. 1461 (1995)

11 K.C. Kao and W. Hwang, *Electrical Transport in Solids*, Vol. 14 (1981)

12 S.I. Choi, *J. Chem. Phys.*, **40** p. 1691 (1964)

13 R.G. Kepler and R.E. Merrifield, *J. Chem. Phys.*, **40**, p. 1173 (1964)

14 I. Sokolik, R.Priestley, A.D.Walser and R.Dorsinville, *Appl. Phys. Lett.*, **69**, p. 4168 (1996)

15 R.G. Kepler, *Phys. Rev. Lett.*, **18**, p. 951 (1967)

16 E. Courtens, A. Bergman and J. Jortner, *Phys. Rev.*, **156**, p. 948 (1967)

17 A.D. Walser, R. Dorsinville, R. Tubino, and R.R. Alfano, *Phys. Rev.B.*, **43**, p. 7194 (1991).

18 M. Pope and C.E.Swenberg, *Electronic Processes in Organic Crystals*, (Oxford University Press, New York), p. 158 (1982)

19 A.J. Campillo, R.C. Hyer, S.L. Shapiro and C.E. Swenberg, *Chem. Phys. Lett.* **48**, p. 495 (1977)

20 M. Pope and C.E. Swenberg, *Electronic Processes in Organic Crystals*, (Oxford University Press, New York) p. 96, 122, & 128 (1982)

21 C.E.Swenberg and N.E.Geacintov, *Organic Molecular Photophysics*, edited by J.B. Birks (Wiley-Interscience, London), Vol. 1, p. 495 (1973)

22 I. Sokolik, R. Priestley, A.D. Walser, R. Dorsinville and C.W. Tang, *Appl. Phys. Lett.*, **69**, p. 4168 (1996)

23 C.W. Tang, S.A. VanSlyke and C.H. Chen, *J. Appl. Phys.*, **65**, p. 3610 (1989)

24 A.J. Campillo, R.C. Hyer, S.L. Shapiro and C.E. Swenberg, *Chem. Phys. Lett.* **48**, p. 495 (1977)

25 U. Goesele, *Chem. Phys. Lett.*, **43**, p. 61 (1976); *Chem. Phys. Lett.*, **46**, p. 196 (1977)

26 J.B. Birks, *Photophysics of Aromatic Molecules*, (Wiley-Interscience), p. 518 (1969)

27 C.W. Tang, S.A. VanSlyke and C.H. Chen, *J. Appl. Phys.*, **65**, p. 3615 (1989)

28 M. Pope and C.E.Swenberg, *Electronic Processes in Organic Crystals*, (Oxford University Press, New York), p. 160 (1982)

29 M. Pope and C.E.Swenberg, *Electronic Processes in Organic Crystals*, (Oxford University Press, New York), p. 122 (1982)

30 C. Hosokawa, H. Tokailin, H. Higashi and T. Kusumoto, *Appl. Phys. Lett.*, **60**, p. 1220 (1992)

31 R.F. Pierret, *Semiconductor Fundamentals*, (Addison-Wesley), Vol. 1, p. 64 (1988)

32 M.A. Diaz-Garcia, F. Hide, B.J. Schwarts, M.R. Anderson, Q. Pei and A.J. Heeger, *Synth. Met.*, **84**, p.455 (1997)

33 S.V. Frolov, W. Gellermann, Z.V. Vardeny, M. Ozaki and K. Yoshino, *Synth. Met.*, **84**, p. 471 (1997)

34 B.J. Schwartz, F. Hide, M.R. Anderson and A.J. Heeger, *Synth. Met.*, **84**, p. 663 (1997)

35 S.V. Frolov, M. Ozaki, W. Gellermann, M. Shkunov, Z.V. Vardeny and K. Yoshino, *Synth. Met.*, **84**, p. 473 (1997)

CHAPTER FIVE

5. QUENCHING OF SINGLET EXCITONS BY PRODUCTS OF PHOTOOXIDATION.

5.1 Introduction

Photooxidation (PO) is one factor which has been shown to quench the photoluminescence (PL) emitted from organic materials.[1] In this process, the combination of light and air/oxygen results in a reduction in the PL and electroluminescence (EL) quantum efficiency, and consequently a reduction in device lifetime. Earlier investigations indicated that operating OLED's in air resulted in a 99% loss of EL intensity in as little as 150 minutes.[2] In Alq_3 based OLED's, the EL intensity was reduced by 50% within 100 hours[3] even when operated under dry argon and with a low drive current. The nature of this degradation was not clearly understood but was attributed to degradation of the metal contacts with ambient air. Operation of devices under such short device lifetimes, even in inert atmospheres, renders OLED's useless for commercial applications.

Degradation of OLED's and device properties has been shown to result from exposure to light, water and oxygen molecules.[4,5,6] This

degradation was related to the corrosion of contacts, the presence and migration of impurities, and to the chemical composition of the emissive material.[7,8] Antoniadis et al.[9] identified the degradation of Alq_3 OLED's with the formation of non-emissive regions or dark spots. The formation and growth of these dark spots were studied under ambient conditions[10] and it was found that the number of black spots did not change with exposure to air. The black spot growth rate however, was mainly dependent on the ambient humidity content. In a dry nitrogen gas chamber where water and oxygen existed only at parts per million, no growth of black spots was observed. However, the growth was accelerated when 100% relative humidity was introduced into the chamber.[11] Dry oxygen in the chamber did not affect the growth rate considerably. From this they concluded that the presence of water in Alq_3 OLED's results in a degradation of the device performance.

To extend the operating lifetime of Alq_3 OLED's, Burrows et al.[6] introduced a simple encapsulation technique to protect the device from the effects of the atmosphere. This resulted in an increase in the device lifetime. A schematic side view of the encapsulated OLED is shown in Figure 5.1. An unencapsulated device showed very little light output remaining after the first 10 hours while the encapsulated device maintained approximately 40% of its original light output even after more than 1000 hours of continuous operation. The improvement of more than two orders

of magnitude in operating lifetime with device encapsulation indicated that reactions with the atmosphere, presumably from exposure to oxygen and water, is a limiting factor leading to device failure.

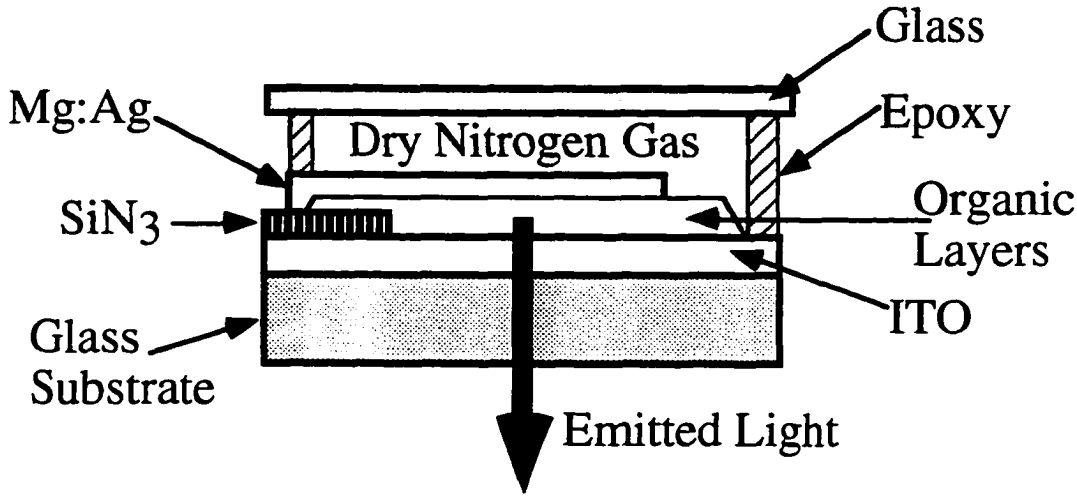

Figure 5.1 Schematic of an encapsulated OLED

A mechanism behind the PL quenching in Alq_3 due to oxidation was proposed by Papadimitrakopoulos et al.[12] and is shown in figure 5.2. Their experiments indicated that in the presence of moisture the Alq_3 molecule undergoes a liberation of an 8-hydroxyquinoline (8-HQ) ligand resulting in a chemical degradation of the compound. Subsequently, in the presence of oxygen, the freed 8-HQ ligand undergoes a condensation reaction which results in the production of additional moisture and a residual non-emissive compound. Only trace amounts of oxygen were required to yield this dark

non-emissive residual byproduct. The moisture produced by the condensation reaction initiates the liberation of additional 8-HQ ligands and the process is repeated. Overall, a reduction in the PL was observed and the presence of water was assumed to be the catalyst for this reaction.

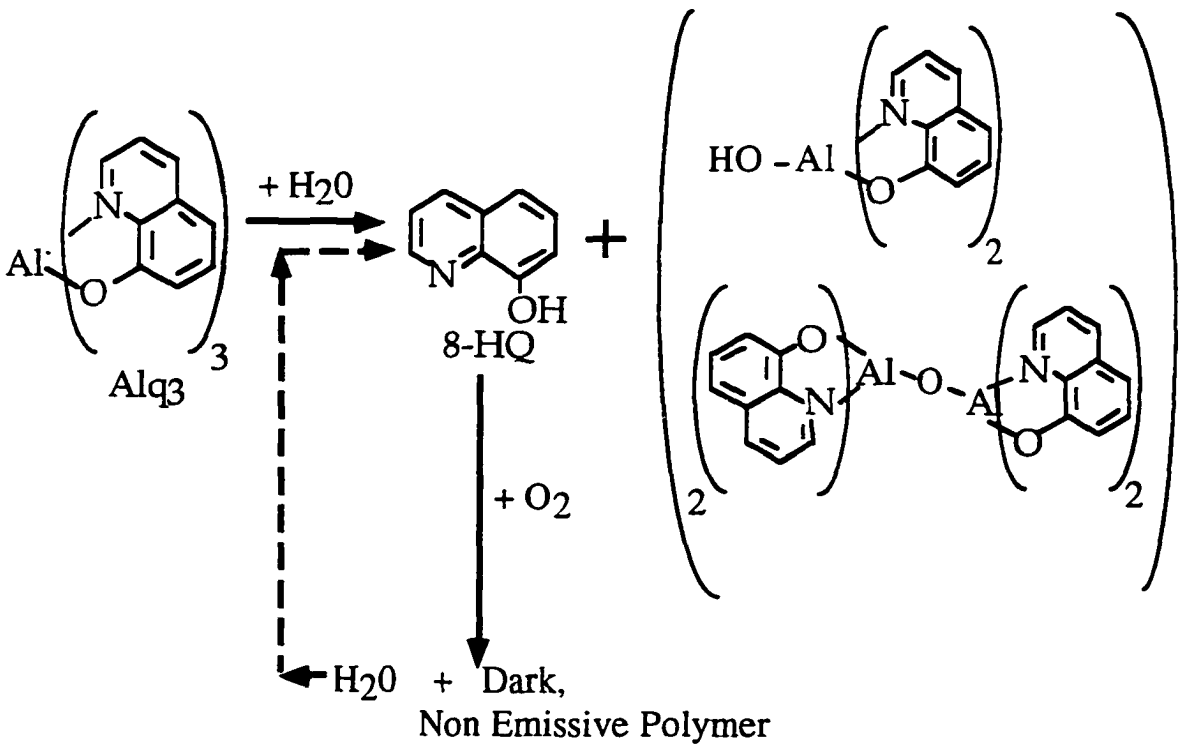

Figure 5.2 Mechanism for the chemical degradation of Alq_3.

In this chapter we have decided to investigate how photooxidation of Alq_3 thin films results in a degradation of the PL intensity. Our objective is to understand how products of PO act as quenchers for singlet excited states. Initially, researchers expected this material to be highly stable and resistant to oxidation. However, we observed for the first time that a

substantial decrease in the PL quantum yield, PL lifetime, and photoconductivity (PC) response does occur due to photooxidation of Alq_3 by oxygen and UV light.

The two mechanisms of Alq_3 degradation suggests that water has an affect on the chemical stability of Alq_3. Therefore, understanding the reactions of Alq_3 with air, oxygen, and UV light would provide valuable information for improving the performance of Alq_3 based OLED's.

5.2 Experimental Setup

The experimental setup used for the measurements performed in this chapter were previously discussed in chapter 3. Equal thin films of Alq_3 were thermally evaporated onto two Auston switches and then transferred to the sample site under inert atmosphere. During all measurements, the sample cell was purged with nitrogen gas to remove any residual oxygen/water molecules. In between measurements, photooxidation was done by illuminating the samples with the full spectrum of a 150 Watt xenon lamp while blowing air or oxygen through the cell. One sample was photooxidized with air and the other with oxygen. This allowed us to examine what affect water has on the degradation of this emitting material. In both cases, photooxidation was done over a 40 minute period with 8 minute intervals between exposure.

5.3 Experimental Results

In our experiment, measurements of photooxidation effects were first conducted using air and UV light. After 40 minutes of PO the peak PL had decreased by 67% of its initial value (pristine sample). However, to identify the effects of water on luminescence quenching, similar measurements were taken on another sample which was photooxidized using pure oxygen. In this case we observed a substantial decrease in the peak PL when oxygen was used as an oxidizing agent. After only 10 minutes of PO the peak PL value decreased by about 67%. From this observation we concluded that pure oxygen has a stronger effect on quenching the PL of Alq_3. These results are shown in Figure 5.3 and they indicate that water vapor, which is always present in air, may not contribute substantially to the PO process.

Yan et al.[13] had previously conducted similar photooxidation experiments in PPV polymers using a Xenon lamp under ambient conditions. Photooxidation of PPV resulted in a rapid decrease in the PL intensity after modest amounts of exposure. This also caused a nonexponential decay in the singlet excited state lifetime as opposed to an exponential decay in pristine samples.

As shown in Figure 5.4 the excited state lifetime of a pristine Alq_3 sample has a single exponential decay with a lifetime of 14-16 nsec.

However, after 40 minutes of photooxidation the decay profile became non-exponential. Examples of nonexponential PL decay dynamics have been reported[14,15,16] and various mechanisms have been proposed to explain the nonexponential behavior. Recent work in PPV demonstrated that the nonexponential behavior arises from exciton quenching at oxidation defects and when these defects are eliminated, the luminescence is exponential with a lifetime near that for PPV in solution.[12]

The changes in the PL decay dynamics we observed allows us to speculate that quenching centers for singlet excitons are created during the PO process. With the production of these quenching sites, possibly at an energy level lower than the first excited state, singlet excitons can rapidly decay to these new states since they provide an efficient channel for non-radiative energy dissipation. PL quenching can therefore be attributed to a direct energy transfer from the excited molecule to a non-emitting quenching site.

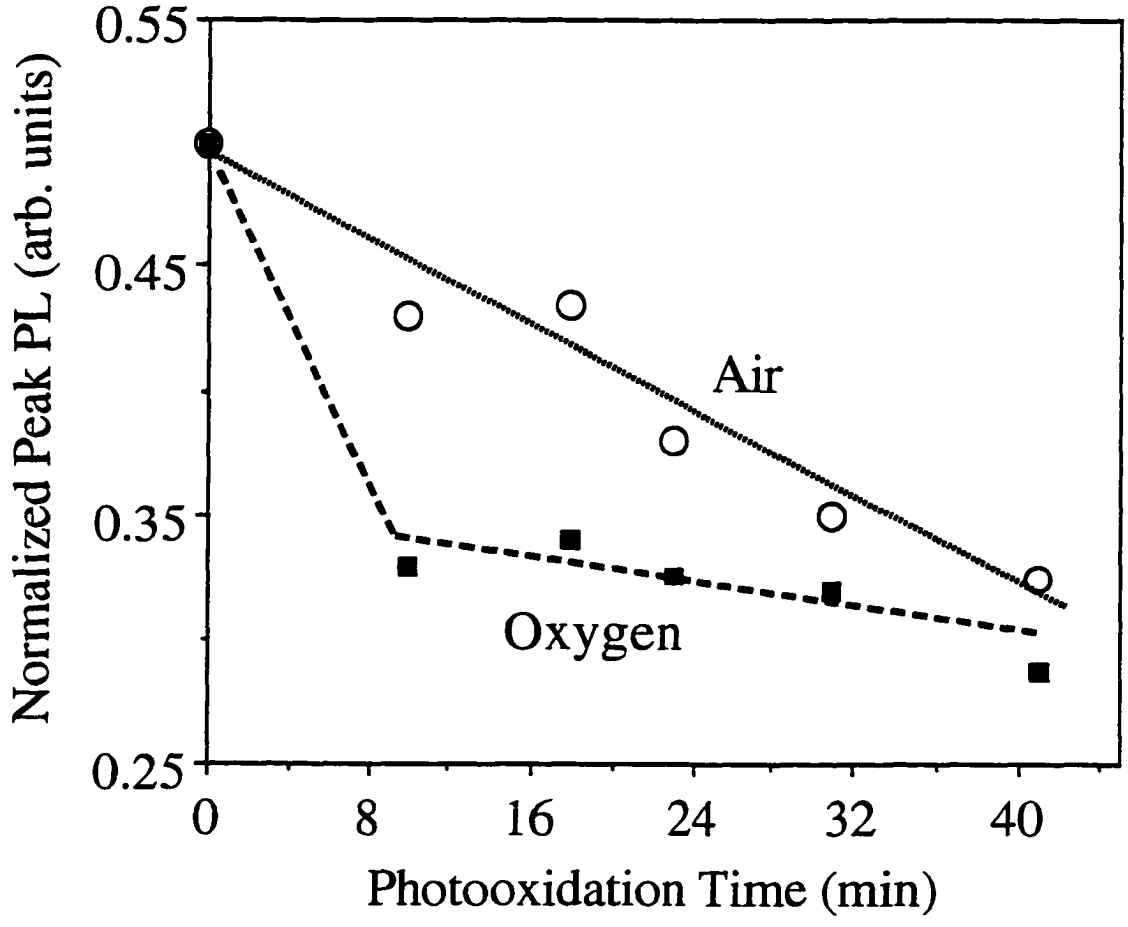

Figure 5.3 Peak PL vs. Photooxidation Time.
Open circles denotes PO under air.
Squares denoted PO under oxygen.
Lines are for reference only.

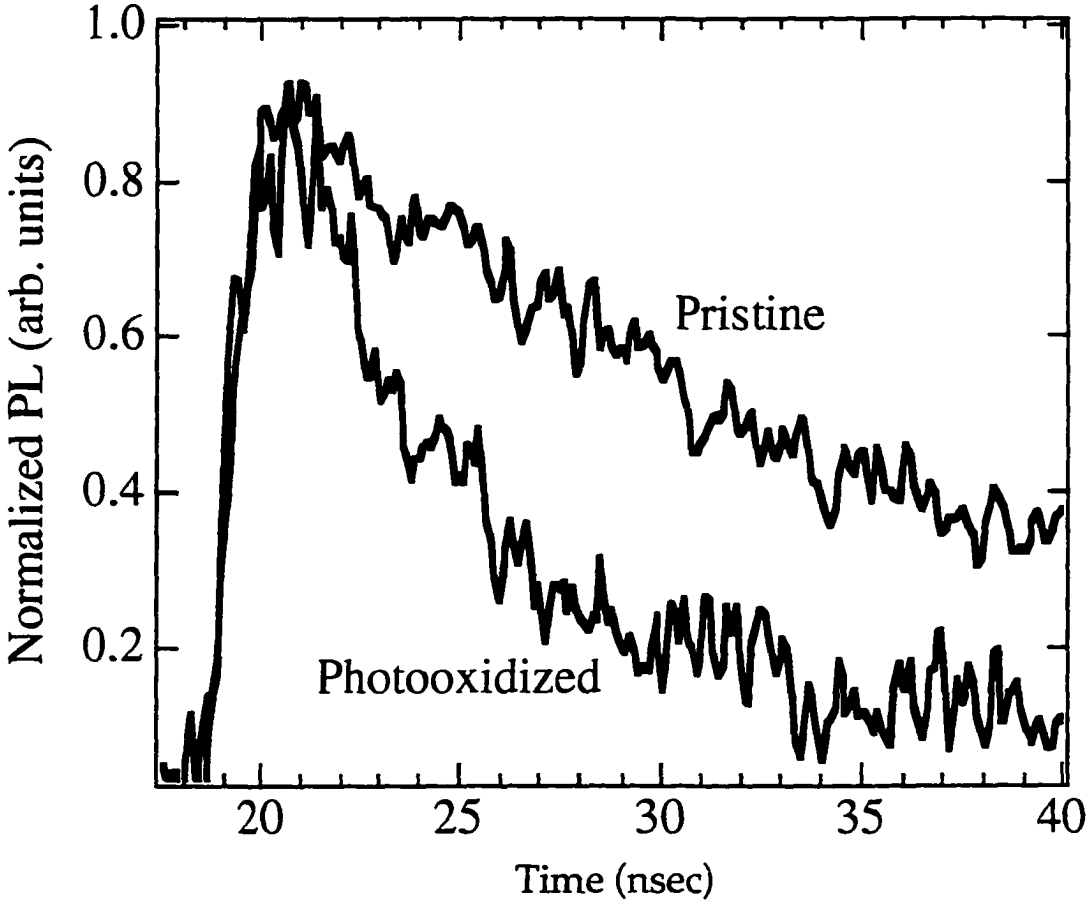

Figure 5.4 PL response of pristine and photooxidized Alq_3 sample.

At high excitation intensities charge carriers generated in Alq_3 contributes to the PC response. These charge carriers are produced from singlet exciton-exciton annihilation.[17] Photooxidation of thin films of Alq_3 was found to reduce the PC response in the case of both air and oxygen. This is shown in Figure 5.5. Again, oxygen was found to reduce the PC response at a faster rate than PO by air.

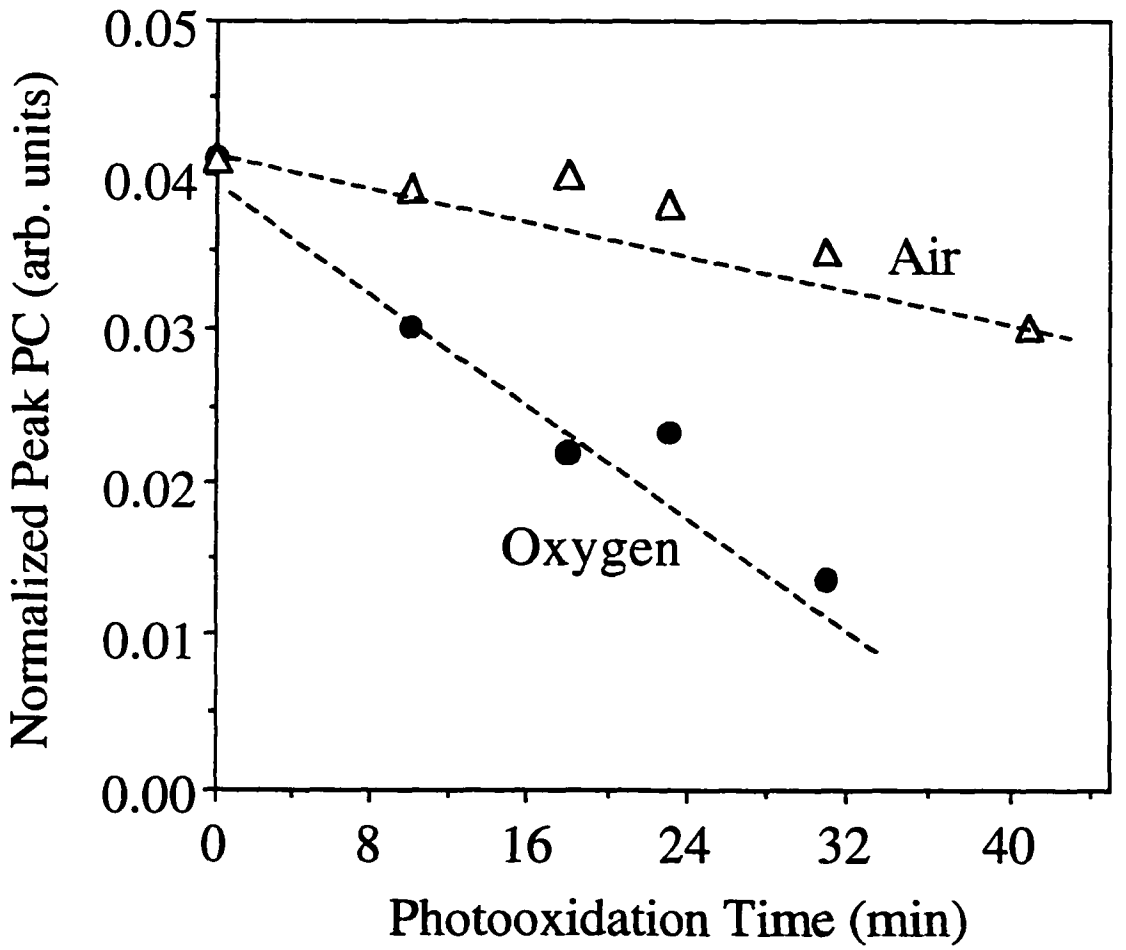

Figure 5.5 Peak photoconductivity vs. photooxidation time. Open triangles denotes PO under air. Circles denoted PO under oxygen.

5.4 Discussion

In our measurements, water was found to have less of an effect in than oxygen in the photooxidation process. This is supported by the significant differences we observed in PL quenching when comparing the presence of pure oxygen with air. Therefore, the PL quenching in Alq_3 is attributed to the presence of oxygen molecules during the photooxidation process. We believe that the PO introduces chemical changes in the Alq_3 molecules and converts these molecules into products of photooxidation, SO_2, defined by:

$$S_0 + h\nu + O_2 \rightarrow S_1 + O_2 \rightarrow S_0 + SO_2 \qquad \text{Equation 5.1}$$

This occurs as a result of the interaction of singlet excitons with oxygen, and contrary to the dark oxidation by water,[18] this reaction required UV light. No changes were observed in the PL intensity when the films were exposed to dry air in the absence of UV light. Likewise, when the films were exposed to UV irradiation while under nitrogen gas flow no changes occurred.

It is also possible that the presence of oxygen results in the replacement of the vinylene groups (C-H) on the 8-HQ ligand with carbonyl groups (C=O). Carbonyl groups are known to possess a strong electron affinity and when formed on the 8-HQ ligand they can possibly cause dissociation of singlet excitons and a reduction in the PL quantum

yield. This was demonstrated in PPV where an increase in the carbonyl groups resulted in a dramatic reduction in PPV photoluminescence.[19] A similar result was also discovered in BCHA-PPV, a PPV derivative and in thiophene based polymer (P3OT). Spectroscopic measurements revealed an growth of the carbonyl peak and a disappearance of the CH_2 and CH_3 groups.

Since PO of Alq_3 resulted in a decrease in the PL response, one would expect to observe a decrease in the PC response since charge carriers in Alq_3 are produced by singlet exciton-exciton annihilation. In our measurements a reduction in the peak PC was observed and we consider a possible mechanisms for this occurrence. In Alq_3, quenching sites produced by PO (SO_2) could result in a direct charge transfer from the excited Alq_3 molecule to the nonradiative SO_2 molecule. A similar mechanism was proposed by Papadimitrakopoulos in Alq_3 for the reduced PL intensity observed due to dark oxidation.[12] The PC response we observed becomes lower since exciton dissociation and charge transfer to the nonradiative SO_2 sites reduces the concentration of singlet excited states that would participate in exciton-exciton annihilation and the photogeneration of charge carriers.

5.5 Conclusion

Despite the fact that the nature of photooxidation luminescence quenching in Alq_3 still remains unknown, we have demonstrated for the first time that the process of photooxidation by oxygen and UV light does take place in Alq_3. Products of PO were found to act as quenching centers for singlet excitons. This resulted in a decrease in the peak PL, the PL excited state lifetime, and the efficiency of photogeneration of charge carriers. The comparison of PO with oxygen and air led us to conclude that moisture (water) has less of an effect than oxygen on the degradation of Alq_3 fluorescence. Our results oppose those of other authors[9.13] who believe that water acts as a catalyst in the degradation of the Alq_3 chemical structure. However, this discrepancy can possibly be attributed to a difference between the mechanism used by Kodak to synthesize our Alq_3 samples and the mechanism used by other authors.

In EL devices, luminescence is produced by the radiative decay of singlet excitons, similar to photoluminescence. Because of this they will also be sensitive to oxygen during operation and they may undergo very similar, if not identical, chemical changes. Permeation of oxygen to the emitting layer in OLED's can occur through pinholes in the cathode electrodes. Even small quantities of oxygen present in the OLED may provide enough reactive material to initiate device degradation. Heat

generated during the EL operation could even speed the photochemical reactions which occur during the PO process. Knowing this, it may be possible to extend the lifetime of the device by encapsulating it from air, but the results of Burrows et al.[6] (previously discussed) show that no encapsulation technique is perfectly impermeable.

1 J.B. Birks, Photophysics of Aromatic Molecules, Wiley-Interscience, New York, p. 492 (1970)

2 Y. Hamada, C. Adachi, T. Tsutsui, and S. Saito, *Jpn. J. Appl. Phys.*, **32**, p. 1812 (1992)

3 C.W. Tang and S.A. VanSlyke, *Appl. Phys. Lett.*, **51**, p. 913 (1987)

4 K. Yoshino, T. Kuwabara, T. Iwasa, T. Kawai, M. Onoda, *Jpn. J. Appl. Phys.*, **29**, p. L1514 (1990)

5 J.C. Scott, J.H. Kaufman, P.J. Brock, R. Dipietro, J. Salem, and J.A. Goitia, *J. Appl. Phys.*, **79**, p. 2745 (1996)

6 P.E. Burrows, V. Bulovic, S.R. Forrest, L.S. Sapochak, D.M. McCarty, and M.E. Thompson, *Appl. Phys. Lett.*, **65**, p. 2922 (1994)

7 C. Adachi, T.Tsutsui, and S. Saito, *Appl. Phys. Lett.*, **56**, p. 799 (1990)

8 L.M. Do, E.M. Han, Y. Niidome, M. Fujihira, T. Kanno, S. Yoshida, A. Maeda, and A.J. Ikushima, *J. Appl. Phys.*, **76**, p. 5118 (1994)

9 H. Antoniadis, M.R. Hueschen, J. McElvain, J.N. Miller, R.L. Moon, D.B. Roitman, and J.R. Sheats, *ANTEC 97*, **724**, p. 1266 (1997)

10 J. McElvain, H. Antoniadis, M. Hueschen, J. Miller, R. Moon, and D. Roitman, *J. J. Appl. Phys.*, **80**, (1996)

11 J.R. Sheats, H. Antoniadis, M. Hueschen, W. Leonard, J. Miller, R. Moon, D. Roitman, and A. Stocking, *Science*, **273**, p. 884 (1996)

12 F. Papadimitrakopoulos, X.M. Zhang, L.L. Thomsen, and K.A. Higginson, *Chem. Mat.*, **8**, p. 1363 (1996)

13 M.Yan, L.J. Rothberg, F. Papadimitrakopoulos, M.E. Galvin, and T.M. Miller, *Phys. Rev. Lett.* **73**, p. 744 (1994)

14 K.S. Wong, *J. Phys. C.*, **20**, p. L187 (1987)

15 M. Furukawa, K. Mizuno, A. Matsui, S.D.D.V. Rughooputh and W.C. Walker, *J. Phys. Soc. Japan*, **58**, p. 2967 (1989)

16 L.J. Rothberg, *Proc. SPIE Int. Soc. Opt. Eng.*, **1910**, p. 122 (1993)

17 A. Walser, I. Sokolik, R. Priestley and R. Dorsinville, *Appl. Phys. Lett.*, **69**, p. 1 (1996)

18 X.-M. Zhang, K.A. Higginson and F. Papadimitrakopoulos, *Electr. Opt. and Magn. Prop. of Org. Sol. State Mater.* III (MRS Symp. Proc. Ser., Vol. 413), p. 43 (1996)

19 F. Papadimitrakopoulos, K. Konstadinidis, T.M. Miller, R. Opila, E.A. Chandross, and M.E. Galvin, *Chem. Mater.*, **6**, p. 1563 (1994)

CHAPTER SIX

6. TEMPERATURE DEPENDENCE OF TRANSIENT PHOTOLUMINESCENCE IN ALQ_3

6.1 Introduction

Since the first observation of its efficient luminescence[1], tris(8-hydroxyquinoline) aluminum (Alq_3) has been widely used as the emitting layer in organic light emitting diodes (OLED's).[2,3] The luminescence from this material originates from the radiative decay of singlet excitons formed by photoexcitation, or in the case of electroluminescence (EL), by charge carrier injection. However, prior to decay, these excitons possess the ability to diffuse and interact with trapping sites resulting in a reduction in the PL efficiency and EL quantum yield.

In this chapter we will investigate the affect of exciton trapping in Alq_3 thin films by measuring the temperature dependence of the transient photoluminescence. Such measurements will assist us in understanding the influence of trapping sites on the PL quantum efficiency in Alq_3. These trapping sites can be identified as defects caused by physical imperfections within the lattice or by the presence of guest molecules which act as

impurities.[4] The important aspect of these traps is that they modify the available energy levels in their vicinity and this often leads to the presence of accessible vacant orbitals located within the energy gap. In organic materials like Alq_3, these vacant orbitals would be located below the LUMO level.[5] We consider that there are defect sites in Alq_3 thin films and these defects act as exciton traps and reduce the exciton lifetime and the PL quantum efficiency. We will demonstrate that the PL quantum efficiency is raised substantially at lower temperatures and this is attributed to a reduction in exciton diffusion to trapping sites.

The dynamics of singlet excited states in organic emitters, namely PPV, has previously been shown to be temperature dependent.[6,7] For example, transient PL measurements on PPV by Lemmer et al.[4] showed an increase in the excited state lifetime of singlet excitations at low temperatures as compared to room temperature. This dependence suggested that diffusion of mobile excitations is reduced at low temperatures resulting in a reduction of exciton quenching at randomly distributed traps and an increase in fluorescence efficiency. In other studies on PPV, Furukawa et al.[8] associated the increase in excited state lifetime at lower temperatures with a reduction in the relaxation of free excitons to nonradiative self-trapped excitons. The thermal activation energy required to overcome the potential barrier separating these two

states is removed at low temperatures thus prohibiting free excitons from relaxing to the nonradiative self-trapped exciton state.

In the case of molecular crystals, Abe et al.[9] observed an increase in the PL and EL intensity at low temperatures in Alq_3 based devices. They associated this increase with a reduction in the nonradiative transition probability typical of molecular crystals at low temperatures.[10] However no analysis on the affects of temperature on the excited state lifetime and the PL quantum yield were performed.

Investigations into the nature of trapping sites in Alq_3 have been reported by Burrows et al.[11] where they suggested that current in Alq_3 based OLED's is limited by a large density of traps. By modeling the temperature dependence of I-V and EL characteristics, information about the energy distribution of these trapping sites were derived. Their results established that a distribution of trapping sites located at 0.15 eV below the LUMO level exists in Alq_3 and the EL observed is produced by the recombination of trapped electrons with holes injected by the hole transport layer. These results support the mechanism behind electron trapping in Alq_3 OLED's. However, they do not address the changes we observed in the PL decay at various temperatures.

We have performed an investigation on the temperature dependence of the time resolved luminescence in Alq_3. We report the dependence of the peak photoluminescence (PL), PL lifetime and PL quantum efficiency

on temperature for pristine films of Alq_3 as determined by transient PL measurements. We have demonstrated that for both low temperature and low excitation, an increase in the peak PL and singlet excited state lifetime is observed which we associate with a reduction in singlet exciton trapping. In addition, it is demonstrated that under low temperature and high excitation conditions, the mutual annihilation of singlet excitons is lowered. This results in a decrease in the exciton diffusion coefficient and exciton diffusion length. In both cases an increase in the fluorescence quantum efficiency is observed relative to room temperature.

6.2 Experimental Setup

The experiments conducted in this chapter were performed on 1-2 μm thick films of Alq_3, thermally evaporated onto the optical switch. Details of the experimental set-up used have been previously discussed in chapter 3. Samples were mounted in a liquid nitrogen pour-fill Dewar and investigated within the temperature range of 300 - 77K. The excitation density ranged from $4x10^{13}$ - $2x10^{15}$ photons/cm^2, allowing us to observe the intensity dependence of the transient behavior.

6.3 Experimental Results

Figure 6.1 shows the transient PL response of Alq_3 for a low excitation intensity ($4x10^{13}$ photons/cm^2) where exciton-exciton annihilation processes can be neglected. At 300K the luminescent response has a single exponential decay with a lifetime of 15-16nsec, consistent with measurements made by Tang et al.[2] in thin films and toluene solutions. Upon reducing the temperature of the sample we observed a gradual increase in the luminescence decay. At 77K the PL decay remained a single exponential with a lifetime of about 20 nsec. Figure 6.2 shows the temperature dependence of the excited state lifetime.

As shown in Figure 6.3, an increase in the peak PL with decreasing temperature coexisted with the changes observed in the excited state lifetime for low excitation. At 77K the peak PL increased by a factor of 2, similar to results obtained by Abe et al.[7] The combined increase in the peak PL and excited state lifetime resulted in an overall increase in the fluorescence quantum yield. This is illustrated in Figure 6.4. At 77K the PL had increased by a factor of 4 as compared to 300K.

Similarly, figure 6.5 shows the transient PL response of Alq_3 from 300K to 77K for a high excitation intensity ($2x10^{15}$ photons/cm^2). At 300K we observed a PL decay which consisted of a fast and slow component. Such response was not observed at low excitation densities. For Alq_3, we

have previously associated this change in PL decay from single exponential to nonexponential with exciton-exciton annihilation which occurs under high excitation.[12] At a reduced temperature of 77K we observed an increase in both PL decay components.

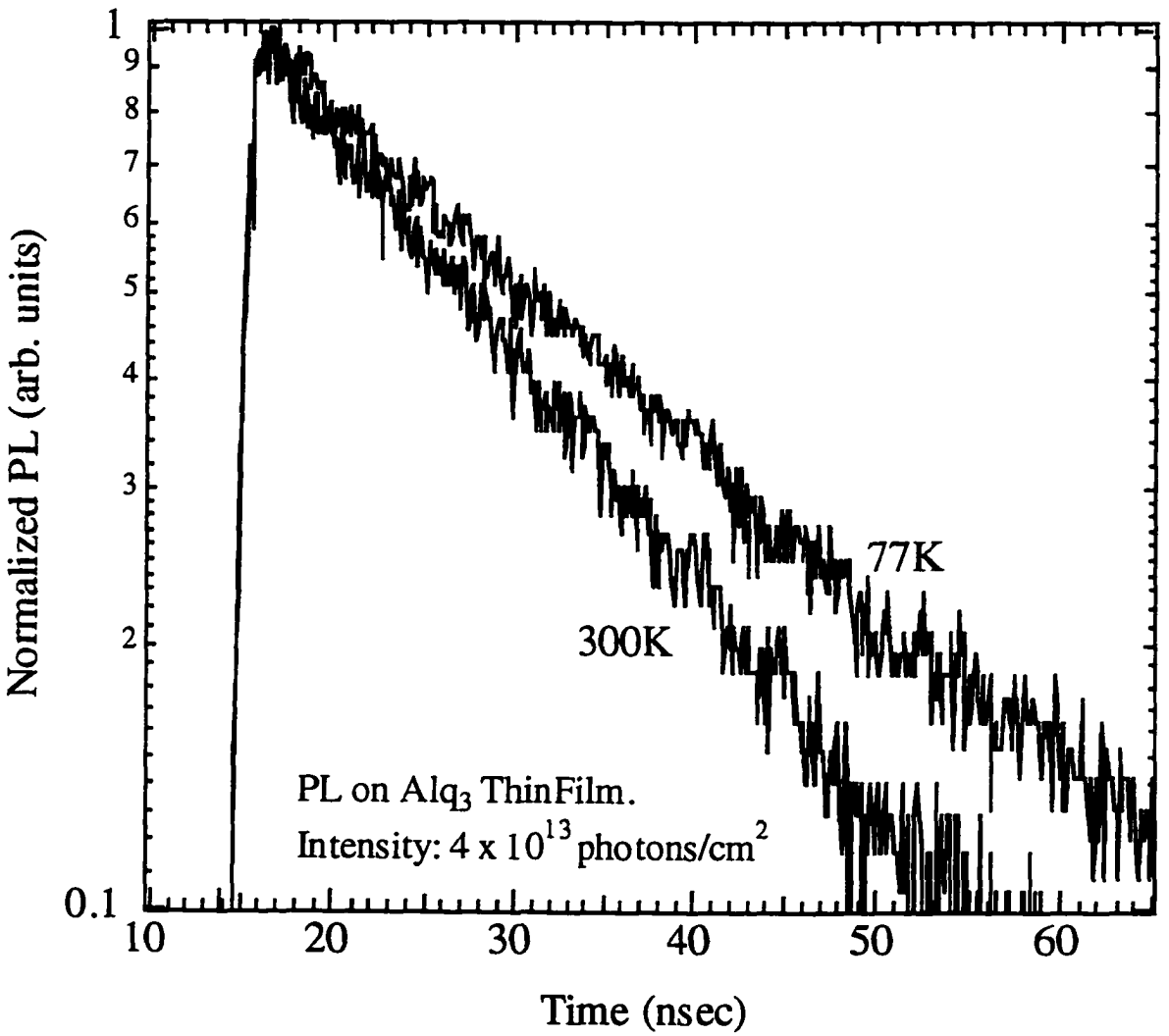

Figure 6.1 PL of Alq_3 at 300K and 77K under low excitation intensity.

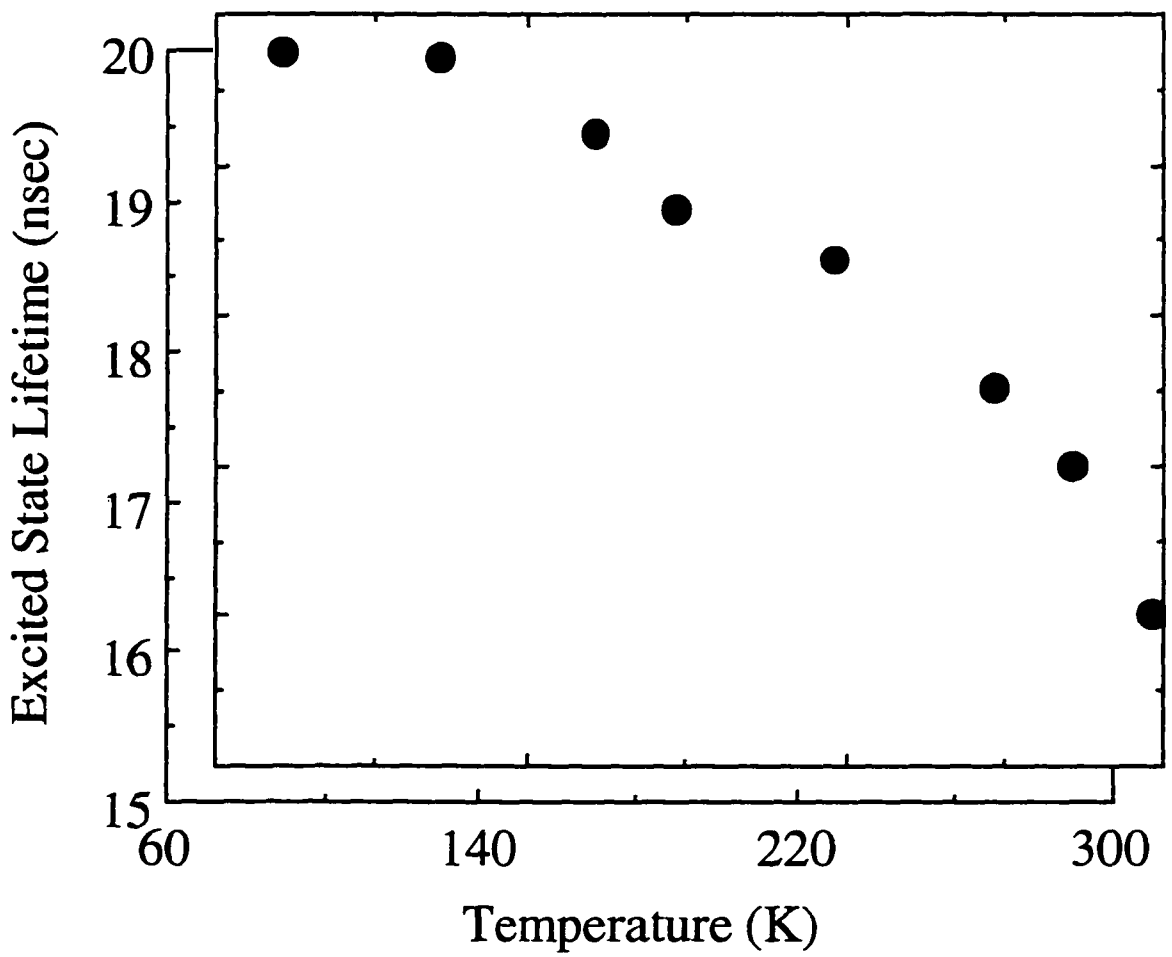

Figure 6.2 Temperature dependence of excited state lifetime in Alq_3 thin film.

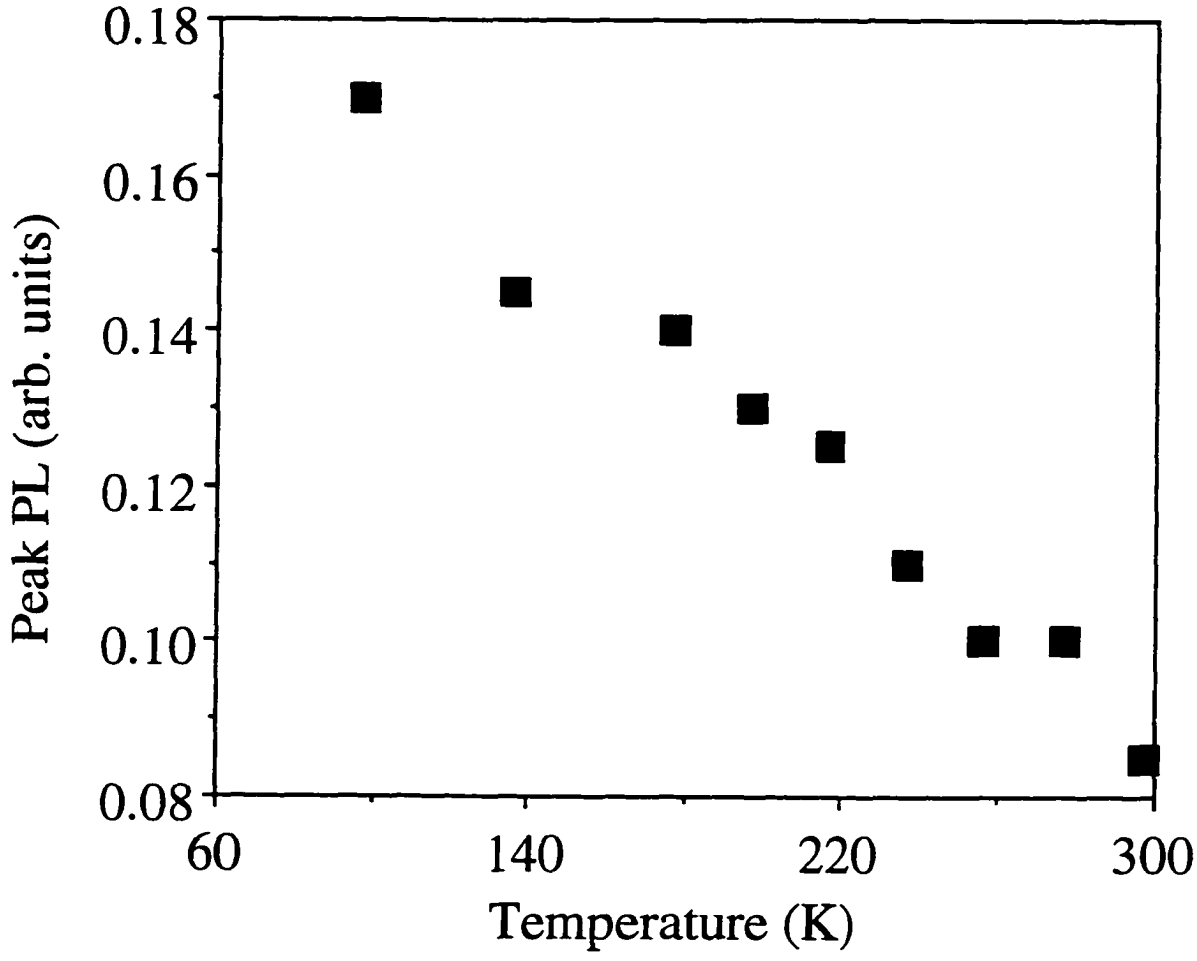

Figure 6.3 Peak PL vs. Temperature in Alq_3 thin film.

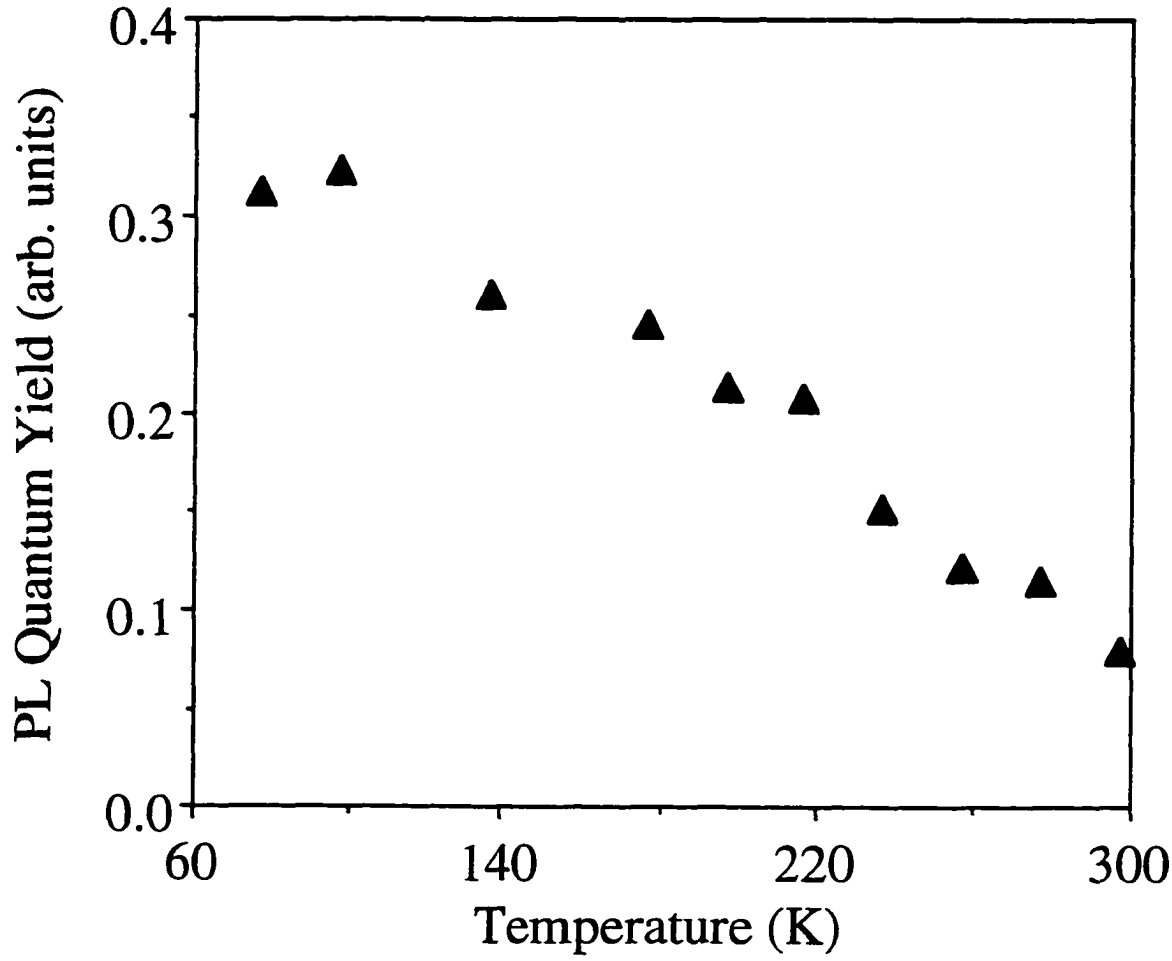

Figure 6.4 Temperature dependence of Alq_3 PL quantum yield.

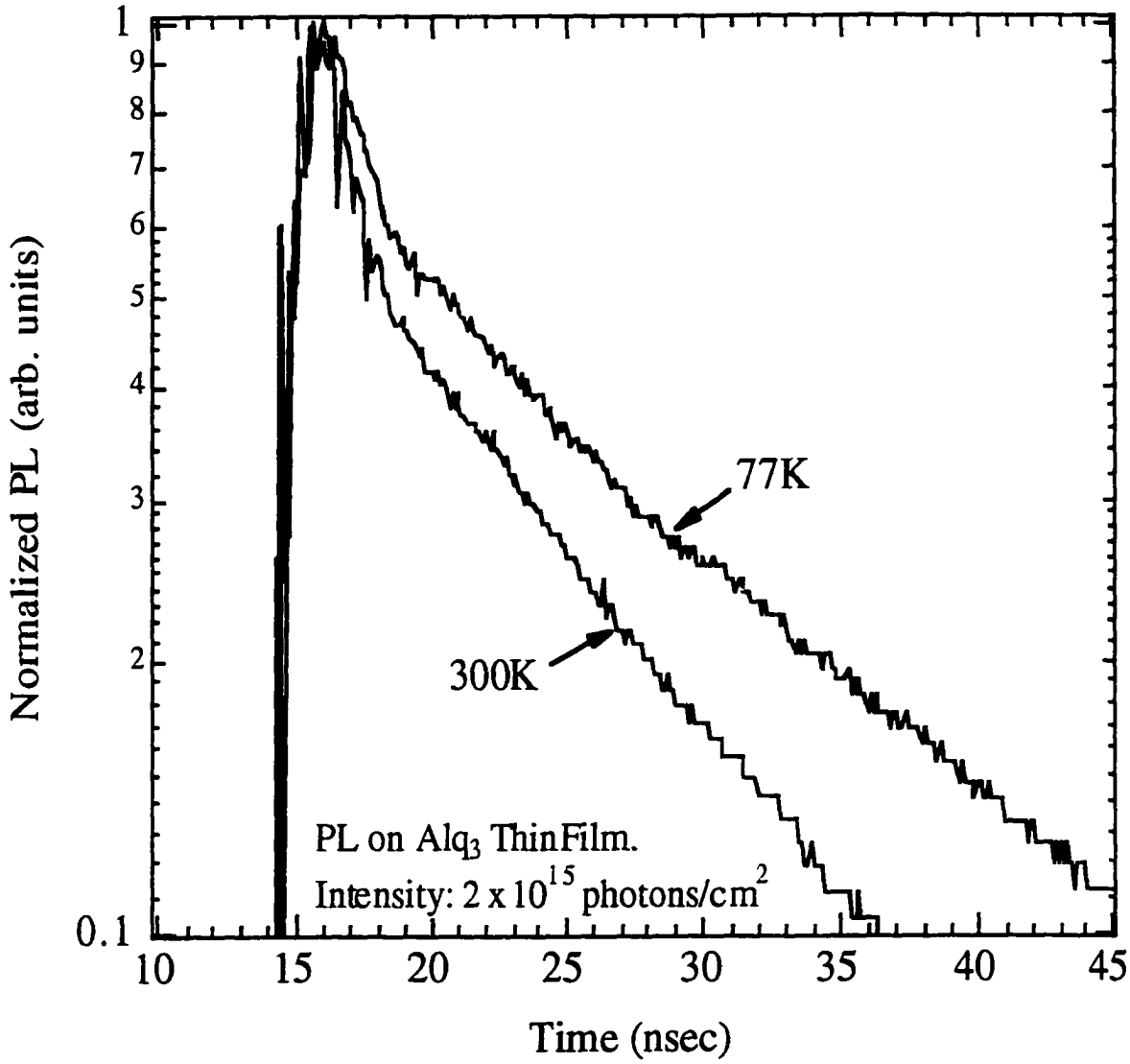

Figure 6.5 PL of Alq_3 at 300K & 77K under high excitation intensity.

6.4 Discussion

Exciton trapping sites exist in crystals and they possess the ability to confine the energy of an exciton that would otherwise diffuse throughout the lattice. Helfrich and Lipsett identified guest molecules such as tetracene doped in anthracene as one type of trap in organic semiconductors. [13] In this case, the highly fluorescent tetracene molecules act as traps for the electronic excitation energies traveling as excitons in the anthracene crystal. In the presence of these traps energy transfer from anthracene excitons occurs suppressing its fluorescence and enhancing the tetracene fluorescence.

The energy transfer process due to the presence of traps can be expressed as:

$$S_1 + \text{Trap} \rightarrow S_{1g} + S_o + \text{phonons} \qquad \text{Equation 6.1}$$

where S_{1g} is the excited trapping molecule or impurity. From the S_{1g} state either a radiative or nonradiative transition can occur. This, however depends on the type of trap involved in the exciton interaction.

In organic crystals this energy transfer was observed to be inhibited at very low temperatures.[14,15] For the case of the impurity molecule anthracene in naphthalene, a significant decrease in the fluorescence quantum yield of anthracene and a corresponding increase in the quantum

yield of naphthalene was observed in cooling the sample from 12K to 5K.[16] Similarly, for tetracene in anthracene, an increase in the quantum yield of anthracene was observed in cooling the sample from 40K to 20K.[14]

In our experiments we have interpreted the observed temperature dependence as a decrease in singlet exciton diffusion at low temperatures which leads to a reduction in exciton trapping. To demonstrate this model quantitatively, we can estimate the bimolecular recombination rate of singlet excitons by using equation 6.2 which describes the concentration of singlet molecular excitons $[S_1]$: [17,18]

$$d[S_1]/dt = \alpha I(t) - k[S_1] - f\gamma_{SS}[S_1]^2 \qquad \text{Equation 6.2}$$

The parameters of the equation have been previously defined in chapter 4. In Alq_3, bimolecular recombination processes can be used to determine the diffusion parameters.

Using equation 6.2 to fit our experimental PL data we extracted the bimolecular recombination rate constant for both 300K and 77K. Theoretical fits provided estimates of $\gamma_{ss} = (8\pm2.5)\times10^{-12}$ cm^3 sec^{-1} and $\gamma_{ss} = (4\pm2)\times10^{-12}$ cm^3 sec^{-1} at 300K and 77K, respectively. These results demonstrate a reduction in the bimolecular recombination rate constant by a factor of two at low temperature.

From the values of γ_{ss} we estimated the diffusion coefficient for singlet excitons, D_s, from the equation:

$$\gamma_{ss} = 8\pi D_s R + 8\pi R^2 (D_s k)^{1/2} \qquad \text{Equation 6.3}$$

where R is the spherical reaction radius.[10,19,20] Taking R = 10Å, we obtained values for D_s within the range of $(3 \pm 1)\times10^{-6}$ cm^2 sec^{-1} at 300K and $(1.6 \pm 0.8)\times10^{-6}$ cm^2 sec^{-1} at 77K. Thus, the diffusion coefficient of singlet excitons in Alq_3 is reduced by about a factor of 2 at low temperature. The diffusion length of singlet excitons, L, was then estimated from equation 6.4:

$$L = (Z\tau D_s)^{1/2} \qquad \text{Equation 6.4}$$

where τ is the singlet lifetime and Z is equal to 6, 4, or 2 for three-, two-, or one-dimensional diffusion, respectively.[8] Assuming that exciton diffusion is three-dimensional in isotropic Alq_3 films, one obtains L=(53 ± 9)Å at 300K and L=(37 ± 10)Å at 77K.

These experimental findings indicates a reduction in the singlet exciton diffusion at low temperatures thus preventing the mobile excitons from reaching traps. This is consistent with the assumption that exciton diffusion to randomly distributed traps is the deactivation channel involved in the nonradiative recombination process.

6.5 Conclusion

From our PL measurements, we have identified that exciton diffusion to defects or trapping sites is an significant non-radiative decay channel for excitons in Alq_3. The increase in the peak PL and the PL excited state lifetime observed at low temperature and low excitation suggests that if exciton-exciton interactions are neglected, then exciton diffusion to trapping sites becomes a primary channel for nonradiative energy dissipation. The decrease in the exciton diffusion coefficient and diffusion length at low temperatures supports the exciton trapping model.

Information regarding exciton diffusion and trapping are valuable for the improvement of Alq_3 based OLED's. The increase in the PL quantum yield observed at 77K suggests that operation of devices at lower temperatures can result in improvements in the EL quantum efficiency. But for commercially viable OLED's and flat panel displays, operation of devices at such low temperature may not be practical. However, other potential devices such as organic lasers which utilize organic light emitting materials as the gain medium can possibly benefit from operation at low temperatures.

1 C.W. Tang and S.A. VanSlyke, *Appl Phys. Lett.* **51**, p, 913 (1987).

2 C. W. Tang, S. A. VanSlyke and C. H. Chen, *J. Appl. Phys.* **65**, p. 3610 (1989)

3 P. E. Burrows, L. S. Sapochak, D. M. McCarty, S. R. Forrest and M. E. Thompson *Appl. Phys. Lett.* **64**, p. 2718 (1994)

4 J.B. Birks, *Photophysics of Aromatic Molecules*, (Wiley-Interscience, London), p. 533 (1970)

5 P.E.Burrows, Z.Shen, V. Bulovic, D.M. McCarty, S.R.Forrest, J.A. Cronin, and M.E. Thompson, *J. Appl. Phys.*, **79**, p. 7991 (1996)

6 U. Lemmer, R.F. Mahrt, Y. Wada, A. Greiner, H. Bassler, and E.O. Gobel. *Appl. Phys. Lett.*, **62**, p. 2827 (1993)

7 I.D.W. Samuel, B. Crystall, G. Rumbles, P.L. Burn, A.B. Holmes and R.H. Friend, Synth. Met., **54**, p. 281 (1993)

8 M. Furukawa, K. Mizuno, A. Matsui, S.D.D.V. Rughooputh and W.C. Walker,*J. Phys. Soc. Jpn.* **58**, p. 2976 (1989)

9 Y. Abe, K.I. Onisawa, S. Aratani and M. Hanazono, *J. Electrochem. Soc.*, **139**, p.641 (1992)

10 K.C. Kao and W. Hwang, *Electrical Transport in Solids* (Pergamon, New York), p. 467 (1981)

11 P.E.Burrows, Z.Shen, V. Bulovic, D.M. McCarty, and S.R.Forrest, *J. Appl. Phys.*, **79**, p. 7991 (1996)

12 I. Sokolik, R. Priestley, A.D. Walser, R. Dorsinville, and C.W. Tang, *Appl. Phys. Lett.*, **69**, p. 4168 (1996)

13 W. Helfrich and F.R. Lipsett, *J. Chem. Phys.*, **43**, p. 4368 (1965)

14 Y. Kanda and H. Sponer, *J. Chem. Phys.*, **28**, p. 598 (1958)

15 L.E. Lyons and J. W. White, *J. Chem. Phys.*, **29**, p. 447 (1958)

16 K. Gschwendter and H.C. Wolf, *Naturwill.*, **48**, p. 42 (1961)

17 M. Pope and C.E. Swenberg, *Electronic Processes in Organic Crystals* (Oxford University Press, New York), p. 158 (1982)

18 C.E. Swenberg and N.E. Geacinotv, in *Organic Molecular Photophysics*, edited by J.B. Birks (Wiley-Interscience, London), Vol. 1, p. 495 (1973)

19 A.J. Campillo, R.C. Hyer, S.L. Shapiro, and C.E. Swenberg, *Chem. Phys. Lett.*, **48**, p. 495 (1977)

20 U. Goesele, Chem. Phys. Lett. **43**, p. 61 (1976); *Chem. Phys. Lett.*, **46**, p. 196 (1977).

CHAPTER SEVEN

7. CONCLUSIONS AND FUTURE DIRECTIONS

This chapter summarizes the results of our experimental studies on Alq_3, a prominent material used as the light emitting layer in OLED's. In addition, we present a description of possible future experiments that may be performed to enhance our understanding of the various light quenching mechanisms in this material. A list of the author's publications and presentations related to this thesis are provided.

7.1 Conclusions

The mechanism behind light emission in Alq_3 is based on the formation of singlet excitons (electron-hole pairs) and the subsequent radiative decay of these excitons. By conducting photoluminescence (PL) measurements we were able to examine various excited state reactions in Alq_3. This allowed us to focus directly on reactions of singlet exciton in the emitting material. Along with the PL, we conducted photoconductivity (PC) measurements. We proposed that the PC in Alq_3 is due to singlet exciton-exciton annihilation and we used this as another observation

channel to understand the reactions of singlet excitons at high singlet exciton concentrations.

First, we examined the effects of singlet exciton-exciton interactions in Alq_3. We have shown that these interactions resulted in a decrease in the peak PL, excited state lifetime and the PL quantum yield. In the case of high intensity photoexcitation of Alq_3 thin films, we observed how the generation of charge carriers originates from singlet exciton-exciton annihilation.

From these measurements we were able to calculate the bimolecular recombination rate constant, the singlet exciton diffusion coefficient and the diffusion length. In OLED's, these parameters are important since they govern the emission zone of the device. The practicality of these exciton-exciton interactions occurring in LED's was examined. Calculations were made showing that under normal device operating conditions, the concentration of singlet excitons in Alq_3 is below the concentration level at which exciton-exciton interactions would occur. Therefore, this reaction may not affect the performance of the device. However, these reactions would need to be addressed in other organic emitting devices such as organic lasers where a large concentration of singlet excitons would exist.

Another key issue we focused on was photooxidation. In order to move the technology of organic EL from being a novelty in an academic laboratory to a commercial product, organic LED's have to demonstrate

satisfactory operating performance when operating under natural environments. Device operation under ambient conditions has been shown to result in degradation of the device. To date, the degradation has been the single most important barrier to commercializing these devices and there is still a great deal of research to be done.

We demonstrated for the first time that the process of photooxidation (PO) in Alq_3 does occur. We showed that PO resulted in a decrease in the PL quantum yield and consequently this can have an adverse affect on the operation of OLED's.

The final issue we examined in this thesis was the temperature dependence of the PL quantum yield in Alq_3. We observed an increase in the peak PL, PL lifetime and PL quantum yield with decreasing temperatures from 300K to 77K. We attributed this increase in the luminescence quantum yield to a reduction in singlet exciton trapping at low temperatures. This model was substantiated by measurements showing a reduction in singlet exciton diffusion coefficient and diffusion length at 77K.

7.2 Future Directions

This section describes future experiments that can be performed to improve our understanding of the reactions of singlet excitons in Alq_3.

We would like to investigate the temperature dependence of the transient photoconductivity (PC) of Alq_3 and correlate these results with those obtained from our photoluminescence (PL) measurements. The PC response in Alq_3 is attributed to singlet exciton-exciton annihilation and we can speculate that a decrease in the PC quantum yield will occur at lower temperatures. Since a decrease in temperature results in a decrease in exciton diffusion, the probability of exciton-exciton interactions followed by the subsequent generation of charge carriers (PC response) may be reduced.

Another model we can use to hypothesize our PC temperature results is the interaction of a singlet exciton with a trapped charge as given by:[1]

$$S_1 + e_T \text{ (or } h_T) \rightarrow S_0^* + e \text{ (or h)} \qquad \text{Equation 7.1}$$

where 'e_T' or 'h_T' represents a trapped electron or hole, respectively, and 'e' or 'h' represents a detrapped electron or hole, respectively. This detrapping process occurs by energy transfer from the singlet exciton to the trapped charge and can result in an increase in the PC quantum yield. However, at low temperatures where we have found singlet excitons to

diffuse less, this detrapping may become less efficient. Results from the temperature dependence measurements on the transient PC response will enhance our understanding of the mechanism for the generation of charge carriers and the dynamics of singlet excitons.

Another measurement we would like to perform involves observing the effects of photooxidation in Alq_3 by conducting FTIR measurements. This will allow us to possibly identify what species are created during the PO process and what is the mechanism behind the luminescence quenching. These measurements will allow us to observe the microscopic changes in the chemical structure of Alq_3 associated with the photochemistry responsible for PL quenching.

---

1 K.C. Kao, and W. Hwang, *Electrical Transport in Solids* (Pergamon, New York), Vol. 14, p. 485 (1981)

7.3 List of Publications and Presentations Related to this Thesis

Scientific Publications

R. Priestley, A.D. Walser, and R. Dorsinville. "Temperature Dependence of Transient Photoluminescence in Tris(8-hydroxyquinoline) Aluminum (Alq_3)." Submitted to Applied Physics Letters (1997)

R. Priestley, A.D. Walser, and R. Dorsinville. "Observation of the Temperature Dependence of the Dynamics of Photoexcited States in Pristine Tris(8-hydroxyquinoline) Aluminum (Alq_3)." Submitted to Materials Research Society (MRS) Abstracts for 1997 Fall Meeting.

R. Priestley, I. Sokolik, A. D. Walser, R. Dorsinville, and C. W. Tang. "Photooxidation Effects on Picosecond Photoluminescence and Photoconductivity in Tris(8-hydroxyquinoline) Aluminum (Alq_3)." *Synth. Met.*, **84**, (1997)

A. D. Walser, I. Sokolik, R. Priestley, and R. Dorsinville. "Simultaneous Measurement of the Transient Photoconductivity and Photoluminescence in Alq_3." *Synth. Met*, **84**, (1997)

I. Sokolik, A. D. Walser, R. Priestley, C. W. Tang, and R. Dorsinville. "Reactions of Singlet Excitons in Tris(8-hyrdoxyquinoline) Aluminum." *Synth. Met*, **84**, (1997)

I. Sokolik, R. Priestley, A. D. Walser, R. Dorsinville, and C. W. Tang. "Bimolecular Reactions of Singlet Excitons in Tris(8-hydroxyquinoline) Aluminum." *Appl. Phys. Lett.* **69**, p. 27 (1996).

A. D. Walser, I. Sokolik, R. Priestley, and R. Dorsinville. "Dynamics of Photoexcited States and Charge Carriers in Organic Thin Films: Alq_3." *App. Phys. Lett.* **69**, p. 12 (1996)

I. Sokolik, A. D. Walser, R. Priestley, C. W. Tang, and R. Dorsinville. "Effect of Photooxidation of the Transient Photoconductivity and Photoluminescence in Alq_3." 1995 Fall MRS Proceedings. Electrical, Optical and Magnetic Properties of Organic Solid State, Vol. 3, MRS Vol 413, p. 65, (1996)

Presentations

R. Priestley, A.D. Walser and R. Dorsinville. "Observation of the Temperature Dependence of the Dynamics of Photoexcited States in Pristine Tris(8-hydroxyquinoline) Aluminum (Alq_3)." Materials Research Society Conference; Boston, MA. December 1997. Poster Presentation

R. Priestley, I. Sokolik, A.D. Walser, R. Dorsinville and C.W. Tang. "Photooxidation Effects on Transient Photoluminescence and Photoconductivity in Alq_3." Optical Society of America Conference; Rochester, NY. October 1996. Oral Presentation

R. Priestley, I. Sokolik, A.D. Walser, C.W. Tang and R. Dorsinville. "Photooxidation Effects on Picosecond Photoluminescence and Photoconductivity in Tris(8-hydroxyquinoline) Aluminum (Alq_3)." International Conference on Science and Technology of Synthetic Metals (ICSM); Snowbird, Utah. July 1996. Poster Presentation

7.4 Bibliography

Abe, Y., K.I. Onisawa, S. Aratani and M. Hanazono, *J. Electrochem. Soc.*, **139**, p.641 (1992)

Adachi, C., T.Tsutsui, and S. Saito, *Appl. Phys. Lett.*, **56**, p. 799 (1990)

Antoniadis, H., M.R. Hueschen, J. McElvain, J.N. Miller, R.L. Moon, D.B. Roitman, and J.R. Sheats, *ANTEC 97*, **724**, p. 1266 (1997)

Auston, D.A., *IEEE J. Quant. Elec.*, **3**, p. 636 (1983)

Avakian, P., *Pure Appl Chem.*, **32**, p. 1 (1974)

Avakian, P., and R.E. Merrifield, *Mol. Cryst.*, **5**, p. 37 (1968)

Bassler, H., G.Schonherr, M.Abkowitz and D.M. Pai, *Phys. Rev. B.*, **24**, p. 3105 (1982)

Birks, J.B., *Photophysics of Aromatic Molecules*, (Wiley Interscience), (1969)

Blatchford, J.W., S.W. Jessen, L.B. Lin, J.J. Lih, T.L. Gustafson, A.J. Epstein and T.M Swager, *Phys. Rev. Lett.*, **9**, p. 1513 (1996)

Bradley, D.D.C., *Adv. Mater.*, **4**, p. 756, (1992)

Bradley, D.D.C., and R.H. Friend, *J. Phys. Cond. Matt.*, **1**, p. 3671 (1989)

Braun, C.L., *Phys. Rev. Lett.* **21**, 215 (1968)

Braun, D. and A.J. Heeger, *Appl. Phys. Lett.* **58**, p. 1982, (1991)

Bredas, J.L., J. Cornil, and A.J. Heeger, *Adv. Mater.*, **8**, No. 5, p. 447 (1996)

Burn, P.L., A.B. Holmes, A. Kraft, D.D.C. Bradley, A.R.Brown, R.H. Friend and R.W. Gymer, *Nature*, **356**, p. 47, (1992)

Burroughes, J.H., D.D.C. Bradley and A.R. Brown, *Nature* **347**, p. 539-541, (1990)

Burrows, P.E., V. Bulovic, S.R. Forrest, L.S. Sapochak, D.M. McCarty, and M.E. Thompson, *Appl. Phys. Lett.*, **65**, p. 2922 (1994)

Burrows, P.E., and S.R. Forrest, *Appl. Phys. Lett.*, **64**, p. 2285 (1994)

Burrows, P.E., L.S. Sapochak, D.M. McCarty, S.R. Forrest, and M.E. Thompson., *Appl. Phys. Lett.*, **64**, p. 20, (1994)

Burrows, P.E., L.S. Sapochak, D.M. McCarty, S.R. Forrest and M.E. Thompson, *Appl. Phys. Lett.*, **64**, p. 2718 (1994)

Burrows, P.E., Z. Shen, V. Bulovic, D.M. McCarty, S.R. Forrest, J.A. Cronin and M.E. Thompson, *J. Appl. Phys.* **79**, p. 1991 (1996)

Burrows, P.E., Z.Shen, V. Bulovic, D.M. McCarty, and S.R.Forrest, *J. Appl. Phys.*, **79**, p. 7991 (1996)

Campillo, A.J., R.C. Hyer, S.L. Shapiro and C.E. Swenberg, *Chem. Phys. Lett.* **48**, p. 495 (1977)

Choi, S.I., *J. Chem. Phys.*, **40** p. 1691 (1964)

Colaneri, N.F., D.D.C. Bradley, R.H. Friend, P.L. Burn, A.B. Holmes, and C.W. Spangler, *Phys. Rev. B.*, **42**, p. 11670, (1990)

Courtens, E., A. Bergman and J. Jortner, *Phys. Rev.*, **156**, p. 948 (1967)

Davydov, A.S., *Theory of Molecular Excitons*, McGraw-Hill, New York (1962)

Diaz-Garcia, M.A., F. Hide, B.J. Schwartz, M.D. McGehee, M.R.Andersson and A.J. Heeger, *Appl. Phys. Lett.*, **70**, p. 3191 (1997)

Diaz-Garcia, M.A., F. Hide, B.J. Schwarts, M.R. Anderson, Q. Pei and A.J. Heeger, *Synth. Met.*, **84**, p.455 (1997)

Do, L.M., E.M. Han, Y. Niidome, M. Fujihira, T. Kanno, S. Yoshida, A. Maeda, and A.J. Ikushima, *J. Appl. Phys.*, **76**, p. 5118 (1994)

Dodabalapur, A., L. Rothberg, and T.M. Miller, *Appl. Phys. Lett.*, **64**, p.2308, (1994)

Etemad, S., A. Pron, A.J. Heeger,, A.G. MacDiarmid, E.J. Mele, and M.J. Rice, *Phys. Rev. B.*, **23**, p. 5137 (1981)

Freeman, D.C., and C.E. White, *J. Am. Chem. Soc.*, **78**, p. 2678 (1956)

Frolov, S.V., M. Ozaki, W. Gellermann, M. Shkunov, Z.V. Vardeny and K. Yoshino, *Synth. Met.*, **84**, p. 473 (1997)

Frolov, S.V., W. Gellermann, Z.V. Vardeny, M. Ozaki and K. Yoshino, *Synth. Met.*, **84**, p. 471 (1997)

Furukawa, M., K. Mizuno, A. Matsui, S.D.D.V. Rughooputh and W.C. Walker,*J. Phys. Soc. Jpn.* **58**, p. 2976 (1989)

Garbuzov, D.Z., V. Bulovic, S.R. Forrest, *Chem. Phys. Lett.*, **249**, p. 433 (1996)

Geacintov, N.E., M. Pope and F. Vogel, *Phys. Rev. Lett.*, **22**, p.593(1969)

Goesele, U., *Chem. Phys. Lett.*, **43**, p. 61 (1976); *Chem. Phys. Lett.*, **46**, p. 196 (1977)

Grem, G., G. Leditzky, B. Ullrich and G. Leising, *Adv. Mater.*, **4**, p. 36, (1992)

Gschwendter, K. and H.C. Wolf, *Naturwill.*, **48**, p. 42 (1961)

Gustafsson, G., Y. Cao, G.M. Treacy, F. Klavetter, N. Colaneri, and A.J. Heeger, *Nature*, **357**, p. 477-479, (1992)

Gymer, R.W., *Endeavour*, **20**, p. 115 (1996)

Hamada, Y., C. Adachi, T. Tsutsui, and S. Saito, *Jpn. J. Appl. Phys.*, **32**, p. 1812 (1992)

Hammerstad, E.O., *Proc. European Microwave Conf.*, p. 268 (1975)

Heisel, F., J.A. Miehe, B. Sipp and M. Schott, *Chem. Phys. Lett.*, **3**, p. 534 (1976)

Helfrich, W., and F.R. Lipsett, *J. Chem. Phys.*, **43**, p. 4368 (1965)

Helfrich, W., and W.G. Schneider, *Phys. Rev. Lett.* **14**, p. 229, (1965)

Heller, A., and E. Wasserman, *J. Chem. Phys.*, **42**, p. 949 (1964)

Hiramoto, M., K. Yoshimura, and M. Yokoyama, *Appl. Phys. Lett.*, **60**, p. 324, (1992)

Holstein, T., *Ann. Phys.*, **8**, p. 343 (1959)

Hoshino, S., and H. Suzuki, *Appl. Phys. Lett.*, **69**, p. 224 (1996)

Hosokawa, C., H. Tokailin, H. Higashi and T. Kusumoto, *Appl. Phys. Lett.*, **60**, p. 1220 (1992)

Kanda, Y. and H. Sponer, *J. Chem. Phys.*, **28**, p. 598 (1958)

Kao, K.C., and W. Hwang, *Electrical Transport in Solids* (Pergamon, New York), Vol. 14, (1981)

Katsume, T., M. Hiramoto, and M. Yokoyama, *Appl. Phys. Lett.*, **66**, p. 2992, (1995)

Kersting, R., U. Lemmer, M. Deussen, H.J. Bakker, R.F. Mahrt, H. Kurz, V.I. Arkhipov, H. bassler, and E.O. Gobel, *Phys. Rev. Lett.*, **73**, p. 1440 (1994)

Kepler, R.G., *Phys. Rev. Lett.*, **18**, p. 951 (1967)

Kepler, R.G., *Phys. Rev.*, **119**, p. 503 (1960)

Kepler, R.G., P.M. Beeson, S.J. Jacobs, R.A. Anderson, M.B. Sinclair, V.S. Valencia and P.A. Cahill, *Appl. Phys. Lett.*, **66**, p. 3618 (1995)

Kepler, R.G., and R.E. Merrifield, *J. Chem. Phys.*, **40**, p.1173 (1964)

Kido, J., *TRIP*, Vol. 2, No.10, p. 350 (1994)

Kido, J., M. Kimura, and K. Nagai, *Science*, **267**, p. 1332, (1995)

Kittel, C., *Introduction to Solid State Physics*, 6 ed. (Wiley) p. 296 (1986)

LabView is a registered trademark of the National Instruments Corporation.

Lee, C.H., G.Yu, and A.J. Heeger, *Phys. Rev. B-Cond. Matt.* **47**, p. 15543 (1993)

Lemmer, U., R.F. Mahrt, Y. Wada, A. Greiner, H. Bassler, and E.O. Gobel. *Appl. Phys. Lett.*, **62**, p. 2827 (1993)

L.E. Lyons and J. W. White, *J. Chem. Phys.*, **29**, p. 447 (1958)

Marks, R.N., J.J.M. Halls, D.D.C. Bradley, R.H. Friend and A.B. Holmes, *J. Phys.: Cond. Matt.*, **6**, p. 1379 (1994)

McElvain, J., H. Antoniadis, M. Hueschen, J. Miller, R. Moon, and D. Roitman, *J. J. Appl. Phys.*, **80**, (1996)

Mori, T., K. Miyachi and T. Mizutani, *J. Phys. D.*, **28**, p. 1461 (1995)

Moridawa, M., C. Adachi, T. Tsutsui, and S. Saito, "Extended Abstracts." The 51th Autumn Meeting of The Japan Society of Applied Physics, p. 1041, (1990)

Moses, D., *Solid State Communications*, **69**, p. 721 (1989)

Murayama, R., "Extended Abstracts." The 54th Autumn Meeting of the Japan Society of Applied Physics, p. 1127, (1993)

Murayama, R., T. Wakioto, H. Nakada, M. Nomura and G. Sato. U.S. Patent 5,227,252.

Northrop, D.C., and O. Simpson, *Proc. Roy. Soc.* **A244**, p. 377 (1958)

Ohmori, Y., M. Uchida, K. Muro and K. Yoshino, *Solid State Comm.*, **80**, p. 605, (1991); Y. Ohmori, M. Uchida, K. Muro and K. Yoshino, *Jpn. J. Appl. Phys.*, **30**, p. L 1938, (1991)

Onsager, L., *Phys. Rev.*, **54**, p. 554 (1938)

Pakbaz, K., Synth. Met., 64, p. 295 (1994)

Parker, C.A., Photoluminescence of solutions,, p. 474 (1968)

Papadimitrakopoulos, F., K. Konstadinidis, T.M. Miller, R. Opila, E.A. Chandross, and M.E. Galvin, *Chem. Mater.*, **6**, p.1563 (1994)

Papadimitrakopoulos, F., X.M. Zhang, L.L. Thomsen, and K.A. Higginson, *Chem. Mat.*, **8**, p. 1363 (1996)

Pierret, R.F., *Semiconductor Fundamentals*, (Addison-Wesley), Vol. 1, p. 64 (1988)

Pope, M., and C.E. Swenberg, *Electronic Processes in Organic Crystals,* (Oxford University Press, New York), (1982)

Pope, M., H.P. Kallmann, and P. Magnante, *J. Chem. Phys.* **38**,p. 2042, (1963)

Rauscher, U., L. Schutz, A. Greiner and H. Bassler, *J. Phys.: Cond. Matt.*, **1**, p. 9751 (1989)

Rice, S.A., and J. Jortner, *Physics and Chemistry of Organic Solid State*, Vol. 3, p. 199 (1967)

Robinson, G., *Electronic Engineering Times*, p. 35, (1997)

Rothberg, L.J., *Proc. SPIE Int. Soc. Opt. Eng.*, **1910**, p. 122 (1993)

Samelson, H., A. Lempicki and C. Brecher, *J. Chem. Phys.*, **40**, p. 2553 (1964)

Samuel, I.D.W., B. Crystall, G. Rumbles, P.L. Burn, A.B. Holmes and R.H. Friend, Synth. Met., **54**, p. 281 (1993)

Sano, T., M. Fujita, T. Fujii, Y. Nishio, Y. Hamada and K. Shibata, "Extended Abstracts." The 41st Spring Meeting, 1994 of the Japan Society of Applied Physics and Related Societies, 25 p-N-2.

Schein, L.B., and D.W. Brown, *Mol. Cryst. Liq. Cryst.*, **87**, p. 1 (1982)

Schwartz, B.J., F. Hide, M.R. Anderson and A.J. Heeger, *Synth. Met.*, **84**, p. 663 (1997)

Scott, J.C., J.H. Kaufman, P.J. Brock, R. Dipietro, J. Salem, and J.A.Goitia, *J. Appl. Phys.*, **79**, p. 2745 (1996)

Sheats, J.R., H. Antoniadis, M. Hueschen, W. Leonard, J. Miller, R. Moon, D. Roitman, and A. Stocking, *Science*, **273**, p. 884 (1996)

Shen, Z., P.E. Burrows, V. Bulovic, D.M. McCarty, M.E. Thompson,and S.R. Forrest, *Jpn. J. Appl. Phys.*, **35**, Part 2, No. 3B, p. L401 (1996)

Sokolik, I., R. Priestley, A.D. Walser, and R. Dorsinville, *Appl. Phys. Lett.*, **69** p. 4168 (1996)

Swenberg, C.E., and N.E.Geacintov, *Organic Molecular Photophysics*, edited by J.B. Birks (Wiley-Interscience, London), Vol. 1, (1973)

Tang, C.W., and S.A. Van Slyke, *Appl. Phys. Lett.* **51**, p. 913, (1987)

Tang, C.W., S.A. VanSlyke and C.H. Chem, *J. Appl. Phys.* **65**, p. 3610, (1989)

Tsutsui, T., *MRS Bulletin*, Vol. 22, p. 40 (1997)

Tsutsui, T., C. Adachi, and S.Saito, in *Photochemical Processes in Organized Molecular Systems*, edited by K. Honda (Elsevier, North Holland, Amsterdam. p. 445, (1991)

Wakayama, N.I., N. Wakayama, and D.F. Williams, *Mol. Cryst. Liq. Cryst.* **26**, p. 275 (1974)

Walser, A., I. Sokolik, R. Priestley and R. Dorsinville, *Appl. Phys. Lett.*, **69**, p. 1 (1996)

Wheller, H.A., *IEEE Trans. Microwave Theory Tech.*, **13**, p. 172 (1965)

Wheller, H.A., *IEEE Trans. Microwave Theory Tech.*, **25**, p. 631 (1977)

Wolf, H.C., and K.W. Benz, *Pure Appl. Chem.*, **27**, p. 439 (1971)

Wong, K.S., *J. Phys. C.*, **20**, p. L187 (1987)

Woo, H.S., S.C. Graham, D.A. Halliday, D.D.C.Bradley, R.H. Friend, P.L. Burn and A.B. Holmes, *Phys. Rev, B.*,

Yang, Y., *MRS Bulletin.* **22**, p. 31 (1997)

Yan, M., L.J. Rothberg, F. Papadimitrakopoulos, M.E. Galvin, and T.M. Miller, *Phys. Rev. Lett.* **73**, p. 744 (1994)

Yoshino, K., T. Kuwabara, T. Iwasa, T. Kawai, M. Onoda, *Jpn. J. Appl. Phys.*, **29**, p. L1514 (1990)

Yu, G., K. Pakbax, and A.J. Heeger, *J. Electron. Mater.*, **23**, p. 925, (1994)

Zhang, X.-M., K.A. Higginson and F. Papadimitrakopoulos, *Electr. Opt. and Magn. Prop. of Org. Sol. State Mater.* III (MRS Symp. Proc. Ser., Vol. 413), p. 43 (1996)

Ziemelis, K.E., A.T. Hussain, D.D.C. Bradle, A.R. Brown, R.H. Friend, and R.W. Gymer, *Nature*, **356**, p. 47 (1992)

IMAGE EVALUATION TEST TARGET (QA-3)

150mm

6"

APPLIED IMAGE, Inc
1653 East Main Street
Rochester, NY 14609 USA
Phone: 716/482-0300
Fax: 716/288-5989